Department of Electrical and Computer Engineering

Optimal Siting, Sizing and Operation of Active Power Line Conditioners (APLCs) in Unbalanced Distribution Networks Embedded with Rooftop PVs for Harmonic Mitigation and Reactive Power Compensation

Saeed Kazemi

This thesis is presented for the Degree of
Master of Engineering Science of
Curtin University

October 2022

Declaration

To the best of my knowledge and belief, this thesis contains no material previously published by any other person except where due acknowledgment has been made. This thesis contains no material that has been accepted for the award of any other degree or diploma in any university.

Saeed Kazemi

15/03/2022

‘To my beloved parents and sister for their endless love and support’

Acknowledgements

I am heartily thankful to my supervisor, Professor Arindam Ghosh and my co-supervisor, Associate Professor Sumedha Rajakaruna for giving me support for the completion of my thesis. I would also like to express my gratitude to my former supervisor, Professor Syed Islam and my former co-supervisor, Dr. Sara Deilami, whose encouragement, supervision, and support from the beginning enabled me to develop an understanding of the subject and guidance throughout my study.

I gratefully acknowledge the scholarship received in the final stage of my study from the Department of Electrical and Computer Engineering at Curtin University of Technology, Perth, Western Australia, Australia.

I would like to express my special gratitude to my beloved parents, Rasoul and Shahla, for their support, patience, and unconditional love during my study. Last but not least, special thanks go to my beloved sister, Reihaneh, for her enormous support and encouragement, which have kept me going every single day.

Abstract

The power quality of distribution networks has been continuously degrading due to the growing integrations of renewable energy sources and nonlinear load applications such as various power electronic devices in modern industries. Nonlinear loads pollute the network by injecting harmonic currents, which may propagate and cause voltage and current waveform distortions. Propagation of current harmonics through power networks can potentially cause voltage instability, voltage distortions, voltage drops across the lines, and line losses, which are some symptoms of poor power quality. Possible solutions to compensate or mitigate harmonic pollutions are custom power devices, as well as active, passive, and hybrid filters. These devices have some limitations in maintaining stability the entire network. Recently, other advance devices such as active power line conditioners (APLCs) and shunt active power filters (SAPF) have attracted much attention owing to the availability of technological advancements in recent years. However, most power industries are still concerned about the impacts of nonlinear loads and are seeking solutions to control the over voltage and power quality of the entire network.

This thesis aims to address the above problems by proposing an approach that uses APLCs in unbalanced smart distribution networks with nonlinear loads and single-phase rooftop photovoltaic cells (PVs) for simultaneous harmonic voltage mitigation and reactive power compensation. The goal is to improve the total voltage harmonic distortion (THDv), regulate the voltage and reduce the voltage unbalance factor (VUF) at all buses with the minimum number and rating of APLCs. A particle swarm

optimisation (PSO) algorithm is employed for optimal sizing, allocation and operation of multiple APLCs in unbalanced distribution networks with rooftop PVs. A Newton-Raphson-based unbalanced harmonic load flow algorithm is developed in MATLAB and used to model the distribution network and calculate the proposed objective functions and optimisation constraints. Two sets of objective functions and constraints will be considered:

- An objective function for the optimal sizing and allocation of multiple APLCs is proposed for the minimisation of THDv, VUF and total size of APLCs while considering constraints to limit the THDv, voltage regulation, VUF, and individual APLC rating (size).

- Another objective function is proposed for the optimal operation of APLCs that will minimise system losses, THDv, and VUF while considering constraints that limit the total harmonic distortion, voltage deviations and VUF.

To examine the capability of the proposed method, balanced and unbalanced IEEE distribution networks containing PVs in different cases with and without APLCs are considered and investigated. Simulations are performed and analysed with and without an upper limit for APLC sizes and considering various weighting factors. Finally, the optimal operation of the system for a 24-hour period is examined.

Contents

List of Figures

List of Tables

Abbreviations

AC	Alternating Current
APLC	Active Power Line Conditioners
ASD	Adjustable-Speed Drive
CSC	Current Source Converters
DC	Direct Current
DHPF	Decoupled Harmonic Load Flow
D-STATCOM	Distribution STATic var COMpensator
DVR	Dynamic Voltage Restorer
FACTS	Flexible AC Transmission Systems
FDHLF	Fast Decoupled Harmonic Load Flow
GS	Gauss-Seidel
GTO	Gate Turn-Off thyristor
HVDC	High-Voltage Direct Current
IEC	International Electro-technical Commission
IEEEE	Institute of Electrical and Electronics Engineers
IGBT	Insulated-Gate Bipolar Transistor
IGCT	Integrated Gate-Commutated Thyristor
NCC	Network Control Center
NR	Newton-Raphson
PCC	Point of Common Connection
PPF	Passive Power Filter
PSO	Particle Swarm Optimization
PV	PhotoVoltaics

PWM	Pulse Width Modulation
SAPF	Shunt Active Power Filter
STATCOM	STATic var COMpensator
SVC	Static VAR Compensator
TDD	Total Demand Distortion
THD_i	Current total harmonic distortion
THD_v	Voltage Total Harmonic Distortion
UDHLF	Unbalanced Decoupled Harmonic Load Flow
UPQC	Unified Power Quality Conditioner
VSC	Variable Speed Drive

Chapter 1

Introduction

1.1 Background

With the constantly increasing demand for electricity and the need for distributed generation, distribution systems have become more complicated. At the same time, the existing power systems also require modification and upgrading. Reliability and performance are important factors in distribution networks. The huge amount of investments involved necessitates careful operation planning of distribution systems. The growing electricity demand can be fulfilled economically and technically by careful distribution network planning. One of the main objectives of distribution network planning is to guarantee that the growing electricity demand within the network can be continuously fulfilled in an optimal way. This could be in terms of high load densities and increasing growth rates. If this objective fails, the electricity supplied to customers will be of poor quality, which means that the electricity demand cannot be fully satisfied.

Because the electricity demand, particularly the need for distributed generation, is increasing constantly, distribution networks are becoming more complicated every day. However, despite of this complexity, the quality of power supplied to the customers must always be satisfactory. This can be achieved by proper designing/planning of networks and effective operation.

Harmonic and power quality problems are introduced in distribution networks by the extensive use of nonlinear load applications. Nonlinear loads such as adjustable speed drives, rectifiers, converters, arc furnaces, and even computer power supplies have significant impacts on the operation and performance of modern electrical distribution systems. Similar to a current source, they inject harmonic currents into the distribution networks, which will propagate and produce potentially dangerous harmonic voltages that distort voltage waveforms at all nodes including the grid at the point of common connection (PCC) [1]. The distorted voltages at the terminals of other linear and nonlinear loads will potentially lead to numerous undesired effects such as maloperation of some protection devices, overheating of motors and transformers, as well as formation of resonances and harmonic resonances with capacitors [2].

After noticing the effect of harmonic distortions on telephone line interferences in the 1920s, several standards have been established to keep the magnitudes of harmonic voltages and currents within acceptable limits. The International Electro-technical Commission (IEC) and Institute of Electrical and Electronics Engineers (IEEE) are two of the institutes that introduced the limits for harmonic voltages [3]. Acceptable limits of harmonic voltage and current distortions are provided by the power quality standards such as the IEEE-519 [4]. The American Electric Power Distribution System investigated and reported the harmonic level of three classes of distributions: residential, industrial, and commercial networks [5]. As required by the standards, maintaining the injected harmonic current magnitudes and the injected total current harmonic distortion (THD_i) below the permissible limits is customers' responsibility at their PCCs, while utility companies are responsible for controlling the total voltage harmonic distortion (THD_v) of the network and the individual buses [1, 4].

Conventionally, passive power filters (PPFs) are used to reduce harmonic distortions; despite their disadvantages of potential resonance, fixed compensation, and large size. To address such issues, active power filters (APFs) have been introduced [6]; however, they are generally more complicated and expensive at high power ratings, and more importantly, these devices are intended to maintain the PCC's injected harmonic currents without considering the THD_v of the rest of the network

[1]. Moreover, maintaining the injected current harmonics at PCCs within the standard limits does not essentially result in tolerable values of the other buses and distortions of the whole network voltages. In this regard, a relatively new generation of APFs called active power line conditioners (APLCs) have been developed [1]. The main difference between the APF and APLC is that the former mitigates harmonic distortions of nonlinear loads at the PCC while the latter minimises the THD_v of the entire system. Furthermore, the APF is always placed next to the nonlinear loads while the location of the APLC within the network needs to be chosen.

The basic compensation principles of APLCs are the same as those of APFs. APFs were proposed in the 1970s. However, in contrast to APFs that inject equal but opposite currents at the PCC to completely eliminate harmonic currents generated by nonlinear loads, APLCs inject harmonic currents to minimise (but not fully eliminate) the THD_v of the entire network or a selected part of the system. Therefore, APLCs aim to address the practical requirement of reducing harmonic distortions to less than the standard values [7-9]. In 1982, the first APLC was used for harmonic compensation of an 800 kVA power system. Later, a hybrid system of 900 kVA-APLC and 6600 kVA-PPF was installed successfully [10]. Currently, APLCs are attracting more attention owing to their ability of compensating for harmonics at lower costs compared to APFs and the possibility of further improving their performance by using the smart meter information [11-13].

Despite the numerous advantages of APLCs compared to APFs, their practical applications are still very limited due to the lack of information and research regarding their optimal location, size and operation. However, there are a few studies on advance approaches for the operation of APLCs. Siting of only one APLC or multiple APLCs is the main contribution of these studies. The preliminary stages toward solving the APLC siting/sizing problem was introduced by references [12, 14, 15]. It was shown that addressing the total harmonic distortion (THD) limitations at all network buses may not be assured by utilising only one APLC, particularly when there are a few nonlinear loads distributed throughout the network.

An analytical optimisation-based algorithm by using nonlinear mixed-integer programming is presented in [16-18] to solve the siting/sizing problem of multiple APLCs. These algorithms are fast but may get trapped in the local minimum points. They are also very sensitive to the initial point/solution and the complexity from several types of nonlinear objective functions. It should be highlighted that the results of these methods may be imprecise if the selection of the initial solution is inaccurate.

The APLC rating and THD values have been considered in [14, 16, 18-20] as the essential component of the objective function. However, there are other factors that also have been taken into consideration by other authors such as harmonic transmission-line loss (HTLL), the telephone influence factor (TIF) and motor load loss (MLL) [15, 17].

To solve the APLC siting/sizing problem, a genetic algorithm (GA) was developed in [19]. The easier implementation and simpler concept compared to the analytical approach are among the advantages of this heuristic algorithm. Differentiation from the nonlinear objective functions and initial solution independency can also be considered as its benefits. However, this algorithm needs adjustment of several parameters, suffers from the local minima, is time consuming, and requires an extensive memory.

Another popular algorithm is the particle swarm optimisation (PSO), which offers all advantages of the heuristic-based algorithms such as the GA with superior speed and accuracy [19]. PSO-based algorithms consume less time, do not require an extensive memory, do not suffer severely from the local minima, and only require a few parameter adjustments. These advantages make the PSO a suitable approach for a wide range of electrical power system problems, such as power system control design, optimal power flow, economic dispatch, reactive power control, and power loss reduction [21-24]. In implementing the PSO, the optimisation problem is carried out by minimising the specific objective function while satisfying the constraints. The variables of the network's power quality are computed by determining the solution of the load flow that generates the value of the objective function. Additionally, obtaining this objective value in the least possible number of iterations is preferable. The level

of harmonic distortion should not exceed the maximum allowable value. A constraint to controlling the harmonic distortion level is involved in the optimisation problem. It is mathematically represented as a THD_v measure. The influence of harmonics is not only on voltage distortion but also on the voltage increment and power loss escalation. The presence of harmonics may amplify the voltage magnitude and power losses. As these two quantities are definitely considered in the problem, taking harmonics into account will significantly influence the optimisation problem [25, 26].

A real distribution system normally consists of a large number of buses with some harmonic generating devices installed on it. In addition, these devices may also have different types. Therefore, a large distribution network containing a number of nonlinear loads requires proper planning. As nonlinear loads typically have different harmonic characteristics, they have to be specifically modelled in load flow calculations, making such calculations very complicated. The computational burden on the problem of optimal sizing/siting of multiple APLCs greatly depends on the load flow calculations Thus, taking a large scale distribution system with multiple nonlinear loads into consideration will increase the computational burden. From the abovementioned discussions, the computational burden is the main obstacle for the optimisation of a large distribution system with multiple nonlinear loads. However, this optimisation needs to be carried out for enhancing the voltage and power quality while reducing the losses.

In addition, for the distribution system operation, the hourly load change is also a problem that needs to be carefully considered. One of the main issues is the variation of the electricity demand, which is very difficult to solve both economically and technically. Several problems, such as power loss escalation, voltage violation, and in general, poor power quality, may accumulate in the distribution systems if not carefully managed. An adaptable enhancement is therefore required to overcome these problems and achieve proper operation of all sized/sited APLCs in the network. The bus voltages and THD must remain within the allowable limits during load changes. The THD level on every bus at every hour must be checked during the optimisation operation.

The bus voltage profiles are influenced by the reactive power, and a lack of adequate reactive power generation can potentially lead to a poor voltage level and even voltage collapse within the power network. Furthermore, the reactive power of network loads reduces the system power factor, increasing losses in the transmission network as well as causing various issues for other network loads [5, 27, 28]. Therefore, compensating for the reactive power is recommended for networks. This can be done by including the fundamental current injection in the operation of APLCs. If the reactive power is compensated, the power losses along the feeder will be minimised and the voltage profile will be further improved [29, 30].

In this study, effective techniques for the problem at hand are developed. The PSO is proposed to solve the optimal siting/sizing and operation of APLCs in unbalanced distribution networks embedded with rooftop PVs. Furthermore, relatively [31, 32] developed and used an accurate and fast decoupled harmonic load flow (FDHLF) algorithm as the backbone of the optimisation problem's calculations. Simulation is initially performed on a distorted balanced IEEE network with multiple nonlinear loads. Then it is extended to an unbalanced distribution system with multiple nonlinear loads. These simulations are all carried out for sinusoidal operating conditions.

1.2 Objectives

Methods for improving the power quality of distribution networks are well researched topics. However, there are research gaps in developing effective methods and customised equipment for enhancing the power quality of an entire network. Furthermore, considering the unbalance factor of a network is a big gap in the existing research.

The aim of this research is to investigate the applications of multiple APLCs in unbalanced smart distribution networks with nonlinear loads and single-phase rooftop PVs for simultaneous harmonic voltage mitigation and reactive power compensation. The main objectives are as follows:

1. To optimally size and locate multiple APLCs in unbalanced distribution networks with nonlinear loads and single-phase rooftop PVs so that the THD_v is maintained within standard levels by developing a modified PSO and an unbalanced DHLF (UDHLF) algorithm.
2. To minimise system losses, voltage fluctuations, and voltage unbalance factors (VUFs) and compensate for the reactive power at the fundamental frequency by optimally operating the APLCs.
3. To implement and evaluate the proposed methods on an IEEE standard network with smart meters over a 24-hour period.

1.3 Thesis Contributions

In this study, a new effective technique is developed and investigated to address the previously discussed issues. In contrast to other proposed techniques that are generally slow in computing the system parameters, using the DHLF to calculate the objective function of the PSO makes the approach faster particularly for larger distribution networks. Additionally, the unbalanced characteristic of distribution networks is also included in the optimisation problem. The unbalance characteristic is always a challenging case in a real network owing to the growing popularity of single-phase PVs and increasing nonlinear loads. Therefore, the approach is implemented for the problem at hand and its influence on the power quality of unbalanced networks is discussed. Maintaining the THD_v of the entire unbalanced network within the standard level and compensating for the network's losses are the main goals of this study. In summary, the main contributions are the following:

1. Development and coding of the UDHLF algorithm.
2. Optimal sizing and sitting of APLCs in unbalanced smart distribution networks with nonlinear loads and single-phase rooftop PVs to limit the THD_v according to IEEE-519 standards [4] using a modified PSO with various weighting factors.
3. Optimal operation of multiple APLCs to minimise system losses, voltage fluctuations, and VUFs.

4. Extending the APLC function to also comprise compensation of reactive power at its fundamental frequency, voltage regulation enhancement and VUF improvement in addition to the conventional harmonic mitigations.
5. Implementation and evaluation of the proposed APLC siting/sizing and operation methods on an IEEE standard network with smart meters over a 24-hour period and then, evaluating the performance of system.

And at the end, recommendations based on the provided results and discussions will be presented.

1.4 Thesis Outline

The rest of this thesis contains the following five chapters. Chapter 2 presents an introduction to the power quality challenges in distribution systems. It discusses the importance of harmonic mitigation techniques on improving the power quality of networks. Some of the available devices to address the problems such as APFs and APLCs are also briefly reviewed. Then, chapter 3 presents some harmonic load flow algorithms and their respective advantages and drawbacks. They are discussed because the harmonic load flow is the backbone of the PSO for computing all parameters of the network. Chapter 4 proposes the PSO-based approach to optimally size and site multiple APLCs in the network. The algorithm is implemented in balanced 18-bus and 123-bus IEEE networks to determine the optimal location and size of the APLCs. In addition, the algorithm's capability of mitigating the THD_v of the entire network is investigated and discussed. The APLC modelling in the proposed approach is also demonstrated. Chapter 5 details the development and extension of the proposed PSO algorithm for unbalanced networks. The algorithm is implemented in an unbalanced network and its ability to mitigate the harmonic distortions and reactive power of the entire network is confirmed. Next, the proposed PSO-based algorithm is implemented for a 24-hour operation of the network and its capability to keep the network's THD under a specific load curve is evaluated. Finally, the conclusions are provided in chapter 6.

Chapter 2

Power Quality in Distribution Network

This chapter discusses some power quality challenges in distribution networks and some approaches to address them.

2.1 Power Quality Challenges

Due to the increasing complexity of distribution systems in terms of operation and structure, power utilities are affected by complex issues. Among them, voltage harmonics, swell, and sag are the most common instability challenges that power utilities are facing [33, 34]. These factors can contribute to the reduction in power quality of power distribution systems [35]. The consequences of power quality issues can cause partial or even full power interruptions in networks. Injecting or absorbing reactive power to/from the network is one of the common approaches for protecting the system against voltage quality issues. In addition, the growing penetration of solar energy generation has added significant technical challenges such as harmonic distortion and voltage rise to power distribution networks. There are a few passive solutions to overcome some of these issues such as lowering the voltage on the secondary side of the transformer by changing its ratio [36] or using larger conductor sizes to decrease the line impedances [37]. However, these methods are not always practical because first, they cannot cover all the problems, and second, they are only

temporary solutions because the networks continuously change. As voltage instability has destructive effects on most electronics equipment, various more effective approaches have been proposed to reduce it.

One of the common approaches is to use capacitor banks to compensate for the reactive power with the aim of power quality improvement. It has been implemented to control and enhance the power factor of connected points by injecting reactive power. Consequently, this improves the network's voltage profile by dipping the flow of reactive power to the distribution line.

Comparing the different types of static synchronous compensator (STATCOM), the voltage source inverter (VSC)-based one has a higher performance, making it more popular. On the other hand, integrated gate-commutated thyristor (IGCT)-, insulated-gate bipolar transistor (IGBT)- and also gate turn-off thyristor (GTO)-based VSCs are more common and being used more in medium-power controllers than in high-power controllers due to some limitations.

However, using inductors or shunt capacitor banks as a conventional method of reactive power compensation has several drawbacks such as large size and weight, resonance, fixed compensation, as well as losses and noise. Finding and implementing an ultimate solution is not easy though because of the high cost of implementing new feeders and uncontrollable compensation of reactive power. Recent approaches to overcome this problem such as the application of STATCOM have demonstrated their success not only for power factor correction but also for other related power quality factors including correction of voltage instability, flicker suppression, and THD control [38, 39]. The main advantages of using STATCOM are the remarkable dynamic features under numerous operating conditions, quick response time, more flexibility in operation and less space requirement.

Distribution STATCOM, known as D-STATCOM, is the recent approach aimed at improving the voltage profile. By using batteries instead of capacitor banks as the energy storage devices, it would be capable of maintaining reactive power at a low voltage range, which can be applied for both frequency and voltage [40]. Its main

application is for protection against oscillations in current and voltage of systems, which may significantly affect sensitive loads [41, 42].

2.2 Harmonics as a Power Quality Problem

The application of nonlinear loads such as adjustable speed drivers, arc furnaces, converters, and rectifiers is growing rapidly in the industrial, commercial, and residential sectors as more power electronic devices are being developed. Consequently, the harmonic levels are increased as well in power distribution networks. The voltage waveforms are being distorted due to the harmonic currents injected into the distribution network by these nonlinear loads. This harmonic distortion leads to a variety of destructive and unwanted impacts on the other loads connected to the PCC. After the detection of harmonics back in the 1920s, harmonic distortion has been calculated based on the ratio of each harmonic amplitude to the fundamental voltage or current of the supply network.

The maximum acceptable THD_v according to IEEE Standard 519-1992 [4] is 5% and is limited to 3% for each individual harmonic voltage in distribution networks of 69kV and below. Table 2.1 and 2.2 present the IEEE Standard 519-1992 for the voltage and current harmonics, respectively.

Table 2.1
Limits of harmonic voltage (IEEE Std. 519-1992) [4]

Bus Voltage *V* at PCC	**Individual Harmonic Distortion (%)**	**Total Harmonic Distortion (THD) (%)**
161 kV ≤ *V*	1.0	1.5*
69 kV ≤ *V* ≤ 161 kV	1.5	2.5
1.0 kV ≤ *V* ≤ 69 kV	3.0	5
***V* ≤ 1.0 kV**	5.0	8.0
* High-voltage systems can have up to 2.0% THD, where the cause is a high-voltage DC terminal, whose effects will have attenuated at points in the network where future users may be connected.		

Table 2.2
Limits of current harmonics in general distribution systems (IEEE Std. 519-1992) [38]

Maximum Harmonic Current Distortion in Percent of I_L						
Individual Harmonic Order (Odd Harmonics)						
I_{sc}/I_L	**h<11**	**11≤h<17**	**17≤h<23**	**23≤h<35**	**35≤h**	**TDD**
>1000	15.0	7.0	6.0	2.5	1.4	20.0
100~1000	12.0	5.5	5.0	2.0	1.0	15.0
50~100	10.0	4.5	4.0	1.5	0.7	12.0
20~50	7.0	3.5	2.5	1.0	0.5	8.0
<20*	4.0	2.0	1.5	0.6	0.3	5.0
I_{SC} = maximum short-circuit current at PCC I_L = maximum demand load current (fundamental frequency component) at PCC TDD = total demand distortion (RSS); harmonic current distortion in % of maximum demand load current						
The limitation of even harmonics is 25% of the odd harmonic limits.						
* The maximum harmonic current distortion of all power generation equipment is limited to these values of current distortion regardless of the actual I_{SC}/I_L.						
Current distortions resulting in a DC offset, e.g. caused by half-wave converters, are not allowed.						

2.2.1 Harmonic Sources

Harmonic sources can be generally categorised in three groups:

1- power electronic equipment including variable speed drives, battery chargers, and most of inverter and rectifier devices;
2- arcing equipment such as arc furnaces and arc welders;
3- saturable equipment including transformers.

2.2.2 Effects of Harmonics

Technically, harmonics have harmful impacts on network components and their operation. Among these are overheating of power transformers, motors, and distribution cables and maloperation of protection equipment, causing harmonic

resonances and low power factor conditions [43]. Consequently, it is crucial to mitigate their impacts on the power network and improve the network efficiency by compensating for the distortions.

2.2.3 Harmonic Mitigation Techniques

Filtering devices are required to eliminate harmonics from the system. In the literature, various filter designs have been presented. Generally, these devices can be categorised as passive and active filters.

2.2.4 Passive Harmonic Filters

The main components of passive filters are capacitors, inductors, and resistors. Their function is to generate resonance at selected harmonic frequencies by tuning the component. They can be either shunt or series connected with the power system. Shunt passive filters are developed to pass those harmonics into the ground through the filter by using a low impedance for selected harmonics. On the other hand, series passive filters are developed to segregate the generated load harmonics from the power source by having a large impedance at selected harmonics [44]. Although passive filters are cheaper than other filters, they are not used widely due to their disadvantages. One of their major limitations is that they cannot be used to eliminate large variations of harmonics components. Moreover, they cannot be used for applications with higher voltages and they have bigger sizes than other filters. Another issue is that they are difficult to be tuned in some cases, for example, when there is interaction between other harmonics injected by other power sources. Another disadvantage of these types of filters is resonance. The cause of resonance condition in passive filters is the interaction between the capacitance component of the filter and the impedance of the power system. In some cases, the harmonic rate of the system can also be increased, resulting in voltage profile problems [45].

2.2.5 Active Filters

Active compensation has been developed and introduced in the 1970s to address the weaknesses of passive filters. There are three configurations for active filters: shunt APF, series dynamic voltage restorer (DVR), and series-shunt unified power quality conditioner (UPQC) [46-56]. Generally, VSCs and current source converters (CSCs) are used as controllers, but VSCs are more popular. In terms of configuration, they can be categorised as single-phase (two-wire) or three-phase (three-wire) devices.

VSCs are popular because they are able to work together with lower switching frequencies and can be employed in multi-step and multi-level converters to increase the power capacity of converters. In addition, energy storage devices can be used instead of DC capacitors in VSCs to exchange active power with the system [57].

APFs act as a harmonic current source injecting harmonic components produced by nonlinear loads but phase shifted by 180°. They compensate for the current harmonics by injecting equal but opposite harmonic compensating current. Fig. 2.1 illustrates the line diagram of a three-phase APF.

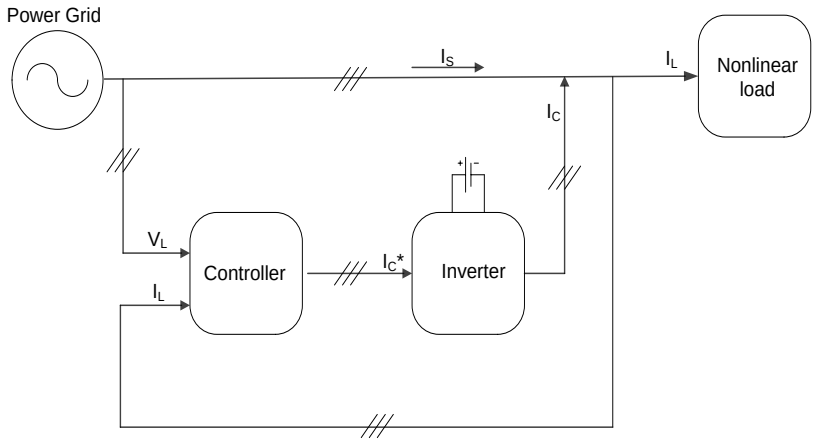

Figure 2.1: Diagram of a three-phase APF [58]

As required by utility providers and standards, customers are the ones responsible for maintaining their injected harmonic currents or THD_i to the network at their PCCs by keeping them below the allowable thresholds. However, utility companies are

responsible for maintaining the THD_V of the network and of each bus within the standard range [4, 43]. Therefore, APFs should be installed at each connection point of nonlinear loads to mitigate their unwanted harmonic currents, which are injected to the network. Similarly, the THD level of related buses reduces to zero by this approach. This is because the exact amount of harmonic currents generated by nonlinear loads is produced and injected to the PCC by the APF, eliminating all harmonic currents at the PCC. The connection of APFs to each nonlinear load of the network is shown in Fig. 2.2.

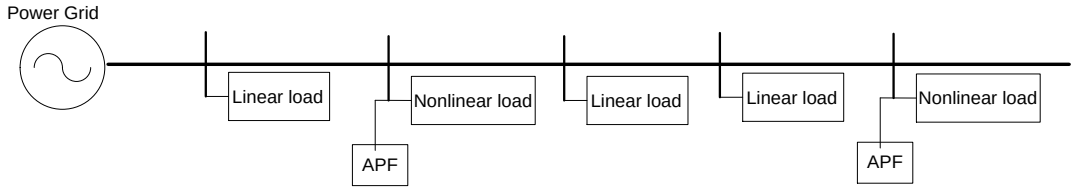

Figure 2.2: Single-line diagram of APFs applied to distribution network

2.2.6 Extraction Techniques of Harmonic Current

Corrections in the frequency domain and time domain are two common and fundamental methods of harmonic current extraction in APF applications [6, 51]. Different types of harmonic extraction techniques are shown in Fig. 2.3. The main advantage of time-domain methods is the fast response in online applications without complicated control techniques. The computational time in this method is relatively shorter than that of the frequency-domain approach because rather than operating on at least one period, it operates on instantaneous values of the distorted waveform. On the other hand, to obtain optimum results, relatively high switching frequencies are required, which consequently results in excessive losses in the semiconductor switches. This is not the case in frequency-domain methods where switching frequencies can be much lower. This is an advantage of using the frequency approach especially for semiconductor switching.

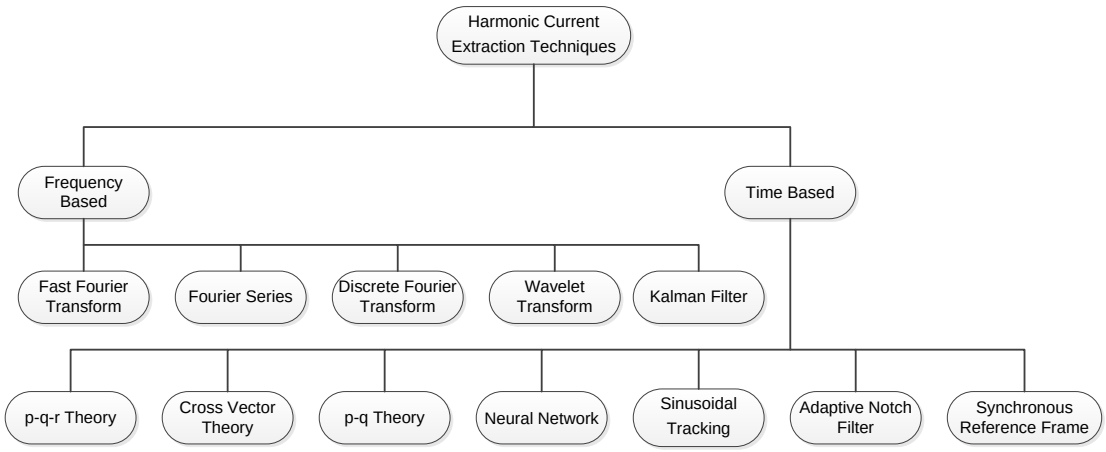

Figure 2.3: Techniques for harmonic extraction [51]

2.2.7 APLCs

Harmonic active filters were first proposed and introduced in the 1970s. Their principal concept is completely eliminating the harmonics of nonlinear loads. However, the entire network is not considered by these devices because compensation of the harmonic injection is only considered for each nonlinear load based on the regulation requiring consumers with nonlinear loads to control their injected harmonics in the network [43]. On the other hand, APLCs are capable of compensating and controlling the harmonics in the entire distribution network to meet network power quality requirements without completely eliminating the harmonic injection [4]. However, optimal siting and sizing of APLCs are necessary to achieve harmonic compensation in the entire network. It can be said that APLCs are enhanced versions of APFs with some dissimilarities [14-18, 20, 59-64]. They compensate for the individual voltage harmonics and THDv of the entire network to maintain it within standard limits while they are only placed at optimal buses as shown in Fig. 2.4. In other words, the reference currents injected by the APLCs do not fully compensate for the distortion of nonlinear loads but are just enough to maintain the harmonic distortions within the limits. However, because of the constraints of online network

data monitoring, the research on APLCs has been very limited and there are fewer research on APLCs than on APFs [14-18, 20, 59-64]. However, this limitation has recently been addressed by introducing smart meters with sophisticated communication networks.

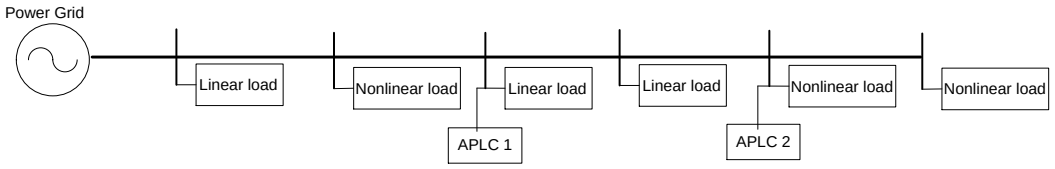

Figure 2.4: Single-line diagram of APLCs connected to distribution network [20]

The current harmonics generated by these APLCs maintain the THD_v of the distribution network within standard values by reducing the harmonic distortion effects of nonlinear loads in the network [20].

Chapter 3

Harmonic Load Flow

3.1 Introduction

This chapter reviews the concepts and formulations of the conventional load flow and the more complicated harmonic load flow studies of the distribution network. Harmonics are considered in load flow calculations due to the widespread existence of nonlinear loads and renewable energy resources in power networks. Harmonic load flow solutions are also required for the optimal siting, sizing and operation of APLCs. This chapter starts with the review of conventional load flow algorithms at the fundamental frequency and then extends the concepts and formulations to include harmonics.

3.2 Conventional Load Flow Formulation for Sinusoidal Operation

Load flow solutions are an indispensable part of any power system's analysis and design. Load flow, also known as power flow, is the formulation and modelling of the electric network at the fundamental power frequency. For given load conditions, load flow studies consist of the calculation of reactive powers and voltage phase angles at the generator buses (PV buses) of the network and voltage magnitudes and voltage phase angles at the load buses (PQ buses). Given the load flow solutions, it is easy to calculate other information such as the real and reactive powers of transmission lines, line power losses and the reactive power of the generation buses. This information is

the backbone of most power system analyses, operations, studies, and optimisations such as optimal operation, management, and control of the network [65-67].

Although the load flow equations of the network can be formulated systematically in various forms, the most common and suitable form for many power system analyses is the node-voltage method. The admittance matrix (Y_{bus}) links the components of the power system and makes the respective calculation much faster. An alternative approach is the mesh-current method, which uses the impedance matrix (Z_{bus}). For example, adding a new load bus will require minor modifications to the admittance matrix by adding a new element, whereas the mesh-current method requires modification of the entire impedance matrix.

The node-voltage method is primarily formulated by generating and computing a set of linear equations in terms of node voltages using load currents. However, only active and reactive load powers are known in power systems, not the load currents. Therefore, an iterative technique is employed to solve the load flow equations, which are nonlinear equations in terms of active and reactive mismatch powers. The Newton–Raphson and Gauss–Seidel are among the methods introduced to solve the load flow problem. Both are briefly discussed here.

The conventional load flow problem can be generally formulated by the following expressions [68]:

$$I_{bus} = Y_{bus} V_{bus} \tag{3.1}$$

where I_{bus} and V_{bus} are the vectors of injection bus currents and bus voltages,respectively, while the bus admittance matrix is Y_{bus}.

For an *n*-bus system, the fundamental bus admittance matrix is defined as

$$Y_{bus} = \begin{bmatrix} Y_{11} & Y_{12} \ldots Y_{1n} \\ Y_{21} & Y_{22} \ldots Y_{2n} \\ . \quad . \quad . \quad . \quad . \\ Y_{n1} & Y_{n2} \ldots Y_{nn} \end{bmatrix} \tag{3.2}$$

where Y_{ii} is the total admittances connected to bus i (i = 1, 2, …, n) and Y_{jk} is the negative of the admittance between buses j and k ($j \neq k$). Note that the admittance matrix Y_{bus} is symmetric because $Y_{kj} = Y_{jk}$.

A single-phase model is fully adequate for representing the load flow of a balanced power system. There are four variables related to every bus of the system [1, 68]: voltage magnitude $\left|\tilde{V}_j\right|$, voltage phase angle δ_j, real power (P), and reactive power (Q). There are three types of buses:

1. Swing bus (also known as slack or reference bus). It is essential to choose this bus to provide the transmission total losses that are unknown until finding the final solution. The initially known parameters are the swing bus voltage amplitude and its phase angle, which are usually set as 1.0 p.u. and 0 rad, respectively.
2. The next bus type is the voltage control (PV) bus. The voltage magnitude V and the real power P are specified for this bus type. The voltage magnitude at the PV bus is fixed by adjusting the excitation of generator field as a voltage regulator. This bus type usually acts as a generation bus at which the generated real power is defined and fixed initially by the generator set points.
3. The last type of bus is the load (PQ) bus which normally refers to a load with specified values of real and reactive powers (P and Q).

The conventional load flow problem is nonlinear because it is formulated in terms of the active and reactive powers; however, the components of the power network in the conventional load flow equations are assumed to be linear [1]. A mathematical solution

of simultaneous nonlinear equations is required to solve the load flow problem of the network. In the following sections, two popular methods for load flow algorithms and their calculation approaches are discussed briefly.

3.2.1 Gauss–Seidel Approach

The Gauss–Seidel approach is an iterative method for solving a set of algebraic equations [1, 69]. After assuming the solution vector, the updated value of a specific variable is obtained by replacing one of the equations in the current value of the rest of variables. Then these variables will be used to update the solution vector. In the next step, the process is applied on all variables to complete one iteration. Finally, the solution vector is converged within a given accuracy by repeating the iteration process. There are some disadvantages of this approach such as the characteristically long solution process due to its slow convergence, and difficulties in handling unusual system conditions such as negative reactive branches. Another drawback is the sensitivity of convergence to the initial values. Moreover, in this approach, each bus is treated independently; therefore, a correction to one bus will require subsequent corrections to all buses connected to it.

To determine the voltage magnitude and angle of each bus, (*n*-1) bus voltage initial parameters (both magnitude and angle) need to be assumed first. Next, the iterative process updates these values in each iteration. The bus *i* current and voltage values are calculated by the following expressions [1, 67-69]:

$$I_i = \frac{\left(P_i - jQ_i\right)}{V_i^*} \tag{3.3}$$

$$V_i = \frac{1}{Y_{ii}}\left[I_i - \sum_{\substack{i=1 \\ i \neq i}}^{n} Y_{ik} V_k \right] \tag{3.4}$$

Substituting (3.3) into (3.4), we obtain the following equation to update the bus *i* voltage:

$$V_i = \frac{1}{Y_{ii}}\left[\frac{(P_i - jQ_i)}{V_i^*} - \sum_{\substack{i=1 \\ i\neq i}}^{n} Y_{ik}V_k\right], \; i = 1, 2, 3, \ldots, n \tag{3.5}$$

where *n* is the bus number except for the slack bus. The most recently updated value of bus *i* voltage should be used for the voltage substituted in the right side of Equation (3.5). Except for the voltage of the swing bus which is fixed, the other voltages are sequentially updated in each iteration. The iteration process continues until the changes in each bus voltage magnitude is less than the prescribed tolerance. This computation approach is called convergence to a solution [1, 67-69].

3.2.2 Newton–Raphson Approach

The Newton–Raphson method is a powerful approach for solving a set of algebraic equations [1, 67-71]. Compared to the Gauss-Seidel, this method is more accurate with better and faster convergence criteria in most cases. Basically, the idea of this approach is calculating the correction terms while considering all of the interactions in the system. In other words, it includes the driving mismatch of active and reactive powers to zero by applying adjustments to the bus voltages.

For each bus *i*, the following equation is valid:

$$P_i + jQ_i = V_i I_i^* \tag{3.6}$$

while

$$I_i = \sum_{k=1}^{n} Y_{ik}V_k \tag{3.7}$$

As a result,

$$P_i + jQ_i = V_i \left[\sum_{k=1}^{n} Y_{ik} V_k \right]^* \tag{3.8}$$

or

$$P_i + jQ_i = |V_i|^2 Y_{ii}^* + \sum_{\substack{k=1 \\ k \neq i}}^{n} Y_{ik}^* V_i V_k^* \tag{3.9}$$

As with the Gauss–Seidel approach, an initial voltage vector is used to start the iteration process. Next, the line powers ($P + jQ$) are calculated and subtracted from the load demands at the respective buses. The resultant error is defined and stored as the mismatch power vector ($\Delta P + j\Delta Q$). The voltages are assumed in polar coordinates and their magnitudes and angles are adjusted as separate independent variables. Two equations in terms of mismatch active and mismatch reactive powers are defined for each bus. It should be noted that every bus injection equation is distinguished with respect to all independent variables.

$$\Delta P_i = \sum_{k=1}^{n} \frac{\partial P_i}{\partial \theta_k} \Delta \theta_k + \sum_{k=1}^{n} \frac{\partial P_i}{\partial |V_k|} \Delta |V_k| \tag{3.10}$$

$$\Delta Q_i = \sum_{k=1}^{n} \frac{\partial Q_i}{\partial \theta_k} \Delta \theta_k + \sum_{k=1}^{n} \frac{\partial Q_i}{\partial |V_k|} \Delta |V_k| \tag{3.11}$$

The mismatch active and reactive power vectors are arranged as a matrix named the Jacobian matrix [1, 67-71]:

$$\begin{bmatrix} \Delta P_1 \\ \Delta Q_1 \\ \Delta P_2 \\ \Delta Q_2 \\ \end{bmatrix} = \underbrace{\begin{bmatrix} \frac{\partial P_1}{\partial \theta_1} & \frac{\partial P_1}{\partial |V_1|} & \cdots \\ \frac{\partial Q_1}{\partial \theta_1} & \frac{\partial Q_1}{\partial |V_1|} & \cdots \\ \cdots & \cdots & \cdots \\ & & \\ & & \end{bmatrix}}_{Jacobian\ matrix} \begin{bmatrix} \Delta \theta_1 \\ \Delta |V_1| \\ \cdots \\ \cdots \\ \end{bmatrix} \tag{3.12}$$

The Newton–Raphson approach is popular in load flow calculations because it has the benefit of Jacobian sparsity. The procedure applies the Gaussian elimination in the solution, which does not calculate explicitly the Jacobian matrix.

3.3 Harmonic Load Flow Solution for Non-Sinusoidal Operation

The network's generators generally supply approximately ideal sinusoidal signals and with typical linear loads, the voltage and current waveforms are nearly sinusoidal as well. The objective of the utility network is to provide a sinusoidal voltage with constant magnitude and frequency to customers.

However, nonlinear loads are common in modern electric power networks. The problem is when the sinusoidal voltage is applied across these loads, they generate a non-sinusoidal or distorted current waveform, which possesses Fourier expansions and is periodic, and inject it to the network [1, 65, 67, 68]. The nonlinearity of these loads causes distorted load currents that propagate through the feeders and result in periodic non-sinusoidal voltage waveforms, which also contain Fourier expansions. The higher frequency components of these expansions are harmonics. Because the effects of the nonlinear loads of the network are additive, the *rms* value of the harmonic voltages might become large [1, 67, 68]. This potentially causes severe impacts on the network and is dangerous. By expressing the harmonic sources in a Fourier expression, the distorted voltage and current waveforms can be examined. The fundamental frequency of a Fourier series should be equal to the power frequency (e.g. 50 Hz or 60 Hz). The

respective harmonic analysis can be used to investigate the source and propagation of these terms across the network [1, 67-71].

Because of the extensive use of nonlinear loads in the industrial sector, harmonic distortions and the growing power quality issues have become main concerns of many utility companies. The line-commutated converter is one of main sources of harmonics and is being widely used for static VAR compensators, high-voltage DC terminal transmission, AC and DC drives, battery chargers, etc. Besides many harmonic generation equipment applied in power networks, a large number of capacitors for power factor correction are also generally applied. Although capacitors are not a source of harmonics themselves, they potentially can affect the response of power systems. In addition, the resonance caused by capacitors can also magnify harmonic distortions in the system.

Harmonic analysis is used to compute the distortion in current and voltage waveforms. It can be used to identify, mitigate, or eliminate the sources of harmonic generations such as harmonic resonances. Therefore, it is an important tool for system design and operation. Resonances at fundamental and harmonic frequencies are due to energy exchange between the inductive and capacitive components and can significantly increase the THD of each bus and the entire network [72]. As a result, it is very essential to take harmonics into consideration for distribution network analysis.

Load flow calculation is one of the main goals of this study. It is frequently applied to evaluate every possible state of the optimisation problem. Choosing a suitable technique for harmonic load flow is important because it affects the precision of the optimisation results.

Because the nature of harmonic signals is primarily dependent on the type of nonlinear load, it is crucial to have an accurate modelling of the loads in harmonic load flow calculations.

In general, there are two distinct categories of power system components for harmonic load flow calculations. The first one is linear loads, which can be modelled by passive components, for example, RLC systems. These loads can be easily modelled by adjusting their impedance according to the respective harmonic

frequency. However, this is not the case for nonlinear loads representing the second group. Some types of direct or iterative approaches need to be used to calculate their unpredictable harmonic transfers. The second group can be modelled with dependent harmonic sources.

Some nonlinear loads such as converters may be modelled as a black box in the solution procedure [73, 74]. This can be virtually extended to other types of nonlinear loads as well.

The classification of harmonic simulation and its related topics are briefly discussed.

3.3.1 Criteria Used for Harmonic Load Flow Classification

There are different classifications for harmonic load flows [18, 72-104]. In the following paragraphs, these classifications and the corresponding solution procedures are briefly discussed.

Modelling of harmonic load flow can be categorised in three different domains. The nonlinear components of the system can be analysed in the frequency (harmonic) domain, time domain, or a hybrid of these two domains. A frequency-scan analysis is used in the frequency domain to calculate the frequency response of the system while the transient-state approach is used in the time domain. Although the latter has good flexibility, it requires a long simulation time for large systems, even when the steady state of the system is calculated by acceleration techniques. On the other hand, the frequency domain leads to less computation cost, but it may be difficult for the models to achieve a good level of accuracy. In this case, a hybrid approach has been implemented to fill the gaps of the other two methods and achieve a good level of accuracy in large systems within a reasonable computation time and cost. This hybrid approach simulates linear elements of the system in the frequency domain while the modelling of nonlinear components is performed in the time domain.

Harmonic load flow can be extended to three-phase networks. However, three-phase load flow is generally applied to unbalanced systems because a single-phase simulation is sufficient for a balanced network.

The different harmonic load flow approaches can be divided in two main categories: coupled and decoupled approaches [102]. All harmonic orders are considered together and solved simultaneously in the coupled approach. By sacrificing computational cost and time, this method provides a good accuracy, but the problem becomes more complicated. On the other hand, the decoupled method solves the problem for each harmonic separately by dividing the system into individual harmonic orders. This will simplify the problem and significantly reduce the computational cost, although at the expense of accuracy. Therefore, this approach is more applicable to real and large systems. Based on the conditions mentioned, the harmonic load flow is briefly described in the following section.

3.3.2 System and Nonlinear Load Modelling Approaches

A. Frequency (Harmonic) Domain

Harmonic domain simulation is the most commonly used and the simplest method for harmonic analysis. Harmonic sources can be assumed as voltage-independent current sources in which the frequency-domain model can be applied [89]. The harmonic domain is a common choice to model many types of power system devices such as linear shunt reactors, transmission lines, and capacitors. These components can be considered as frequency-dependent components. Their terminal behaviour for a specific harmonic order can be represented by a harmonic admittance matrix. Thus, harmonic analysis based on a frequency scan is the best choice to analyse large-scale power networks because of computational efficiency.

B. Time Domain

Time domain is the only choice for an accurate modelling of time-varying components and some other nonlinear loads such as transformers with saturated iron core.

Numerical integration is used to model and solve a power system represented by a set of nonlinear differential equations. This approach also requires a detailed model of all system components.

The transformer with saturated iron core is one of the devices that the time domain approach can analyse. Nonlinear magnetising properties of device is the reason. An overexcited transformer is the worst case because its saturated core generates some uncharacteristic harmonics [85]. However, the frequency approach can be used if the transformer is assumed operating in normal situations with a linear behaviour under the harmonic frequency. As a result, an incremental harmonic domain matrix can be used to model the transformer by harmonic load flow. However, time domain is still more suitable for modelling this transformer because its behaviour is affected by complex phenomena even in the steady state.

The time domain approach is especially suitable for synchronous generators and motors. They are nonlinear loads not because of the saturation effects, but mainly due to the power and torque characteristics that directly affect the generation and consumption of voltages and currents [75]. Switched (time-varying) components are other devices in which the time domain approach is used for simulations.

C. Hybrid Time–Frequency Domain

The frequency domain approach significantly reduces the modelling accuracy of nonlinear and time-varying components. On the other hand, utilising the time domain will increase the complexity of the component model, which results in excessively long computation times. Thus, to achieve the capabilities and advantages of both frequency and time domains, a comprehensive hybrid methodology is proposed. The capability of this approach had been investigated by applying it to a large power network and it was reported to be effective [75, 83].

In this hybrid approach, the time domain is used to individually model the nonlinear elements of the network while the frequency domain is used to model the linear elements by using the most suitable method. In the time domain method, acceleration techniques are usually implemented to find the steady state. The

complicated iteration process consisting of several levels of nested iterations is a challenging part to achieve maximum flexibility, which may be encountered by using the hybrid approach [102]. Some of the main features of this approach are as follows:

1. An accelerating technique is used to obtain a time-domain steady-state solution; it has a good accuracy, making numerical integration unnecessary. Moreover, the piecewise-linear nature of the device provides an advantage.
2. The time domain is used for the modelling of electronic devices such as converters.
3. The frequency domain is used for the modelling of linear devices.
4. Power or voltage specification is considered to determine the operation point of these devices.
5. To determine the operation point of the entire system, power specification is used by the load flow. Fulfilling all the conditions is guaranteed by an iterative process.
6. Harmonic interaction is approached by an iterative method. This interaction is an effect of voltage harmonics on the production of current harmonics by nonlinear devices.

3.3.3 Balance of Three-Phase System

A. Single-Phase Representation

A balanced power network (or assumed so) is mainly represented and modelled by single-phase diagram. Except for the unbalanced condition in the system, the load flow simulation normally implements a single-phase representation and calculation of the power network [102]. However, considering a three-phase representation of the load system potentially increases its complexity. In addition, the single-phase harmonic load flow can also be extended into a three-phase harmonic while considering the network's unbalanced state.

A balanced harmonic load flow system can be decomposed into its nonlinear and linear components. The following algorithm is generally implemented in a harmonic load flow simulation for calculation purposes:

1. Dividing the system components into nonlinear and linear parts.
2. Using the harmonic domain to model the network loads as impedances from the specified powers and calculating their corresponding voltages by the fundamental load flow.
3. Calculating the harmonic currents generated by the nonlinear components.
4. Formulating and solving the system unknowns by an iterative approach.

B. Three-Phase Representation

As mentioned, due to the unbalanced condition of any system, a three-phase harmonic load flow approach might be essential. Practically, power networks can accentuate any unbalanced voltage because the system is not perfectly symmetric. Uncharacteristic harmonic frequencies caused by an asymmetric system is one of reasons that a three-phase approach for harmonic load flow is required.

In addition, the following conditions may cause system unbalance [102]:

1. Asymmetry in the network components can cause structural unbalance, resulting in coupling between sequence admittance matrices. This can lead to complexity in the system computations and increase the memory requirement. An iterative approach has been introduced to avoid solving the coupled system. Current sources are used to model the coupling terms, and sequence voltages of previous iterations are used to calculate their values. To include these terms in a conventional positive sequence load flow, power terms need to be used for modelling.

2. The difference in active and reactive powers of load causes system unbalance. Converting three-phase bus specifications into positive-sequence elements can solve this; thus, the load flow is required to be applied only for the positive sequence, while a nodal analysis is enough for negative and zero sequences.

The group of positive, zero, and negative sequence can be applied to simultaneously solve the three-phase load flow problem by an iterative process and calculate the phase voltages. These voltages can then be used to update current injections of negative and zero sequence of loads and positive sequence of active and reactive powers, and updating compensation currents caused by unbalanced components. Zero- and negative-sequence bus admittance matrices do not need to be updated because they are invariant. The voltage criterion has been used to test the convergence of the method. When each successive voltage change is within the allowable tolerance, the iteration process is stopped.

3.3.4 Solution Approach

As previously mentioned, the available methods for the harmonic load flow problem can be categorised into decoupled and coupled approaches. Consideration of the coupling between harmonics is the main difference between these two approaches. In contrast to the coupled approach, the couplings and interactions among harmonic orders are omitted in the decoupled approach.

All harmonics are simultaneously considered in the coupled approach calculations because a harmonic order is coupled with other harmonic frequencies; therefore, its solutions are acquired by determining other harmonics values. This method includes an exact modelling of the nonlinear load characteristics, which is expressed as a relation between the injected harmonic voltages and their causes, that is, harmonic currents. However, due to unavailability of an exact nonlinear load model, this approach may be difficult to apply into a practical (industrial) system [94].

The decoupled method splits the problem into specific harmonic orders to simplify the solution. Consequently, less computational cost is required for this approach. The decoupled technique only requires the current magnitude and phase angle, which can be simply calculated from measurements, making the approach feasible for extensive application. However, the result of this method is not as precise as that of the coupled approach.

3.4 Harmonic Load Flow Classification

The harmonic load flow algorithms can be categorised into seven classes based on the criteria mentioned in section 3.2. The decoupled approach is employed in this research for harmonic load flow calculations. Simulation results of the decoupled harmonic method are provided in section 3.5.

3.4.1 DHLF

This approach calculates the harmonic load flow while neglecting the harmonic coupling. The following equation provides the model of the connection line between bus *i* and bus *i+1* at the fundamental frequency:

$$y_{i,i+1} = \frac{1}{R_{i,i+1} + jX_{i,i+1}} \tag{3.13}$$

where $R_{i,i+1}$ is the line section resistance between bus *i* and *i*+1, and $X_{i,i+1}$ is the line section inductive reactance between bus *i* and *i*+1. Then, the bus voltage magnitude and its phase angle are computed by solving the following mismatch equations [72, 81, 105]:

$$P_i - \sum_{j=i-1}^{i+1} \left|Y_{ji}^1\right| \left|V_j^1\right| \left|V_i^1\right| \cos(\delta_i^1 - \delta_j^1 - \theta_{ji}^1) = 0 \tag{3.14}$$

$$Q_i - \sum_{j=i-1}^{i+1} \left|Y_{ji}^1\right| \left|V_j^1\right| \left|V_i^1\right| \sin(\delta_i^1 - \delta_j^1 - \theta_{ji}^1) = 0 \tag{3.15}$$

where

$$Y_{ji}^1 = \left|Y_{ji}^1\right| \angle \theta_{ji}^1 = \begin{cases} y_{i-1,i}^1 + y_{i+1,i}^1 & if\ j = i \\ -y_{ji}^1 & if\ j \neq i \end{cases} \tag{3.16}$$

and

V_i^1: Fundamental voltage at bus i

$y_{i+1,i}^1$: Branch admittance between bus i and i+1

P_i: Total active power at bus i; $P_i = P_{li} + P_{ni}$

P_{li}: Linear active loads at bus i

P_{ni}: Nonlinear active loads at bus i

Q_i: Total reactive power at bus i; $Q_i = Q_{li} + Q_{ni}$

Q_{li}: Linear reactive loads at bus i

Q_{ni}: Nonlinear reactive loads at bus i

Superscript 1 represents the fundamental frequency in the above symbol. If there is a capacitor at any bus, then its admittance should be added to (3.16).

The following equation calculates the power loss of the connection line between bus i and $i+1$ at the power frequency:

$$P_{loss(i,i+1)}^1 = R_{i,i+1}\left(\left|V_{i,i+1}^1 - V_i^1\right|\left|y_{i,i+1}^1\right|\right)^2 \tag{3.17}$$

A integration of passive components and current sources are employed to model the harmonic load flow at higher frequencies [72] .A general model of linear loads to form the respective fundamental frequency's active and reactive powers is a resistor in parallel with an inductance [105]. Ideal harmonic current sources are used to represent nonlinear loads that injects harmonic currents into the network [101]. These sources may determine the characteristics of the voltage waveform and additional losses at any harmonic frequency.

The most commonly used approach for modelling distribution networks is the admittance-matrix-based harmonic load flow because the frequency-scan method is its fundamental structure [85]. In this method, the system's admittance matrix of elements is required to be adapted according to the respective harmonic order. At higher frequencies, the skin effect is negligible and can be ignored. Therefore, the resulting shunt capacitor admittances, nth load harmonic frequency admittances, and feeder

admittances are respectively represented by the following expressions [72, 77, 78, 81, 82, 90, 105]:

$$y_{li}^{n} = \frac{P_{li}}{\left|V_i^1\right|^2} - j\frac{Q_{li}}{n\left|V_i^1\right|^2} \tag{3.18}$$

$$y_{ci}^{n} = ny_{ci}^{n} \tag{3.19}$$

$$y_{i,i+1}^{n} = \frac{1}{R_{i,i+1} + jnX_{i,i+1}} \tag{3.20}$$

where Q_{ii} and P_{ii} are the linear reactive and active loads at bus *i*, respectively.

Although the line impedance and shunt capacitors have accurate models at higher frequencies, the characteristics of composite customer loads are sometimes not well known.

Fig. 3.2 shows the equivalent distribution of a radial system given in Fig. 3.1 at the *n*th harmonic frequency.

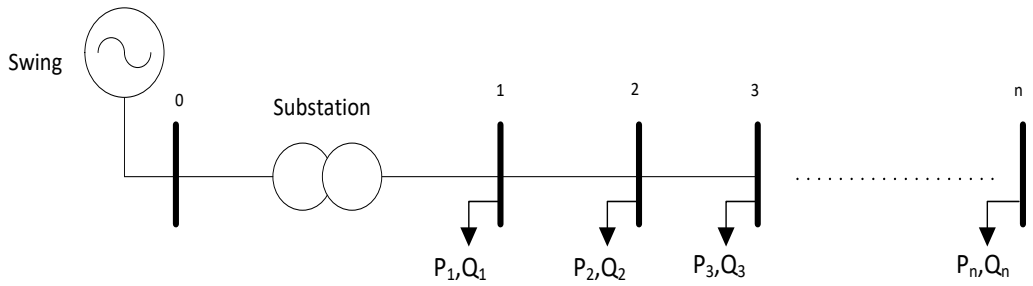

Figure 3.1: Single-line diagram of radial distribution feeder

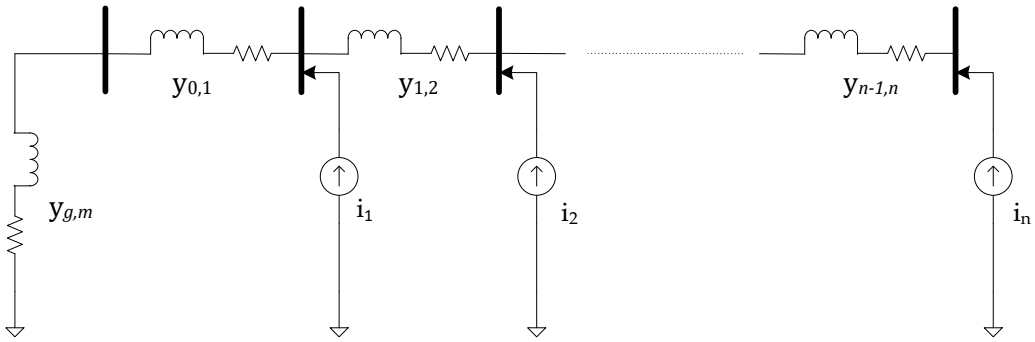

Figure 3.2: Equivalent distribution system circuits at *n*th harmonic frequency without linear portion of load

The nonlinear loads in Fig. 3.2 are represented by current sources for the simulation of the harmonic load flow. Fig. 3.2b shows a more simplified circuit which is sometimes applied in the harmonic analysis where the shunt admittances representing linear loads are ignored.

The load composition has been considered in a straightforward model as given in [72, 81, 90]. In these models, the *n*th harmonic current injected at bus *i* by the harmonic current source, which represents a nonlinear load, is computed as follows:

$$I_i^1 = [(P_{ni} + jQ_{ni})/V_i^1]^* \tag{3.21}$$

$$I_i^n = C(n)I_i^1 \tag{3.22}$$

where I_i^n is the *n*th harmonic order current which makes I_i^1 the fundamental current. *C(n)* is the ratio of the *n*th current harmonic to the fundamental one. Field test and Fourier analysis can be used to obtain *C(n)* for all users along the distribution network [72, 81, 90]. The magnitude of harmonic orders injected by nonlinear loads tends to decrease at a rate that is inversely proportional to the harmonic order. However, the phase angle cannot be validated because it highly depends on the nonlinear load type [81].

Loop equations are proposed to each harmonic frequency for DHLF calculation. It should be noted that the source nodes are included in every loop formation. Once

the admittance matrix and the corresponding harmonic current are modified, the harmonic load flow can be derived by solving the following harmonic load flow equation [72, 82, 85, 90]:

$$Y^n V^n = I^n \tag{3.23}$$

At any bus *i*, the *rms* voltage is defined by the following equation:

$$|V_i| = \left(\sum_{n=1}^{N} |V_i^n|^2 \right)^{1/2} \tag{3.24}$$

where *N* is upper order of the considered harmonics in the calculation. Using the following equation, the THD_v at bus *i* (THD_{vi}) can be obtained after calculating the load flow for different harmonic orders:

$$THD_{vi}(\%) = \left[\frac{\left(\sum_{n\neq 1}^{N} |V_i^n|^2 \right)^{1/2}}{|V_i^1|} \right] \times 100\% \tag{3.25}$$

The following equation expresses the power loss of the line between buses *i* and *i+1* at the *n*th harmonic frequency [81, 90, 105]:

$$P_{loss(i,i+1)}^n = R_{i,i+1} \left(|V_{i,i+1}^n - V_i^n| y_{i,i+1}^n | \right)^2 \tag{3.26}$$

Finally, the system total loss is given by the following expression:

$$P_{loss}^n = \sum_{n=1}^{N} \left(\sum_{i=0}^{m-1} P_{loss(i,i+1)}^n \right) \tag{3.27}$$

where *m* is the bus number. Fig. 3.3 illustrates the flowchart of the DHLF.

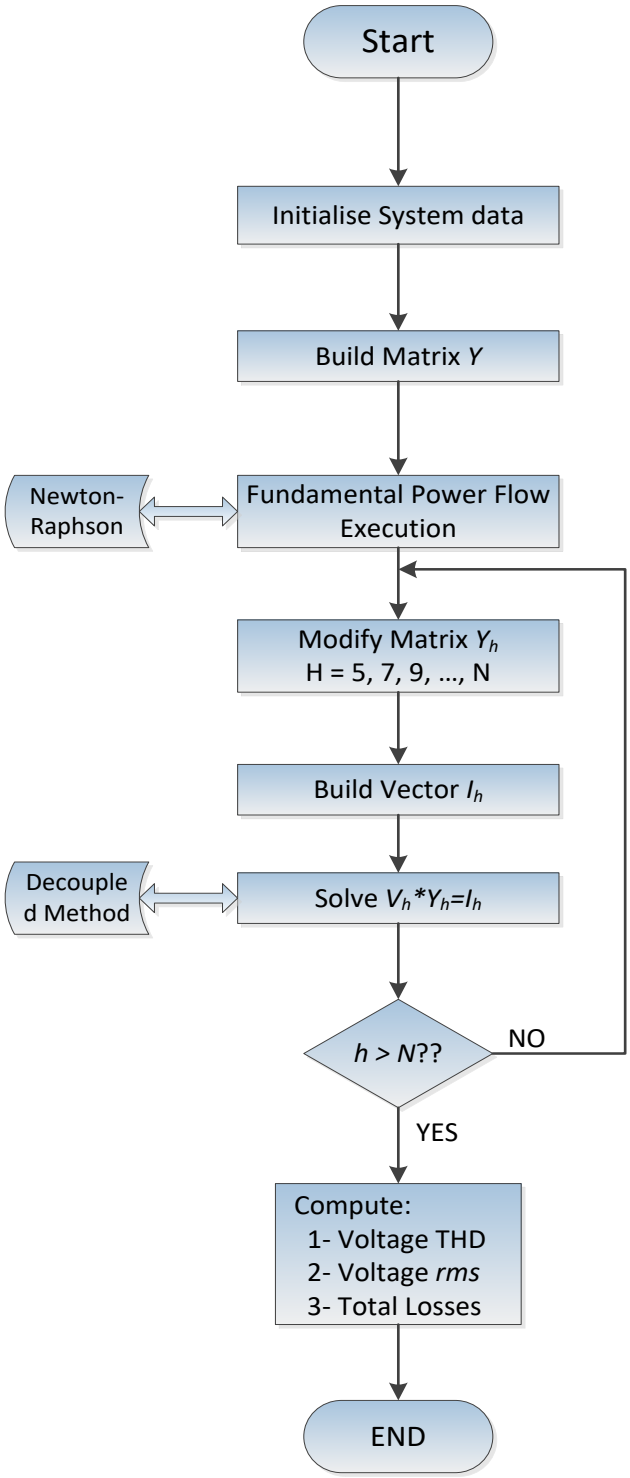

Figure 3.3: Flowchart of DHLF

3.4.2 Fast Harmonic Load Flow [86]

The forward/backward sweep techniques and the equivalent current injection transformation are employed in this method to find the solution to the harmonic load flow problem. The complex power S_i for bus i is:

$$S_i = (P_i + jQ_i),\ i = 1, ..., N \tag{3.28}$$

while at the k-th iteration, the equivalent current injection $\left(I_i^k\right)$ is given by the following equation:

$$I_i^k = I_i^r\left(V_i^k\right) + jI_i^i\left(V_i^k\right) = \left(\frac{P_i + jQ_i}{V_i^k}\right)^* \tag{3.29}$$

where V_i^k is the bus i voltage at the same iteration

At each iteration, the injection current equivalent needs to be transformed for the fundamental load flow. However, the transformation is not required because the harmonic injection currents are already given. Fig 3.4 illustrates the harmonic currents injection in a part of the lateral distribution system.

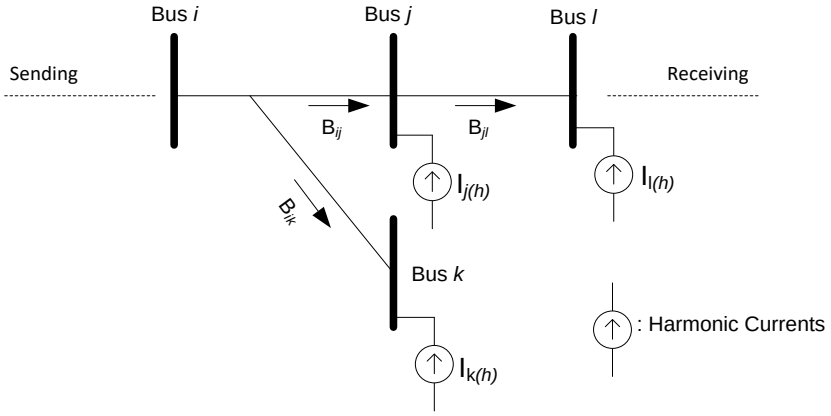

Figure 3.4: Harmonic current injection in a distribution system [86]

The following expressions shows the interactions between the harmonic currents and branch currents:

$$B_{jk}^{(h)} = -I_{k}^{(h)} \tag{3.30}$$

$$B_{jl}^{(h)} = -I_{l}^{(h)} \tag{3.31}$$

$$B_{ij}^{(h)} = B_{jk}^{(h)} + B_{jl}^{(h)} - I_{k}^{(h)} \tag{3.32}$$

where *I* and *B* are the injection current and branch current, respectively. It can be seen that by adding the injection current of the recipient bus toward the transmitting bus, the relation between the harmonic injection currents and branch currents can be obtained. The general expression can be formulated as follows:

$$B_{ij}^{(h)} = -I_{k}^{(h)} + \sum_{j} B_{jl}^{(h)} \tag{3.33}$$

In addition, the relationships between the branch currents and bus voltages are given as

$$\begin{aligned} V_{j}^{(h)} &= V_{i}^{(h)} - B_{ij}^{(h)} * Z_{ij}^{(h)} \\ V_{k}^{(h)} &= V_{j}^{(h)} - B_{jk}^{(h)} * Z_{jk}^{(h)} \\ V_{l}^{(h)} &= V_{j}^{(h)} - B_{jl}^{(h)} * Z_{jl}^{(h)} \end{aligned} \tag{3.34}$$

where $Z^{(h)}$ is the *h*th harmonic equivalent impedance of the line section.

To solve the bus voltages, the branch currents have to be calculated for a radial distribution. The general expression can be formulated as follows:

$$V_{j}^{(h)} = V_{i}^{(h)} - Z_{ij} * B_{ij}^{(h)} \tag{3.35}$$

By computing the sending bus voltage forward to the feeder's receiving one, the bus voltages can be acquired. It should be noted that the power network components are adjusted based on each harmonic order.

3.4.3 Modified Fast Decoupled Load Flow [84]

The conventional fast decoupled load flow is extended and generalised by this method to accommodate harmonic sources. This method enjoys the decoupled and reduced features to explore the harmonic load flow applications. A mathematical nonlinear model needs to be employed and integrated into an existing fast decoupled load flow approach to achieve this objective. By applying this method, the modelling of nonlinear loads can be combined in the main algorithm without substantially sacrificing the computation time.

The bus injection current vector for the *h*th harmonic is given by the following equation:

$$I^{(h)} = Y^{(h)}V^{(h)} \tag{3.36}$$

where $Y^{(h)}$ is the system's admittance at the *h*th harmonic order. The introduced current at any busbar *p* can be formulated as follows:

$$I_p^{(h)} = \sum_{l=1}^{n} Y_{p,l}^{(h)} V_l^{(h)} \tag{3.37}$$

This expression shows how the voltage magnitude and angle change in each harmonic order because of the introduced harmonic currents.

The following equation shows the complete matrix of the Newton–Raphson harmonic load flow:

$$\begin{bmatrix} \Delta W \\ \Delta I \\ \dots \\ \Delta I^{(h)} \end{bmatrix} = \begin{bmatrix} J^{(1)} & J^{(k)} & \dots & J^{(h)} \\ OT^{(k)} & O & \dots & O \\ \dots & & & \\ O & & & T^{(n)} \end{bmatrix} \begin{bmatrix} \Delta X^{(1)} \\ \Delta X^{(k)} \\ \dots \\ \Delta X^{(n)} \end{bmatrix}; \; k = 5, \ldots, \mathrm{h} \tag{3.38}$$

Implementing the decoupling features is challenging in the harmonic load flow study because of the resulting harmonic Jacobian matrix, which is not block diagonalised. This can be addressed by applying a direct diakoptical technique, which is a suitable approach for modified systems without the need for re-inverting the admittance matrix. The approach can be easily and rapidly applied with the fast decoupled load flow. Harmonic sources are treated in this approach in the same way as in the fundamental load flow.

The integrated AC network with a nonlinear load can be defined at nonlinear bus by the following equation:

$$Y\hat{V} = \hat{I} \tag{3.39}$$

where $\hat{V}$ is the voltage of the integrated network, and $\hat{I}$ is the injected harmonic current.

The current $\hat{I}$ can then be defined as follows:

$$\hat{I} = I + I_h \tag{3.40}$$

Thus,

$$\hat{V} = Y^{-1}(I + I_h) \tag{3.41}$$

$$\hat{V} = Y^{-1}I + Y^{-1}I_h \tag{3.42}$$

$$\hat{V} = V + Y^{-1}I_h \tag{3.43}$$

where V is the vector of the fundamental voltage.

In addition, the fast decoupled expressions for the system without nonlinear loads are given by the following equations:

$$B'\Delta\delta = \Delta\delta / V \tag{3.44}$$

$$B''\Delta V = \Delta Q / V \tag{3.45}$$

By including a harmonic generating source:

$$B'\Delta\delta = \Delta P / V - C\,\Delta P_h / V \tag{3.46}$$

$$B''\Delta V = \Delta Q / V - C\,\Delta Q_h / V \tag{3.47}$$

where ΔP_h and ΔQ_h are the injected harmonic real and reactive powers, respectively.

$$\Delta\,\hat{\delta} = B'^{-1}\Delta P / V - B_b^{'-1} C\,\Delta P_h / V \tag{3.48}$$

$$\Delta\,\hat{V} = B_b^{''-1}\Delta Q / V - B_b^{''-1}\,C\,\Delta Q_h / V \tag{3.49}$$

or

$$\Delta\,\hat{\delta} = \Delta\delta - \Delta B_b^{'}\,\Delta P_h / V \tag{3.50}$$

$$\Delta\,\hat{V} = \Delta V - \Delta B_b^{''}\,\Delta Q_h / V \tag{3.51}$$

$$\Delta B = B_b^{-1} C \tag{3.52}$$

$B_b^{'}$ and $B_b^{''}$ are the B matrices for each frequency.

Divergence has been reported when using this approach because of the following divergence causes:

1. determining the converter operation points by the iteration loop;
2. dependency of the current mismatch relationship solution to different factors such as the harmonic injected currents, system admittance at each frequency, and harmonic voltages calculated from the previous iteration;
3. solution might not be achieved in some harmonic orders;

4. nonlinear load integration into the fundamental system.

The occurrence of resonance does not cause any divergence in this approach, unlike in other harmonic load flow methods. However, this approach suffers from other challenges such as estimating the initial condition of the harmonic variables, which is also reported in other approaches.

3.4.4 Modified Newton–Raphson [91, 93]

One of the most popular approaches is the Newton–Raphson, which has been implemented extensively for this calculation. This approach iteratively forces the mismatch equations including the active and reactive powers to zero by adjusting the bus voltages in the solution. By extending the number of simultaneous nonlinear equations, the harmonics can be included in the Newton–Raphson load flow approach to reflect not only the *P* and *Q* mismatch but also the *S* and *I* conservation. While this potentially makes the Jacobian matrix larger, it is very rare. The relation between *V* and *I* for every harmonic order was studied in [92].

It is necessary to review the concept of active and reactive powers before reformulating the Newton–Raphson for harmonic load flow. The following equations express the voltage *v(t)* and current *i(t)* considering their *rms* harmonic components.

$$v(t) = a_0 + \sum_{k=1}^{\infty} a_k \sin(k\varpi_0 t + \phi_k) \tag{3.53}$$

and

$$i(t) = c_0 + \sum_{k=1}^{\infty} c_k \sin(k\varpi_0 t + \theta_k) \tag{3.54}$$

The following equation defines the active power *P*:

$$P = a_0\ c_0 + \sum_{k=1}^{\infty} a_k c_k \cos(\theta_k - \phi_k) \tag{3.55}$$

The following equation expresses the reactive volt ampere Q:

$$Q = \sum_{k=1}^{\infty} a_k c_k \sin(\theta_k - \phi_k) \tag{3.56}$$

Despite the active power P, this reactive volt ampere does not have the conservation characteristic. The apparent volt ampere S is given by

$$S = \sqrt{\left(\sum_{k=0}^{\infty} a_k^2\right)\left(\sum_{l=0}^{\infty} c_l^2\right)} \tag{3.57}$$

Similarly, this quantity does not have the conservation characteristic. For sinusoidal $v(t)$ and $i(t)$

$$S^2 = P^2 + Q^2 \tag{3.58}$$

However, this equation does not comply with the non-sinusoidal case. The distortion volt ampere D as a discrepancy term is given as follows:

$$D = \sqrt{S^2 - P^2 - Q^2} \tag{3.59}$$

Slack bus and conventional load buses, which include PV and PQ buses, and linear loads are treated in the usual way in the extended Newton–Raphson algorithm for harmonic load flow calculation. However, the active power P is known and the apparent power S is specified for the nonlinear buses inclusively. In addition, the type of nonlinearity of loads should be assumed to be known to specify the relationship between the harmonics of the load. All harmonic power balance equations, ΔP, and

ΔQ are zero at all non-slack buses. The ΔP and ΔQ functional form in the conventional case is a function of $|V_{bus}|$ and θ_{bus} while the Y_{bus} must be modified at harmonic frequencies. While only the first-order harmonic power is known at nonlinear loads, the specific values of active and reactive powers are known at linear buses at all harmonic orders.

Although the above expressions are adequate to find the solution of the harmonic load flow problem, two supplementary expressions are essential for nonlinear buses: current and apparent power balances. The current balance at the fundamental frequency is given in Eq. (3.60) for the three-phase full-wave bridge rectifier as the nonlinear load shown in Fig. 3.5. It can be shown that other nonlinear loads with known characteristics can also be analysed in the same way.

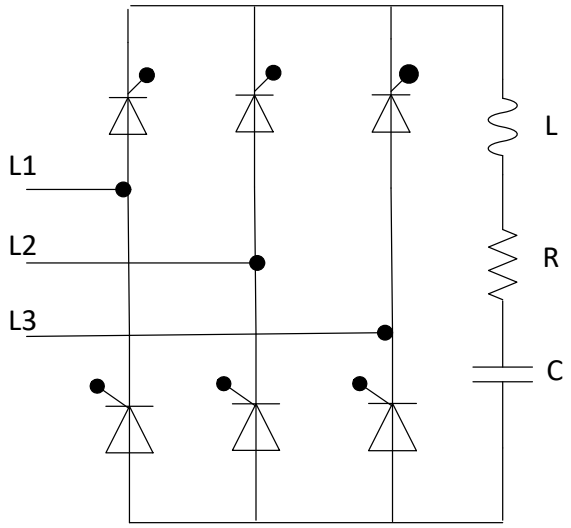

Figure 3.5: Full-wave bridge rectifier with general load

$$\begin{bmatrix} I_{r,m}^{(1)} \\ I_{i,m}^{(1)} \\ I_{r,m+1}^{(1)} \\ I_{i,m+1}^{(1)} \\ \cdots \\ I_{i,n}^{(1)} \end{bmatrix} = \begin{bmatrix} g_{r,m}^{(1)}(v_m^{(1)}, v_m^{(5)}, ..., \alpha_m, \beta_m) \\ g_{i,m}^{(1)}(v_m^{(1)}, v_m^{(5)}, ..., \alpha_m, \beta_m) \\ \\ \cdots \\ \\ g_{i,n}^{(1)}(v_n^{(1)}, v_n^{(5)}, ..., \alpha_n, \beta_n) \end{bmatrix} \tag{3.60}$$

where β_m is commutating resistance or DC voltage, and α_m is triggering angle at bus *m*. $I_{r,m}^{(1)}$ and $I_{i,m}^{(1)}$ are the first harmonic real current and the first harmonic imaginary current injected by nonlinear load at bus *m*, respectively. Buses *m* to *n* are nonlinear.

The above expression can be rewritten for all buses (linear and nonlinear) at all harmonic frequencies.

$$\begin{bmatrix} I_{r,1}^{(h)} \\ I_{i,1}^{(h)} \\ \cdots \\ I_{i,m-1}^{(h)} \\ I_{r,m}^{(h)} \\ I_{i,m}^{(h)} \\ \cdots \\ I_{i,n}^{(h)} \end{bmatrix} = -\begin{bmatrix} 0 \\ \\ \\ \\ \dfrac{}{g_{r,m}^{(h)}(v_m^{(1)}, v_m^{(5)}, ..., \alpha_m, \beta_m)} \\ g_{i,m}^{(h)}(v_m^{(1)}, v_m^{(5)}, ..., \alpha_m, \beta_m) \\ \cdots \\ g_{i,n}^{(h)}(v_n^{(1)}, v_n^{(5)}, ..., \alpha_n, \beta_n) \end{bmatrix} \tag{3.61}$$

The harmonic admittance $Y_{bus}^{(h)}$ is the model of linear bus harmonic responses (bus 1 to *m*–1); additional injection currents at harmonic frequencies are set as zero. The following equation expresses the apparent power balance at each nonlinear bus *j*:

$$S_j^2 = \sum_h (P_j^{(h)})^2 + \sum_h (Q_j^{(h)})^2 + \sum D_j^2 \tag{3.62}$$

$g_{r,m}$, $g_{i,m}$, …, $g_{r,n}$, and $g_{i,n}$ are used to calculate $\sum D_j^2$, which is the total distortion power at nonlinear bus *j*. It means that these power distortions are not treated as independent variables. Then, the injected powers *P* and *Q* of the nonlinear devices get updated by the apparent power balance at the nonlinear buses.

The conventional approach in the reformulated Newton–Raphson harmonic load flow is using the model of the frequency-based component and then updating the Jacobian matrix. Then, the load flow program is executed for each harmonic order. By

imposing the suitable divergences ΔM to zero and using the Jacobian matrix j, the calculation is carried out. The correction term ΔU, as shown in the following expression, should be obtained in the process:

$$\Delta M = J.\Delta U \tag{3.63}$$

For the harmonic load flow approach,

$$\begin{bmatrix} \Delta W \\ \Delta I^{(1)} \\ \Delta I^{(5)} \\ \Delta I^{(7)} \\ \dots \end{bmatrix} = \begin{bmatrix} J^{(1)} & J^{(5)} & J^{(7)} & \dots & 0 \\ YG^{(1,1)} & YG^{(1,5)} & YG^{(1,7)} & \dots & H^{(1)} \\ YG^{(5,1)} & YG^{(5,5)} & YG^{(5,7)} & \dots & H^{(5)} \\ YG^{(7,1)} & YG^{(7,5)} & YG^{(7,7)} & \dots & H^{(7)} \\ \dots & & & & \end{bmatrix} \begin{bmatrix} \Delta V^{(1)} \\ \Delta V^{(5)} \\ \dots \\ \\ \Delta\alpha \end{bmatrix} \tag{3.64}$$

where all elements are sub-matrices or sub-vectors divided from ΔM, J, and ΔU. The following equations illustrate the sub-elements:

$$\Delta V^{(h)} = \left(V_1^{(h)}\Delta\theta_1^{(h)}, \Delta V_1^{(h)}, \dots, \Delta V_n^{(h)}\right)^t \; ; h = 1, 5, 7, \dots \tag{3.65}$$

$$\Delta\alpha = \left(\Delta\alpha_m, \Delta\beta_m, \dots, \Delta\beta_n\right)^t \tag{3.66}$$

$$\Delta W = \left(P_1^{(s)} - f_{1,1}, Q_1^{(s)} - f_{1,2}, \dots, Q_n^{(s)} - f_{n,2}\right)^t \tag{3.67}$$

which is the mismatch of active and reactive powers.

$$\Delta I^{(1)} = \left(I_{r,m}^{(1)} + g_{r,m}^{(1)}, I_{i,m}^{(1)} + g_{i,m}^{(1)}, \dots, I_{i,n}^{(1)} + g_{i,n}^{(1)}\right)^t \tag{3.68}$$

which is the mismatch of the fundamental current.

$$\Delta I^{(h)} = \left(I_{r,1}^{(h)}, I_{i,1}^{(h)}, \dots, I_{i,m-1}^{(h)}, I_{r,m}^{(h)} + g_{r,m}^{(h)}, I_{i,m}^{(h)} + g_{i,m}^{(h)}, \dots, I_{i,n}^{(h)} + g_{i,n}^{(h)}\right)^t, \; h \neq 1 \tag{3.69}$$

which is the mismatch of the harmonic currents

$J^{(1)}$: Fundamental Jacobian

$J^{(h)}$: Harmonic h Jacobian

$$= \left[\begin{array}{c} 0_{2(m-1)},2n \\ \hline \begin{array}{l} \textit{partial derivatives of } P \\ \textit{and } Q \textit{ with respect to } V^{(h)} \\ \textit{and } \theta^{(h)}. \textit{These are formed} \\ \textit{in the conventional way} \end{array} \end{array} \right] \tag{3.70}$$

$0_{2(m-1)},2n$ defines a $2(m-1) \times 2n$ zero matrix and the Y_{bus} used to generate $J^{(h)}$ is $Y_{bus}^{(h)}$. In addition,

$$(YG)^{(h,j)} = \begin{cases} Y^{(h,h)} + G^{(h,h)} & h = j \\ G^{(h,j)} & h \neq j \end{cases} \tag{3.71}$$

where:

$Y^{(h,h)}$: Matrix of the hth harmonic (linear) line current partial derivative with respect to the hth harmonic bus voltage.

$G^{(h,h)}$: Matrix of the hth (nonlinear) harmonic load current partial derivative with respect to the hth harmonic bus voltage.

$G^{(h,j)}$: Matrix of the hth nonlinear harmonic load current partial derivative with respect to the jth harmonic bus voltage, which is given by the following matrix:

$$G^{(h,j)} = \begin{bmatrix} 0_{2(m-1),2(m-1)} & 0_{2(m-1),2(n-m+1)} & & & \\ & \dfrac{\partial g_{r,m}^{(h)}}{V_m^{(j)}\partial\theta_m^{(j)}} & \dfrac{\partial g_{r,m}^{(h)}}{\partial V_m^{(j)}} & 0 & 0 \\ & \dfrac{\partial g_{i,m}^{(h)}}{V_m^{(j)}\partial\theta_m^{(j)}} & \dfrac{\partial g_{i,m}^{(h)}}{\partial V_m^{(j)}} & & \\ 0_{2(n-m+1),2(m-1)} & 0 & ... & 0 & \\ & 0 & 0 & \dfrac{\partial g_{r,m}^{(h)}}{V_m^{(j)}\partial\theta_m^{(j)}} & \dfrac{\partial g_{r,m}^{(h)}}{\partial V_m^{(j)}} \\ & & & \dfrac{\partial g_{i,m}^{(h)}}{V_m^{(j)}\partial\theta_m^{(j)}} & \dfrac{\partial g_{i,m}^{(h)}}{\partial V_m^{(j)}} \end{bmatrix} \tag{3.72}$$

For harmonic loads, these partial derivatives can be acquired by differentiating the sinusoidal steady state of Eq. 3.73. For the fundamental frequency, only the last 2(*n*-*m*+1) rows exist because the linear buses do not include the fundamental current balance. In addition, $H^{(h)}$ is the partial derivative of real and imaginary currents of non-sinusoidal loads with respect to commutation resistance β and triggering angle α.

$$H^{(h)} = diag\begin{bmatrix} \dfrac{\partial g_{r,t}^{(h)}}{\partial\alpha_t} & \dfrac{\partial g_{r,t}^{(h)}}{\partial\beta_t} \\ \dfrac{\partial g_{i,t}^{(h)}}{\partial\alpha_t} & \dfrac{\partial g_{i,t}^{(h)}}{\partial\beta_t} \end{bmatrix} \begin{matrix} t = m,...,n \\ h = 1,5,7,... \end{matrix} \tag{3.73}$$

This completes the harmonic load flow algorithm.

3.4.5 Comparison of Harmonic Load Flow Algorithms

A comparison of the characteristics of harmonic load flow algorithms has been summarised in [32]. Based on their argument and discussions, DHLF offers practically accurate results. In addition, it is verified that DHLF is reasonably adequate for

harmonic load flow calculation. This approach provides a compromise between the result accuracy and calculation complexity. It is further verified that the precision of the results is significantly affected by the accuracy of the nonlinear load modelling. These verifications are necessary to ensure that the optimisation employing DHLF will generate precise results. The harmonic load flow is the backbone of the optimal problem that takes harmonics into consideration. In the problem, the harmonic load flow calculations will be repeatedly performed to assess every possible solution. Therefore, it is not surprising if the precision of the optimisation results is significantly affected by the accuracy of the harmonic power calculation.

3.5 Simulation Results of DHPF

This part discusses the output of the coded DHLF approach by implementing it on a distorted IEEE 18-bus network [15]. The simulation result includes the THDv, fundamental voltage, and *rms* harmonic voltage.

The coded program is executed in MATLAB R14 version 7 using a PC with an Intel Core i7 3.4 GHz processor and 8 GB RAM. The following simplified work flow indicates the coded DHLF:

Start
Read system and nonlinear load data;
For fundamental frequency (h = 1)
    Build fundamental admittance matrix;
    Run fundamental load flow;
    Save the fundamental voltages and calculate the fundamental losses;
For harmonic frequencies (h = 5, 7, 11, …, N) ; N : maximum harmonic order considered
    Adjust the harmonic admittance matrix;
    Define the harmonic injection current vector;
    Calculate the harmonic voltage;
    Save the harmonic voltage and calculate the harmonic losses;
Calculate
    The *rms* harmonic voltage for every bus;
    The THD_v for every bus;
    Calculate the total real and reactive losses for the entire system;
Display the results
End

3.5.1 IEEE 18-Bus Network

The system involves three nonlinear loads placed at buses 5, 9, and 23. This network is similar to the systems used in [77-79]. These loads are involved in the simulation using the fundamental real and reactive powers while they are considered as harmonic sources in the harmonic frequencies that inject harmonic currents into the network. The DHLF is employed to obtain the *rms* voltage and THD_v. The maximum harmonic order considered is the 11th. Fig. 3.6 illustrates the system.

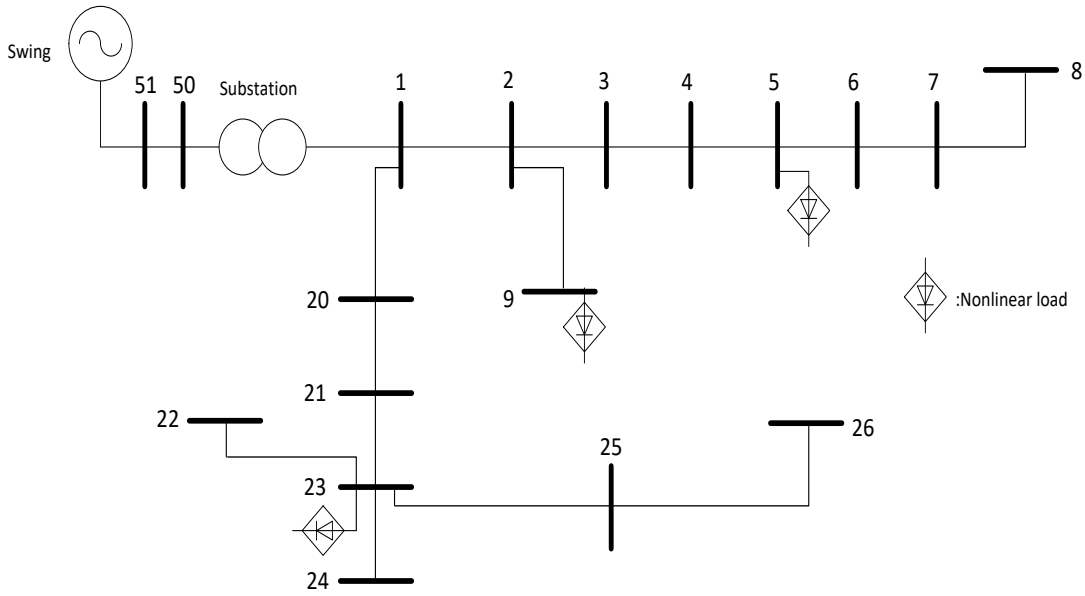

Figure 3.6: Distorted IEEE 18-bus system without APLCs [15]

The system consists of several linear loads and three nonlinear loads placed at buses 5, 9, and 23. For this preliminary simulation, only the 5th and 7th harmonics are considered. The detailed specifications of the distribution network are given in Table 3.1 and Table 3.2. The network's line parameters of connected buses are given in Table 3.3. The waveform of the selected nonlinear loads is illustrated in Fig. 3.7.

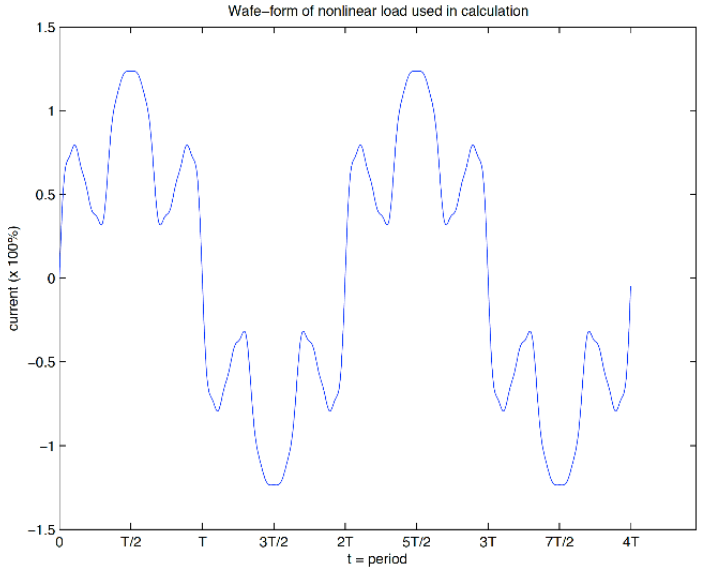

Figure 3.7: Waveform of nonlinear load

Table 3.1
Parameters of balanced IEEE 18-bus distribution network

Item	**Qty.**	**Item**	***P*** **(MW)**	***Q*** **(MVAr)**
Bus	18	Total Generation Capacity	30	-5.0 to +10.0
Generator	1	Online Capacity	30	-5.0 to +10.0
Committed Generator	1	Generation	17.981	5.6225
Linear Load	14	Linear Load	8.6	5.33
Nonlinear Load	3	Nonlinear Load	9	6.78
Branch	18	Total Harmonic Losses	0.698	3.649

Table 3.2
Linear loads of IEEE 18-bus distribution network

Bus No.	Real Power (MW)	Reactive Power (MVAr)
1	0	0
2	0.2	0.12
3	0.4	0.25
4	1.5	0.93
5	0	0
6	0.8	0.5
7	0.2	0.12
8	1	0.62
9	0.5	0.31
20	1	0.62
21	0.3	0.19
22	0.2	0.12
23	0.8	0.5
24	0.5	0.31
25	1	0.62
26	0.2	0.12
50	0	0
51	0	0

Table 3.3
Line parameters of IEEE 18-bus distribution network

From Bus	To Bus	Resistance (p.u.)	Reactance (p.u.)	Total Line Charging Susceptance (p.u.)
1	2	0.00431	0.01204	0.000035
2	3	0.00601	0.01677	0.000049
3	4	0.00316	0.00882	0.000026
4	5	0.00896	0.02502	0.000073

5	6	0.00295	0.00824	0.000024
6	7	0.0172	0.0212	0.000046
7	8	0.0407	0.03053	0.000051
2	9	0.01706	0.02209	0.000043
1	20	0.0291	0.03768	0.000074
20	21	0.02222	0.02877	0.000056
21	22	0.04803	0.06218	0.000122
21	23	0.03985	0.0516	0.000101
23	24	0.0291	0.03768	0.000074
23	25	0.03727	0.04593	0.0001
25	26	0.02208	0.0272	0.000059
25	26	0.02208	0.0272	0.000059
50	1	0.00312	0.06753	0
50	51	0.0005	0.00344	0

The simulation results of the system calculated by the DHLF are presented in Table 3.4. The system has high distortion due to the nonlinear loads, which caused 0.69 MW and 3.65 MVAr of total harmonic real and reactive losses, respectively. The THD values of all buses exceed the 5% limit, which is not acceptable in terms of power quality. The maximum THD of the network is approximately 15% at bus 24.

Table 3.4
Bus voltage summary of system containing nonlinear loads

Bus No.	**Fundamental Value**	**R.M.S Value**	**THD_v**
1	1.0044	1.0096	10.164648
2	0.9961	1.0008	9.772536
3	0.9896	0.9946	10.016083
4	0.9861	0.9911	10.019377
5	0.9785	0.9831	9.686219

6	0.9774	0.9821	9.803033
7	0.975	0.98	10.106627
8	0.969	0.974	10.103638
9	0.9842	0.9876	8.296791
20	0.9788	0.9858	11.96461
21	0.9619	0.9699	12.981798
22	0.9602	0.9682	12.98176
23	0.9296	0.9374	12.967322
24	0.9323	0.9427	14.995782
25	0.9256	0.9351	14.360754
26	0.9252	0.9347	14.36055

Chapter 4

Optimal Sizing and Allocation of Multiple APLCs for Harmonic Mitigation and Reactive Power Compensation

4.1 Introduction

Generally, harmonic distortions are compensated by APFs while reactive power compensation is handled by STATCOM. Although these shunt devices are employed in distribution networks for reactive power and harmonic compensation, this approach needs one device for each nonlinear load. Therefore, some other custom power devices such as APLCs are proposed to maintain the harmonics of the entire distribution system and meet the specified requirement of the network by IEEE Standard 519-1992 [4].

Although there are many studies based on compensation of either the voltage harmonic distortion in the network or the reactive power, simultaneously compensating both is only examined in few studies [106-111]. A custom APF was proposed in [106] to compensate for the harmonics and reactive power of single-phase linear and nonlinear loads. By a combination of parallel and series active filters, a universal active filter configuration was proposed in [107] for transformerless single-phase network applications. Some of STATCOM applications capable of eliminating network harmonics were discussed in [108-111]. A custom power device called UPQC was proposed and investigated in other studies [112-115] to maintain the bus voltage

and also compensate the line current distortion. The proposed UPQC consists of series and shunt converters.

Compensating the harmonic and voltage distortions of only one load at the PCC is considered in all the studies mentioned. Compensating for the entire network is just considered and discussed in [115] by placing the UPQC in the radial distribution network; however, only the reactive power compensation is studied. The objective function proposed for siting the UPQCs contains the rating of UPQC, percentage of nodes with under-voltage problems, and network power losses.

Application of a shunt APLC is proposed in this chapter to compensate both the harmonic distortion and reactive power of the entire radial distribution network. Two PSO-based algorithms are proposed to first optimally locate (place) and size (rating) and then optimally control (operate) multiple APLCs in a distorted distribution network. It should be noted that the network relies on a smart meter to measure and transmit data to the control centre. The objective function is to minimise the total APLC injected current and the overall network THD_v while the maximum allowable network THD_v, individual bus voltage harmonics, and fundamental voltage (V_{Fund}) of each bus are the constraints for an optional limit of the maximum APLC size. The 18-bus and 123-bus IEEE networks are used for detailed simulations to present and analyse a distorted system with few nonlinear loads. In addition, the importance of the weighting factors of the objective function is investigated by analysing their impacts on the APLC size and THD_v of the system.

4.2 Optimal Sizing and Allocation of Multiple APLCs for Harmonic Mitigation

Decoupled harmonic current sources are used to model the APLCs as they inject harmonic currents at the PCCs. A PSO-based algorithm is proposed for the optimal sizing and siting of multiple APLCs. The rating (size) of APLC placed on bus *m* can be given as:

$$I_{m,\ APLC-size} = I_{m,APLC-Fund} + I_{m,APLC-Harmonicc} \tag{4.1}$$
$$= I^1_{m,\ APLC} + \sqrt{\sum_{h=2}^{H} \left|I^h_{m,\ APLC}\right|^2}, \qquad m = 1, \dots, M, h = 2, \dots, H$$

where *h* and *m* represent the harmonic order and bus number, respectively, while *H* and *M* are their maximum values.

Minimising the APLC sizes and the overall network THD_v is the objective function for optimally sizing and allocating multiple APLCs:

$$\min F = W_{THD} * THD_{v-system} + W_{size} * I_{APLC\ size} \tag{4.2}$$
$$= W_{THD} * \sum_{m=1}^{M} \left(\sqrt{\sum_{h=2}^{H} \left|V^h_m\right|^2} \Big/ |V^1_m| \right) + W_{size} * \sum_{m=1}^{M} I_{m,\ APLC\ size}$$

where W_{size} and W_{THD} represent respectively the weighting factors for network APLC size and THD_v, while V^1_m and V^h_m are the bus *m* fundamental and harmonic voltages, respectively. The PSO runs the DHLF at each iteration to calculate the network parameters of the objective function. The upper limits for the THD_v and individual voltage harmonics of each bus, and the lower limit for V_{Fund} according to the IEEE-519 standard [1, 4] are the selected constraints associated with Eq. (4.2):

$$V_{Fund-m} \geq 0.9\ p.u. \tag{4.3}$$

$$THD_{m,k} = \left(\sqrt{\sum_{h=2}^{H} \left|V^h_m\right|^2} \Big/ |V^1_m| \right) \leq THD^{limit}_{v-bus} = 5\% \tag{4.4}$$

$$\left(\frac{|V^h_m|}{|V^1_m|}\right) \leq |V|^{limit}_{bus} = 0.03 \tag{4.5}$$

where $V_{Fund\text{-}m}$ is the fundamental voltage of bus *m*.

Fig. 4.1a shows the flowchart of the proposed PSO-based algorithm, which is employed to find the solutions to Eqs. (4.2)-(4.5). In simple terms, an APLC system is temporarily placed at each of the buses except for the swing bus and then an optimisation solution for the equations is executed by the PSO. At the final stage, only APLCs with ratings greater than zero or the desired lower limit (if applicable) are selected to be placed in the network.

4.3 Optimal Online Operation of APLCs for Harmonic Mitigation and Reactive Power Compensation

Fig. 4.1b shows the flowchart of the proposed PSO-based algorithm employed for online control of the APLCs that have been optimally sized and sited as discussed in the previous section (Fig. 4.1a). The problem formulation is similar to that in Fig. 4.1a with the following differences:

- APLCs are already fixed and placed at the optimal locations specified by the first proposed PSO algorithm (Fig. 4.1a).
- Network parameters are updated at time steps Δt for a period of 24 h. The second PSO is executed for every time step Δt to find the optimised solution of the following objective function:

$$\min F = W_{THD} \times THD_{v-system}(t) + W_{size} \times I_{APLC\ size}(t) + W_{loss} \times F_{loss}(t)$$

$$= W_{THD} \times \sum_{m=1}^{M} \left(\sqrt{\sum_{h=2}^{H} \left| V_m^h(t) \right|^2} \Big/ |V_m^1(t)| \right)$$

$$+ W_{size}$$

$$\times \sum_{m=1}^{M} I_{m,\ APLC\ size}(t)$$

$$+ W_{loss}$$

$$\times \sum_{h=1}^{H} \left| \sum_{m_1=1}^{M} \sum_{m_2=1}^{M} \frac{R_{m_1,m_2}^h}{(Z_{m_1,m_2}^h)^2} \left| Vbus_{m_1}^h(t) \right. \right.$$

$$\left. \left. - Vbus_{m_2}^h(t) \right|^2 \right|; m_1, m_2 = 1, 2, \ldots, M; m_2 > m_1; for\ t$$

$$= \Delta t, 2\Delta t, 3\Delta t \tag{4.6}$$

where Z_{m_1,m_2}^h and R_{m_1,m_2}^h are respectively the line impedance and the resistance for harmonic order *h* between buses m_1 and m_2.

- The maximum size of the installed APLCs based on their ratings is an additional constraint:

$$I_{k,APLC\ size} = \sqrt{\sum_{h=1}^{H} \left| I_k^h \right|^2} \leq I_{k,max} \tag{4.7}$$

where $I_{k,,max}$ and *k* are the ratings and optimal locations of APLCs, respectively, as specified by the first PSO algorithm.

In summary, the flowchart of the second PSO algorithm shown in Fig. 4.1b contains the following main steps:

1) The APLCs are placed at the selected optimal buses determined by first PSO algorithm (Fig 4.1a). The optimal location, rating, and quantity of APLCs are known at this stage.

2) On an online basis with time steps of Δt, the smart meters of the network send the measured power quality parameters to the network's central control through the communication network. Then, the second PSO algorithm (Fig. 4.1b) is executed to find the optimal APLC reference currents. These reference currents are sent to the APLCs to update their operation values.

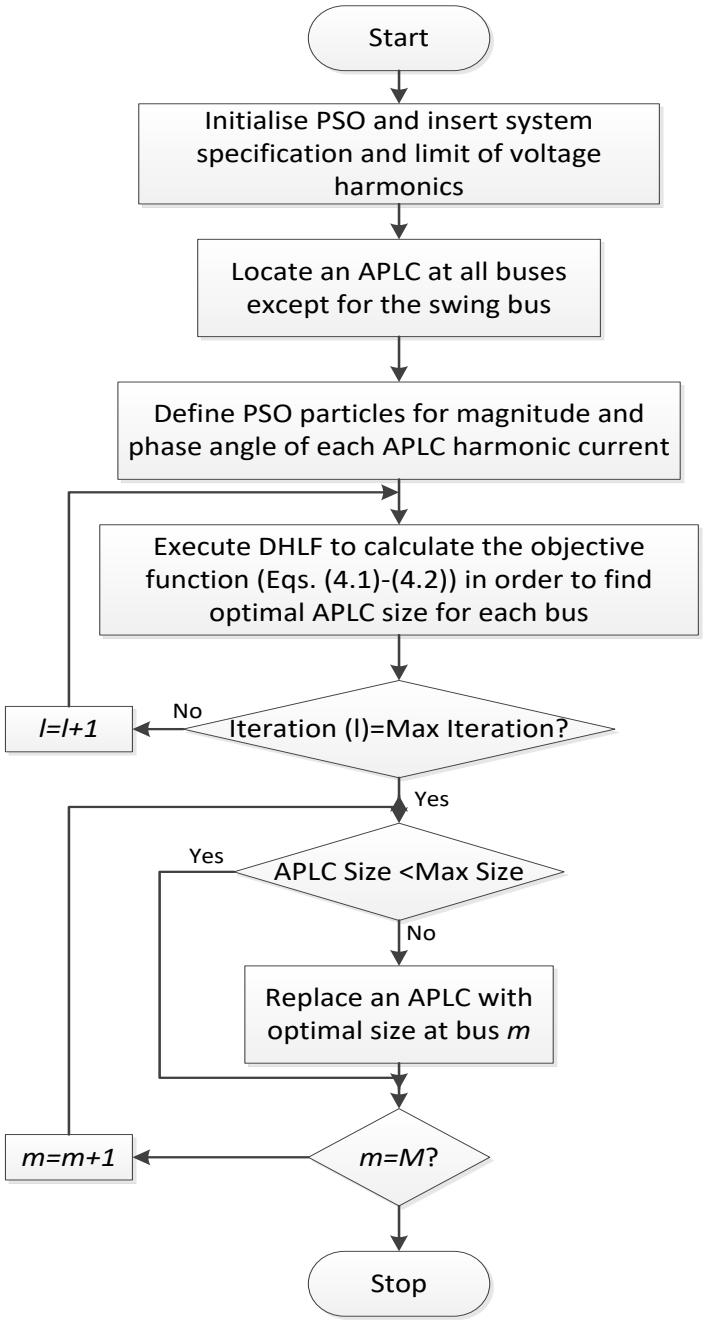

(a)

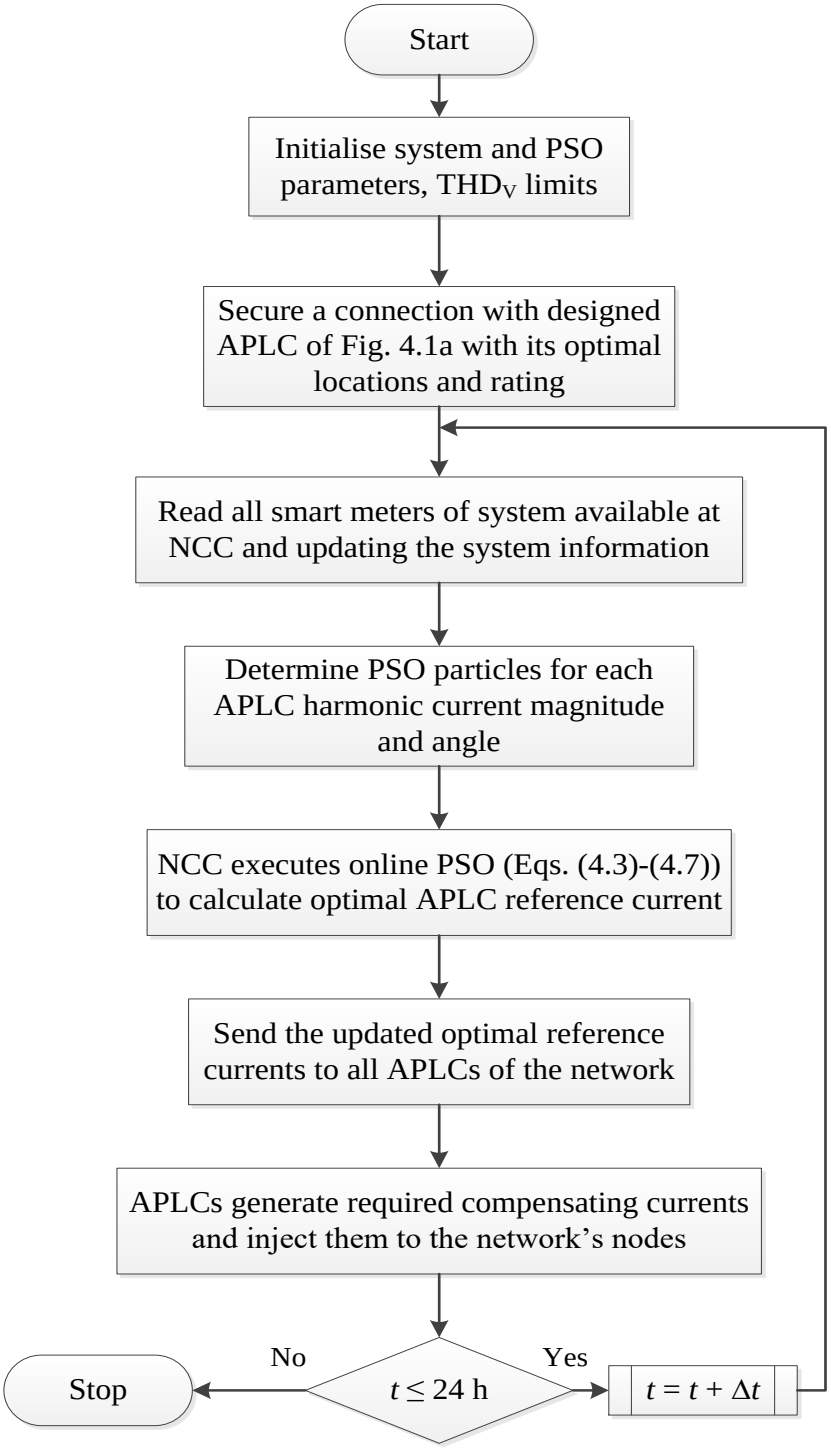

(b)

Figure 4.1: Flowchart of proposed PSO algorithm using DHLF approach: (a) design and (b) operation

4.4 Simulation Results of Balanced 18-bus IEEE System

The same 18-bus IEEE network of Fig. 3.6 is considered to evaluate the performance of the proposed approaches for optimal sizing and siting of multiple APLCs on distorted networks. The load and network line connection parameters are given in Tables 3.1–3.3. Three nonlinear loads are placed at buses 5, 9, and 23 of the system. The nonlinear loads are modelled as decoupled harmonic current sources. Their injected current harmonics are presented in Table 4.1 as a percentage of the fundamental component. The decoupled injected current harmonics of each nonlinear load are fixed and independent of the network operating conditions because these injected currents only depend on the type of load with rated voltage excitation. The optimal siting and sizing simulations are performed for the worst-case scenario with maximum linear and nonlinear loading conditions.

Tables 4.2–4.3 present the results of two simulated study cases. These cases are 1) Case 4-I: optimal siting/sizing of APLCs with equal weighting factors of objective function (W_{THD} = 0.5 and W_{APLC} = 0.5) and 2) Case 4-II: optimal siting/sizing of APLCs considering unequal objective function weighting factors (W_{THD} = 0.05 and W_{APLC} = 0.95).

Table 4.1
Injected current harmonics of nonlinear loads in Fig 3.6 used in Case 4-I and Case 4-II (as a percentage of the fundamental component)

Harmonic order	Magnitude (%)	Angle (deg)
1	100	0
5	20	0
7	14.3	0
11	9.1	0
13	0	0
17	0	0

By implementing the PSO on the simulated distribution system, the PSO has chosen buses number 2 and 25 as the sites of APLCs. This simulation is performed with PSO

initial values of 100 iterations and a population of 5000. The objective function versus iteration is also illustrated in Fig. 4.2. From Table 4.2, it is evident that the APLCs improve the performance of the network by decreasing the THD_v values and maintaining them within the standard limit (5%). Fig. 4.3 shows the system with APLCs.

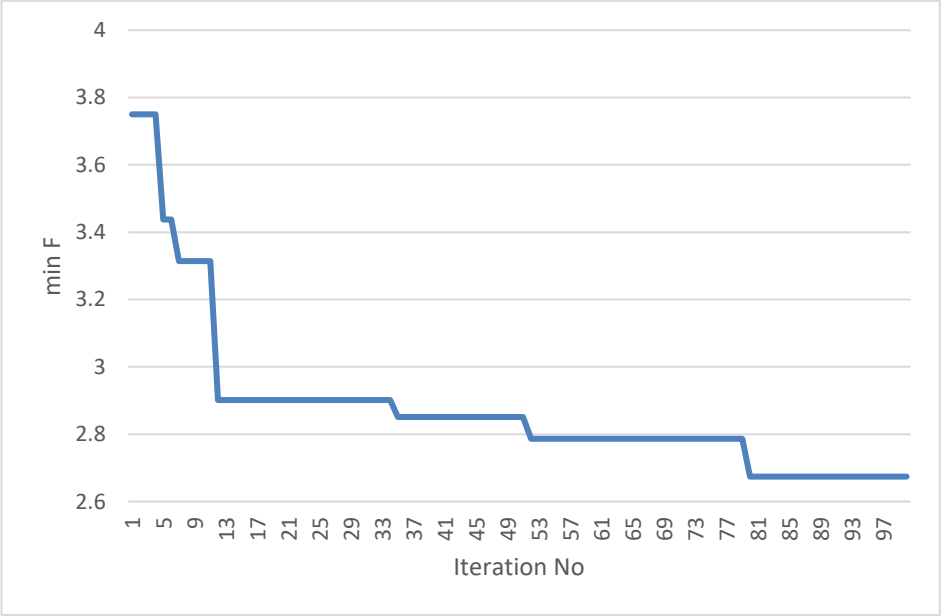

Figure 4.2: Convergence curve of objective function (Case 4-I)

The second case is used to investigate the effect of the weighting factors on the sizing of APLCs. As indicated in Table 4.3, the THD_v limit for the network is still satisfied while the total size of APLC has been reduced by 14%, which is a significant reduction from the required APLC system to fulfil the THD_v requirement. However, THD_v of some buses are close to the 5% margin in Case 4-II as they are highlighted in Table 4.3. Both cases are compared in Fig. 4.4 with the system without an APLC. It is shown that both could successfully maintain the system's THD within 5%.

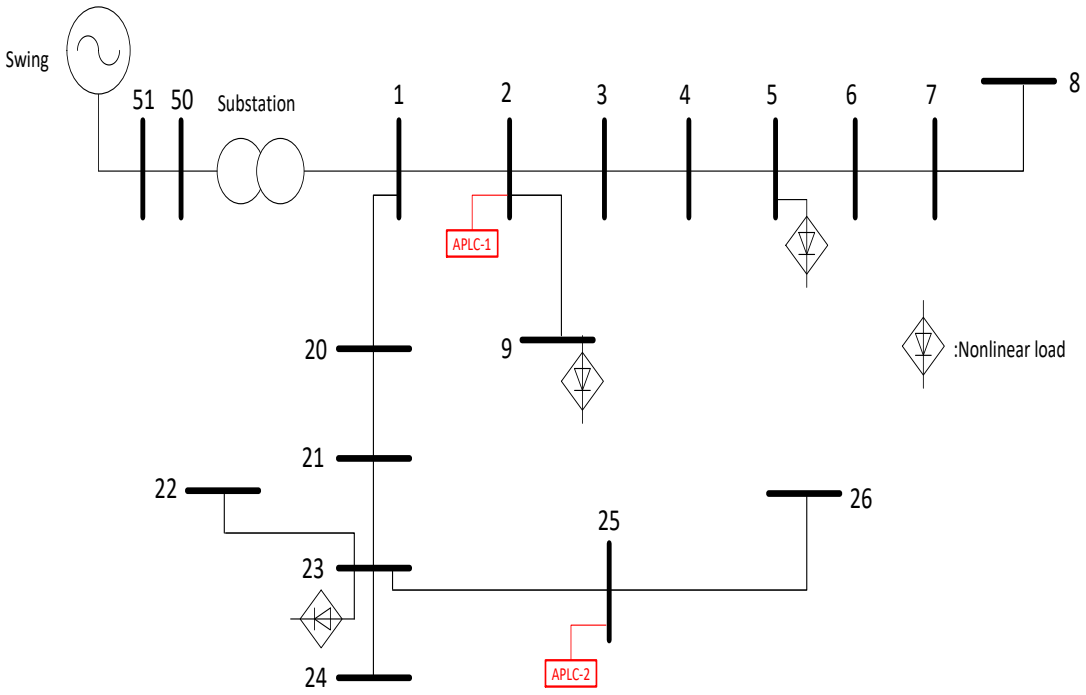

Figure 4.3: Distorted IEEE 18-bus system with APLCs

Table 4.2
System parameters with optimal sizing and allocating of multiple APLCs with equal weighting factors (Case 4-I)

Bus No.	**Fundamental Value**	**R.M.S Value**	**THD_v**
1	1.004	1.004	2.793
2	0.996	0.996	3.241
3	0.989	0.989	1.850
4	0.986	0.986	1.120
5	0.978	0.978	1.333
6	0.977	0.977	1.349
7	0.975	0.975	1.39
8	0.969	0.969	1.390
9	0.984	0.984	1.465
20	0.978	0.978	1.497
21	0.961	0.961	0.521
22	0.960	0.960	0.521
23	0.929	0.929	1.84

24	0.932	0.932	2.127
25	0.925	0.925	1.109
26	0.925	0.925	1.109

Table 4.3
System parameters with optimal sizing and allocating of multiple APLCs with unequal weighting factors (Case-4-II)

Bus No.	**Fundamental Value**	**R.M.S Value**	**THD_v**
1	1.004	1.005	4.367
2	0.996	0.997	4.605
3	0.989	0.990	3.54
4	0.986	0.986	2.93
5	0.978	0.978	1.12
6	0.977	0.977	1.133
7	0.975	0.975	1.168
8	0.969	0.969	1.168
9	0.984	0.984	2.872
20	0.978	0.979	3.844
21	0.961	0.962	3.278
22	0.96	0.960	3.278
23	0.929	0.929	1.848
24	0.932	0.932	2.137
25	0.925	0.926	3.887
26	0.925	0.925	3.887

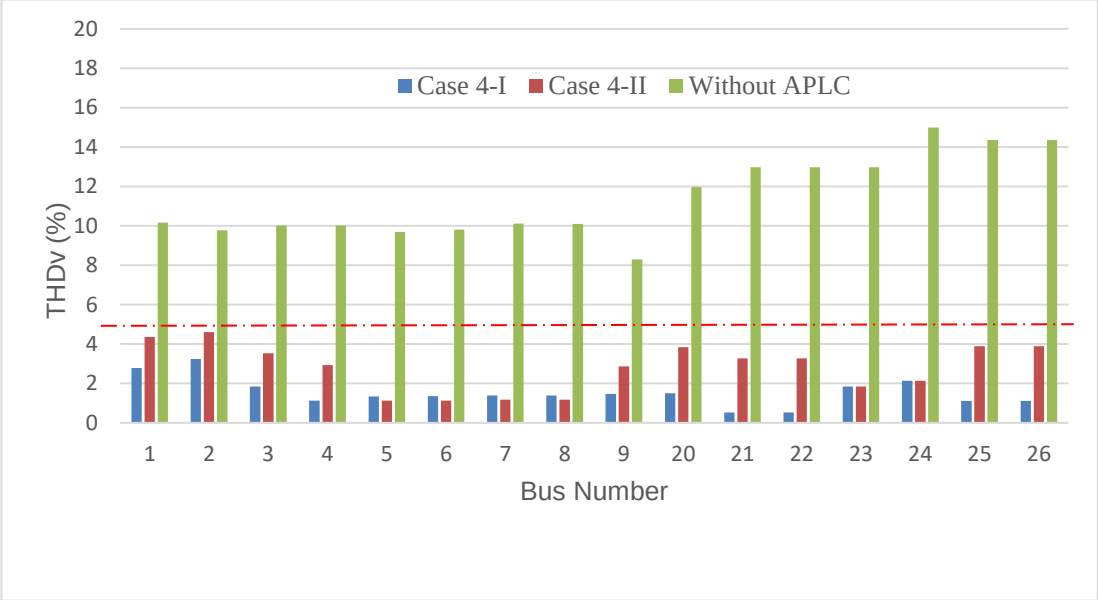

Figure 4.4: Comparison of THD_v for all buses of Case 4-I, Case 4-II, and network without APLC

According to the results of Case 4-I and Case 4-II, it is better to select a larger weighting factor for $W_{APLC\ size}$ from practical and technical points of view. As shown, this will result in lower costs because of less maintenance and investment costs by using smaller and fewer APLC units, while the voltage quality remains within the acceptable threshold.

4.5 Case 4-III: Simulation Results of Balanced 123-Bus IEEE System

One of the main advantages of using DHLF as the backbone of the system parameter calculations is its faster computing time compared to other methods, which makes it practical to implement for larger systems. To assess the performance of the proposed approach on larger and more complicated distribution networks, an IEEE 123-bus network [116] has been chosen. For this simulation, multiple types of nonlinear loads have be added to the system. Table 4.4 presents the injected current harmonics of the nonlinear loads placed at buses 13, 15, 21, 25, 40, 54, 64, 74, 78, 100, 106, and 610.

Their respective current waveforms are presented in Fig. 4.5. The loads and network connection line parameters are presented in Tables 4.5–4.8 and the single-line diagram of the network is shown in Fig. 4.6.

Table 4.4
Types and injected current harmonics of nonlinear loads used in Case 4-III (as a percentage of the fundamental component)

Type	**Harmonic**											
	5		**7**		**11**		**13**		**17**		**19**	
	Mag (%)	θ (deg)	Mag (%)	θ (deg)	Mag (%)	θ (deg)	Mag (%)	θ (deg)	Mag (%)	θ (deg)	Mag (%)	θ (deg)
IEEE6pulse1	80	0	14.3	0	9.1	0	7.7	0	5.9	0	5.3	0
IEEE6pulse2	19.1	0	13.1	0	7.2	0	5.6	0	3.3	0	2.4	0
ABB_ACS600_6P	42	0	14.3	0	7.9	0	3.7	0	3.2	0	2.3	0
Rockwell_6pulse_VFD	23.5	111	6.1	109	4.6	-158	4.2	-178	1.8	-94	1.4	-92
Toshiba_PWM_ASD	82.8	-135	77.5	69	46.3	-62	41.2	139	14.2	9	9.7	-155

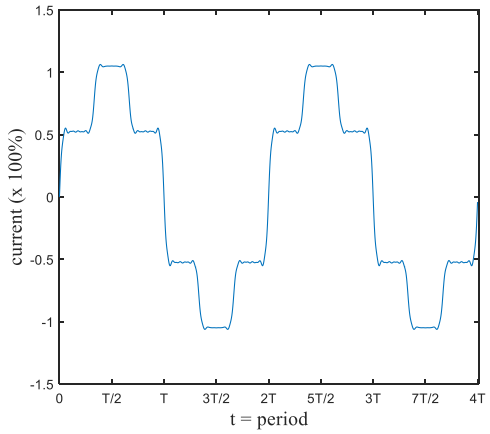

(a)

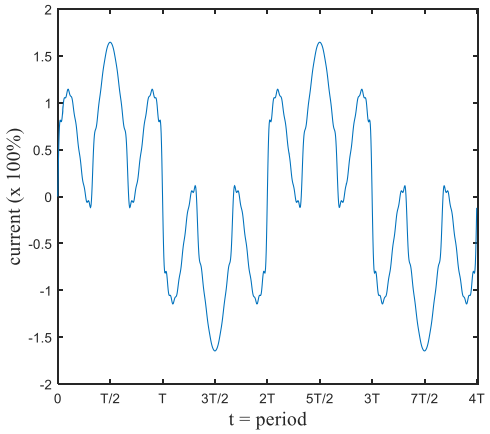

(b)

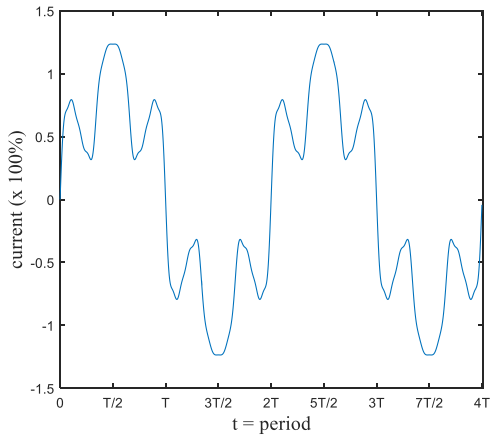

(c)

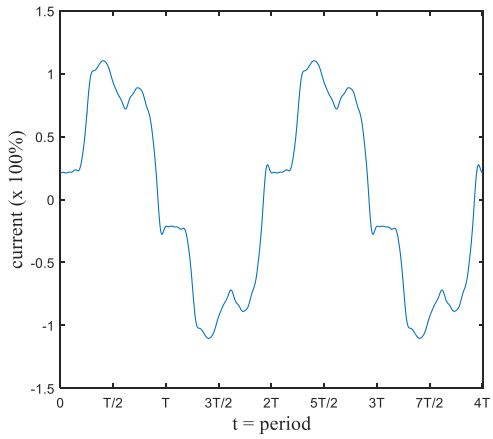

(d)

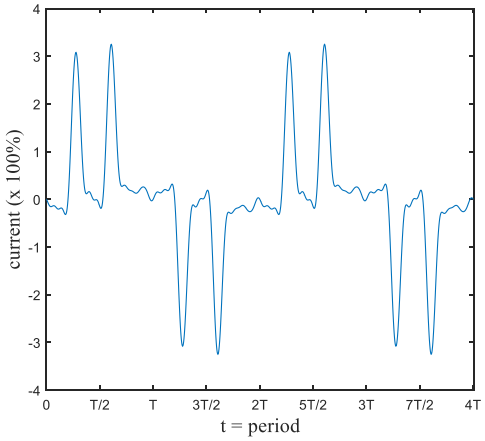

(e)

Figure 4.5: Current waveform of nonlinear loads used in the simulation; (a) IEEE6pulse1; (b) IEEE6pulse2; (c) ABB_ACS600_6P; (d) Rockwell_6pulse_VFD; (e) Toshiba_PWM_ASD;

Table 4.5
Nonlinear loads of IEEE 123-bus distribution network (Case 4-III)

Bus No.	**Type**	**Real Power (MW)**	**Reactive Power (MVAr)**
13	IEEE6pulse2	0.03705	0.0264
15	IEEE6pulse1	0.04725	0.0294
21	ABB_ACS600_6P	0.05745	0.0396
25	Rockwell_6pulse_VFD	0.0531	0.02685

40	Toshiba_PWM_ASD	0.0711	0.04395
54	IEEE6pulse2	0.0573	0.02265
64	IEEE6pulse1	0.03195	0.01395
74	ABB_ACS600_6P	0.03855	0.0258
78	Rockwell_6pulse_VFD	0.0576	0.0213
100	Toshiba_PWM_ASD	0.03705	0.0276
106	IEEE6pulse1	0.0288	0.0141
610	Rockwell_6pulse_VFD	0.05775	0.02925

Table 4.6
Parameters of simulated IEEE 123-bus distribution network

Item	**Qty.**	**Item**	***P* (MW)**	***Q* (MVAr)**
Bus	123	Total Generation Capacity	30	-5.0 to +10.0
Generator	1	Online Capacity	30	-5.0 to +10.0
Committed Generation	1	Generation	1.9073	1.2488
Linear Load	40	Linear Load	1.37	0.76
Nonlinear Load	12	Nonlinear Load	0.57	0.32
Branch	122	Total Harmonic Losses	0.117352	0.262207

Table 4.7
Linear loads of IEEE 123-bus distribution network (Case 4-III)

Bus No.	**Real Power (MW)**	**Reactive Power (MVAr)**
1	0.03847	0.01922
7	0.01923	0.00961
9	0.03847	0.01922
10	0.01923	0.00961
11	0.03847	0.01922
19	0.03847	0.01922
20	0.03847	0.01922
28	0.03847	0.01922
29	0.03847	0.01922
33	0.03847	0.01922
35	0.03847	0.01922
37	0.03847	0.01922

42	0.01923	0.00961
45	0.01923	0.00961
46	0.01923	0.00961
47	0.03419	0.02646
48	0.06838	0.05291
49	0.03419	0.02646
51	0.01923	0.00961
52	0.03847	0.01922
53	0.03847	0.01922
55	0.01923	0.00961
60	0.01923	0.00961
63	0.03847	0.01922
65	0.03419	0.02646
68	0.01923	0.00961
69	0.03847	0.01922
70	0.01923	0.00961
71	0.03847	0.01922
76	0.10257	0.07937
79	0.03847	0.01922
82	0.03847	0.01922
88	0.03847	0.01922
94	0.03847	0.01922
98	0.03847	0.01922
109	0.03847	0.01922
111	0.01923	0.00961
112	0.01923	0.00961
113	0.03847	0.01922
114	0.01923	0.00961

Table 4.8
Line parameters of the IEEE 123-bus distribution network (Case 4-III)

From Bus	**To Bus**	**Resistance (p.u.)**	**Reactance (p.u.)**	**From Bus**	**To Bus**	**Resistance (p.u.)**	**Reactance (p.u.)**
1	2	0.037103	0.022444	60	62	0.014481	0.032063
1	3	0.053004	0.032063	60	160	0.005793	0.012825

1	7	0.017378	0.038475	61	610	0.005793	0.012825
3	4	0.042403	0.02565	62	63	0.010137	0.022444
3	5	0.068905	0.041681	63	64	0.020274	0.044888
5	6	0.053004	0.032063	64	65	0.024618	0.054507
7	8	0.011585	0.02565	65	66	0.018826	0.041681
8	12	0.047704	0.028856	67	68	0.042403	0.02565
8	9	0.047704	0.028856	67	72	0.01593	0.035269
8	13	0.017378	0.038475	67	97	0.014481	0.032063
9	14	0.090107	0.054507	68	69	0.058304	0.035269
13	34	0.031802	0.019238	69	70	0.068905	0.041681
13	18	0.047789	0.105807	70	71	0.058304	0.035269
13	152	0.005793	0.012825	72	73	0.058304	0.035269
14	11	0.053004	0.032063	72	76	0.011585	0.02565
14	10	0.053004	0.032063	73	74	0.074206	0.044888
15	16	0.079506	0.048094	74	75	0.084806	0.0513
15	17	0.074206	0.044888	76	77	0.02317	0.0513
18	19	0.053004	0.032063	76	86	0.040548	0.089776
18	21	0.017378	0.038475	77	78	0.005793	0.012825
18	135	0.005793	0.012825	78	79	0.013033	0.028856
19	20	0.068905	0.041681	78	80	0.027515	0.060919
21	22	0.111308	0.067332	80	81	0.010137	0.022444
21	23	0.014481	0.032063	81	82	0.014481	0.032063
23	24	0.116609	0.070538	81	84	0.143111	0.086569
23	25	0.01593	0.035269	82	83	0.014481	0.032063
25	26	0.020274	0.044888	84	85	0.100708	0.060919
25	28	0.011585	0.02565	86	87	0.026067	0.057713
26	27	0.01593	0.035269	87	88	0.037103	0.022444
26	31	0.047704	0.028856	87	89	0.01593	0.035269
27	33	0.106008	0.064125	89	90	0.053004	0.032063
28	29	0.017378	0.038475	89	91	0.013033	0.028856
29	30	0.020274	0.044888	91	92	0.063605	0.038475

30	250	0.011585	0.02565	91	93	0.013033	0.028856
31	32	0.063605	0.038475	93	94	0.058304	0.035269
34	15	0.021202	0.012825	93	95	0.017378	0.038475
35	36	0.037652	0.083363	95	96	0.042403	0.02565
35	40	0.014481	0.032063	97	98	0.01593	0.035269
36	37	0.063605	0.038475	97	197	0.005793	0.012825
36	38	0.053004	0.032063	98	99	0.031859	0.070538
38	39	0.068905	0.041681	99	100	0.017378	0.038475
40	41	0.068905	0.041681	100	450	0.046341	0.102601
40	42	0.014481	0.032063	101	102	0.047704	0.028856
42	43	0.106008	0.064125	101	105	0.01593	0.035269
42	44	0.011585	0.02565	102	103	0.068905	0.041681
44	45	0.042403	0.02565	103	104	0.148411	0.089776
44	47	0.014481	0.032063	105	106	0.047704	0.028856
45	46	0.063605	0.038475	105	108	0.018826	0.041681
47	48	0.008689	0.019238	106	107	0.121909	0.073744
47	49	0.014481	0.032063	108	109	0.095407	0.057713
49	50	0.014481	0.032063	108	350	0.057926	0.128251
50	51	0.014481	0.032063	109	110	0.063605	0.038475
52	53	0.011585	0.02565	110	111	0.121909	0.073744
53	54	0.007241	0.016031	110	112	0.026502	0.016031
54	55	0.01593	0.035269	112	113	0.111308	0.067332
54	57	0.020274	0.044888	113	114	0.068905	0.041681
55	56	0.014481	0.032063	135	35	0.021722	0.048094
57	58	0.053004	0.032063	150	1	0.02317	0.0513
57	60	0.043444	0.096188	152	52	0.02317	0.0513
58	59	0.053004	0.032063	160	67	0.020274	0.044888
60	61	0.031859	0.070538	197	101	0.014481	0.032063

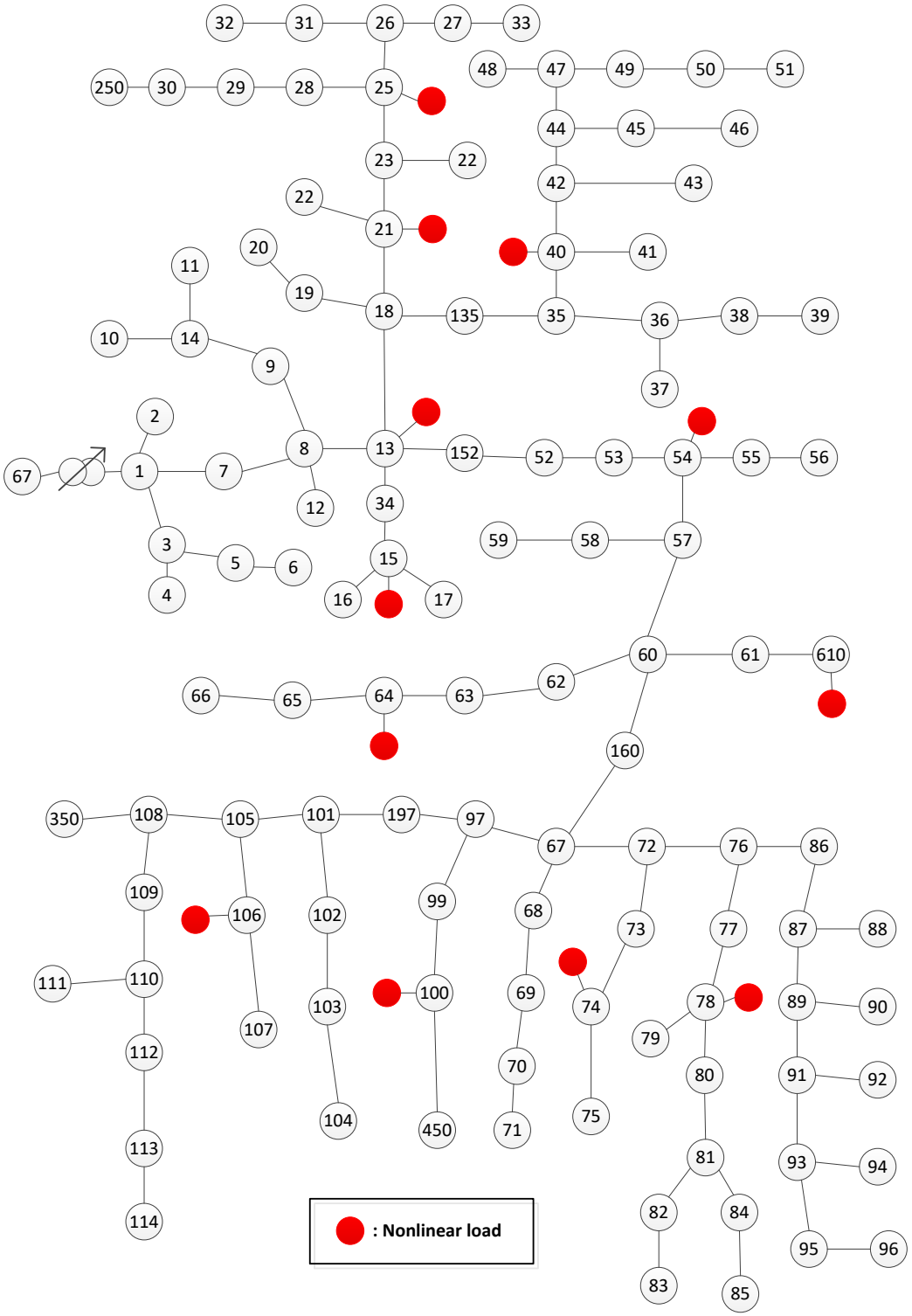

Figure 4.6: Single-line diagram of 123-bus IEEE network (Case 4-III)

By executing the proposed PSO on the 123-bus distribution system, buses number 34, 65, 71, 75, 103, and 113 have been chosen by the algorithm as the APLC sites. This simulation is performed with PSO initial values of 100 iterations and a population of 20,000. The THD_v values of the system before and after putting the APLCs are compared in Table 4.9. It is shown that the optimally sited/sized APLCs can improve the performance of the network by decreasing the THD values and maintaining them within the standard limit (5%). This means that the proposed approach can successfully fulfil the requirement of large and complex distribution networks. The THD_v values are also visually compared in Fig. 4.7. Furthermore, Fig. 4.8 shows the system with optimal location of the chosen APLCs.

Table 4.9
THD values of 123-bus IEEE network without and with multiple optimally sited/sized APLCs (Case 4-III)

Bus No	**THD without APLC**	**THD with APLC**	**Bus No**	**THD without APLC**	**THD with APLC**
1	3.398	10.335	63	1.545	10.966
2	3.398	10.335	64	2.141	10.985
3	3.398	10.335	65	3.004	10.984
4	3.398	10.335	66	3.004	10.984
5	3.398	10.335	67	0.616	11.007
6	3.398	10.335	68	0.626	11.004
7	3.457	10.515	69	0.639	11.001
8	3.498	10.637	70	0.655	10.999
9	3.497	10.636	71	0.668	10.997
10	3.497	10.634	72	0.928	10.995
11	3.497	10.634	73	1.338	11.051
12	3.498	10.637	74	1.873	11.123
13	3.560	10.827	75	2.448	11.123
14	3.497	10.635	76	0.903	10.962
15	4.148	10.881	77	0.859	10.903
16	4.148	10.881	78	0.849	10.888
17	4.148	10.881	79	0.849	10.888
18	2.724	11.125	80	0.849	10.887
19	2.724	11.123	81	0.849	10.887
20	2.724	11.122	82	0.849	10.886

21	2.620	11.132	83	0.849	10.886
22	2.620	11.132	84	0.849	10.887
23	2.568	11.100	85	0.849	10.887
24	2.568	11.100	86	0.903	10.956
25	2.511	11.064	87	0.902	10.954
26	2.511	11.064	88	0.902	10.953
27	2.511	11.063	89	0.902	10.953
28	2.511	11.064	90	0.902	10.953
29	2.511	11.063	91	0.902	10.952
30	2.511	11.063	92	0.902	10.952
31	2.511	11.064	93	0.902	10.952
32	2.511	11.064	94	0.902	10.951
33	2.511	11.062	95	0.902	10.952
34	4.103	10.859	96	0.902	10.952
35	2.727	11.332	97	0.819	11.058
36	2.727	11.331	98	1.208	11.110
37	2.727	11.330	99	2.036	11.241
38	2.727	11.331	100	2.497	11.325
39	2.727	11.331	101	0.743	11.068
40	2.905	11.460	102	0.962	11.068
41	2.905	11.460	103	1.277	11.068
42	2.904	11.455	104	1.277	11.068
43	2.904	11.455	105	0.615	11.078
44	2.903	11.452	106	0.723	11.107
45	2.903	11.451	107	0.723	11.107
46	2.903	11.451	108	0.820	11.072
47	2.903	11.450	109	1.321	11.062
48	2.903	11.449	110	1.659	11.058
49	2.903	11.449	111	1.659	11.057
50	2.903	11.449	112	1.801	11.057
51	2.903	11.449	113	2.396	11.053
52	2.644	10.884	114	2.396	11.052
53	2.270	10.909	135	2.696	11.165
54	2.035	10.925	150	3.322	10.103
55	2.035	10.925	152	3.379	10.838
56	2.035	10.925	160	0.643	10.960
57	1.396	10.931	197	0.781	11.060
58	1.396	10.931	250	2.511	11.063
59	1.396	10.931	350	0.820	11.072
60	0.838	10.947	450	2.497	11.325
61	0.983	10.866	610	1.010	10.852
62	1.250	10.958			

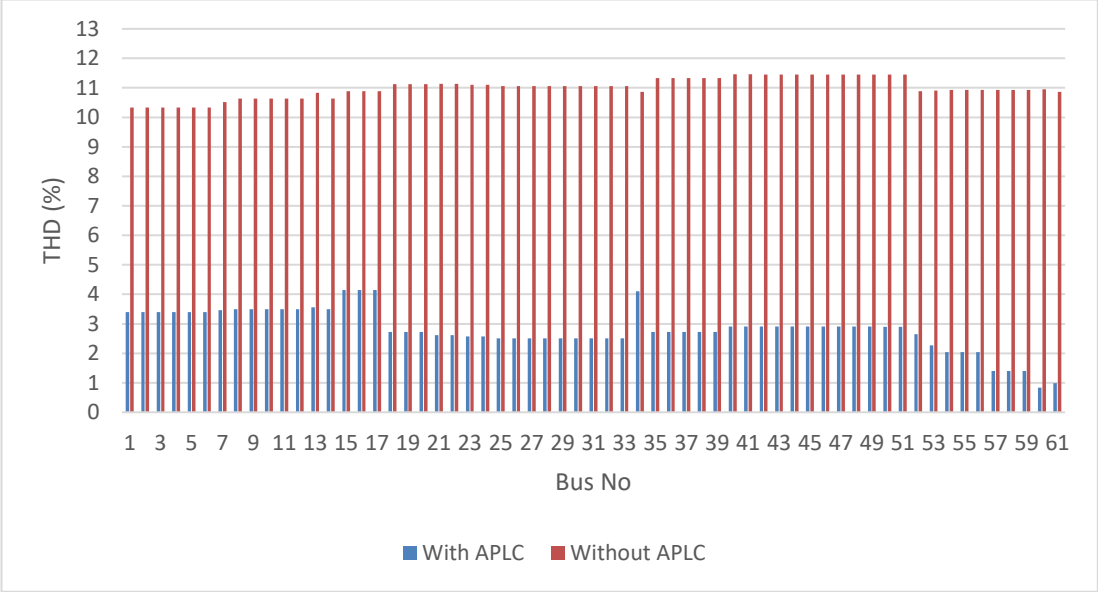

(a)

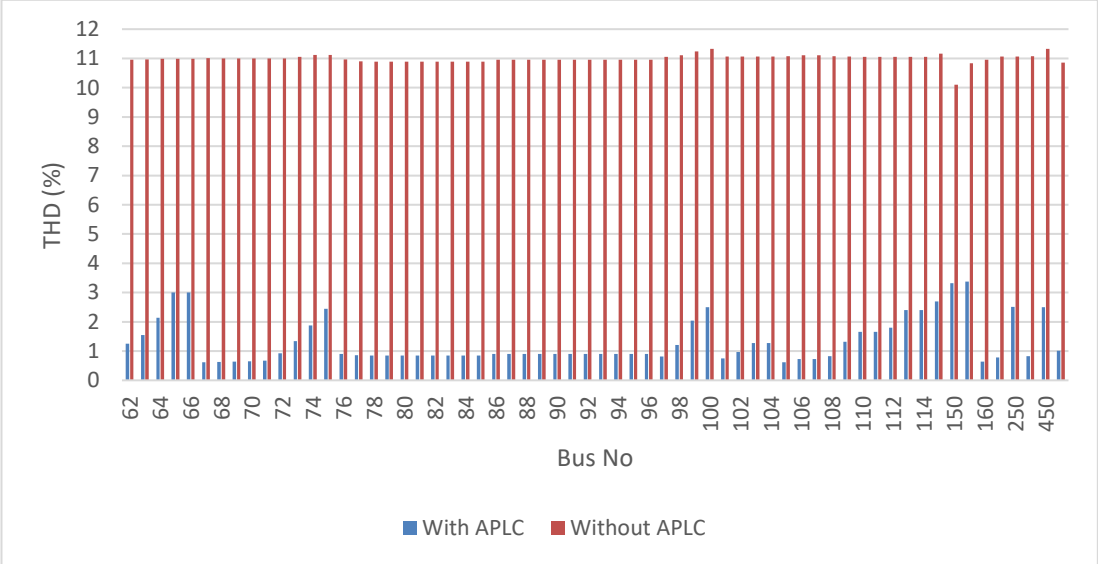

(b)

Figure 4.7: Comparison of THD_v of all buses with and without APLCs on 123-bus IEEE distribution network (Case 4-III): a) buses 1–61; b) buses 62–123

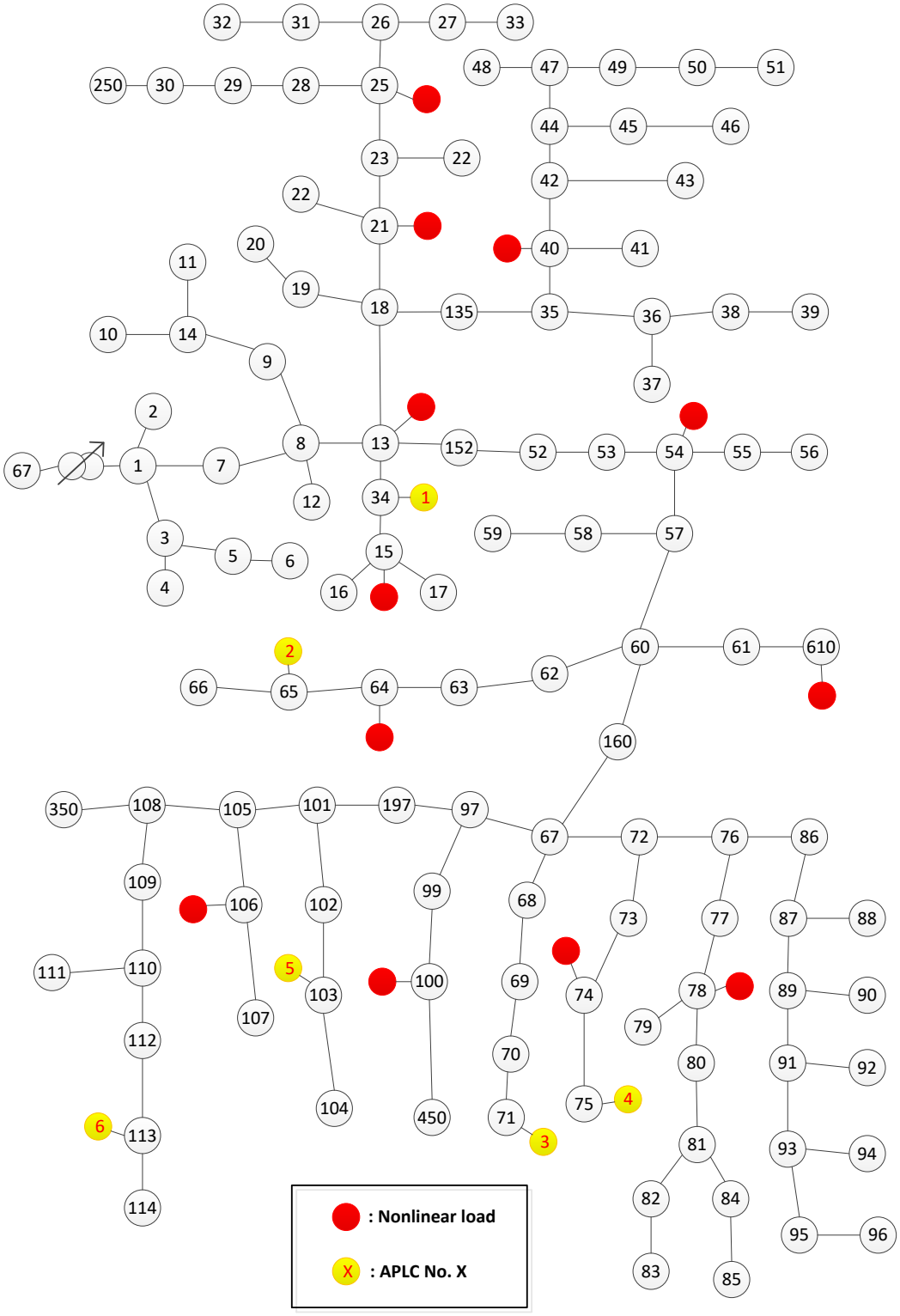

Figure 4.8: Single-line diagram of 123-bus IEEE network with optimally sited/sized APLCs (Case 4-III)

CHAPTER 5

Optimal Sizing, Allocation, and Operation of Multiple APLCs for Harmonic Mitigation and Reactive Power Compensation in Unbalanced Distribution Network

5.1 Introduction

Although APLCs usually generate a balanced set of three-phase currents with controllable amplitude and phase angle, distribution networks are generally unbalanced due to the following: 1) unequal load currents are drawn from the three-phase power system by using most of the industrial three-phase loads and 2) the single-phase loads cannot be distributed symmetrically in the three-phase distribution network. Voltage and THD_v imbalances in the system are power quality problems in an unbalanced distribution network that affect other customers within the network. Furthermore, even small imbalances can cause unbalanced electromagnetic torques and overheating in many inductive loads such as induction motors as they are very sensitive to voltage imbalances. Therefore, it is very crucial to address these issues in unbalanced networks.

This chapter presents the harmonic mitigation and reactive power compensation in an unbalanced distribution system including balanced and unbalanced large industrial loads as well as local loads, thus, illustrating how APLCs can mitigate the

total harmonic distortion and voltage instability problems in unbalanced distribution networks. Similar to the solution for the balanced networks, the PSO-based approach is implemented and evaluated for optimally sizing, siting, and operating the APLCs in the unbalanced distribution network. However, the network is more complex and requires significantly higher computation time for finding the optimal solution.

5.2 Simulations for Optimal Siting and Sizing of APLCs in Unbalanced Distribution Network

The simulated network in this study is the unbalanced version of the 18-bus IEEE network shown in Fig. 5.1. Letters A, B, and C in the yellow circles show the phases where the single-phase PV units are fitted. For example, node 4 has a single-phase PV connected to phase C. The optimal siting/sizing simulations are executed for the worst-case scenario with maximum linear and nonlinear loading conditions. In this study, five cases are simulated and the respective results are presented in the following sections.

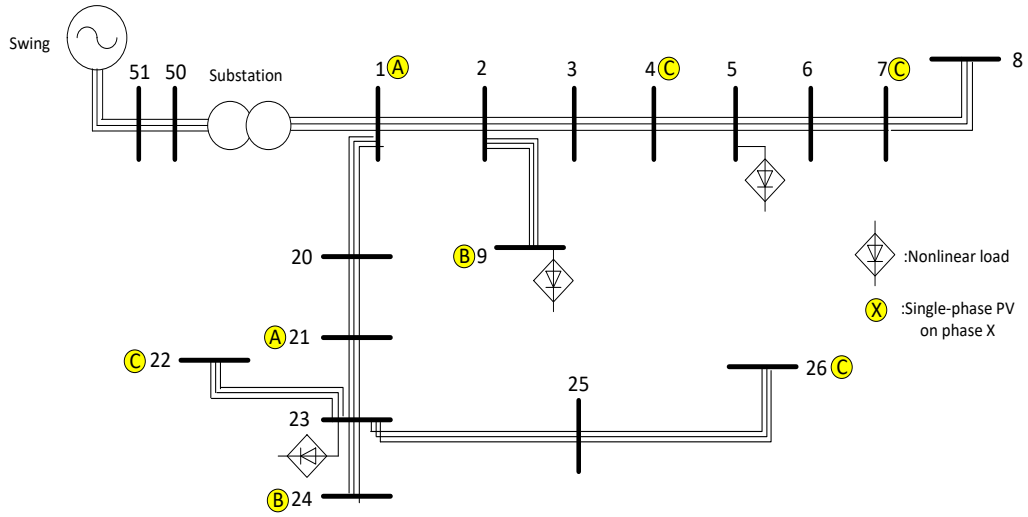

Figure 5.1: Distorted unbalanced IEEE 18-bus system used for simulation (Case 5-I)-(Case 5-II)

5.2.1 Case 5-I: System Operation of Unbalanced Distribution Network without APLCs

The worst operating condition of the system, i.e. with the maximum values of all linear and nonlinear loads, is considered. The simulation results of performing the DHLF approach on the system without any APLC are presented in Table 5.1. Fig. 5.2 shows the THD_v of all buses for each phase (columns 3, 5, and 7 of Table 5.1). It is shown that the THD_v of all buses exceed the acceptable level of 5% for all three phases, which means that the entire network is highly distorted. The most distorted bus of the system is bus 26 with a THD_v of 14.21% (phase B), which is expected because of its remote location from the swing bus (bus 1).

Table 5.1
Bus voltage summary of unbalanced-network containing nonlinear loads (Case 5-I)

Bus No.	R.M.S Value - Phase A (p.u.)	THD_v of Phase A (%)	R.M.S Value - Phase B (p.u.)	THD_v of Phase B (%)	R.M.S Value - Phase C (p.u.)	THD_v of Phase C (%)
1	1.039	13.803	1.0405	13.856	1.037	13.822
2	1.037	13.850	1.0378	13.903	1.033	13.863
3	1.036	13.885	1.035	13.936	1.029	13.892
4	1.035	13.903	1.0337	13.954	1.027	13.908
5	1.033	13.954	1.0298	14.002	1.024	13.952
6	1.033	13.954	1.0289	14.003	1.024	13.952
7	1.032	13.955	1.0278	14.003	1.022	13.952
8	1.030	13.956	1.0258	14.004	1.020	13.953
9	1.035	13.911	1.0359	13.964	1.031	13.921
20	1.026	13.89	1.0317	13.969	1.030	13.934
21	1.017	13.96	1.0263	14.055	1.026	14.02
22	1.016	13.962	1.0256	14.057	1.025	14.022
23	1.004	14.085	1.0174	14.208	1.019	14.172
24	1.004	14.086	1.0147	14.208	1.019	14.173

25	0.998	14.084	1.0174	14.211	1.01	14.175
26	0.998	14.083	1.0174	14.212	1.016	14.176
50	1.058	13.568	1.0585	13.571	1.058	13.569
51	1.059	13.554	1.0596	13.554	1.059	13.554

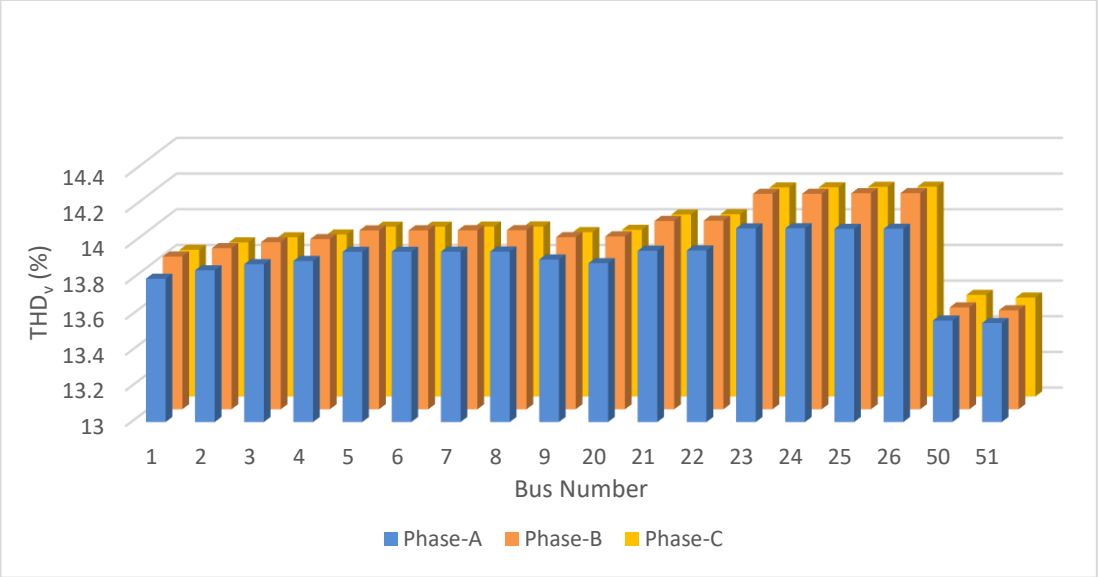

Figure 5.2: Simulation results of unbalanced network containing nonlinear loads (Case 5-I)

5.2.2 Case 5-II: System Operation of Unbalanced Distribution Network with Optimal Sizing and Allocating of Multiple APLCs with Equal Weighting Factors of THD_v and APLC Size

The proposed PSO algorithm in Fig 4.1a is utilised to solve the optimal siting and sizing of multiple APLCs for the unbalanced 18-bus IEEE network shown in Fig 5.1. Table 5.2 presents a summary of the simulation results. The THD_v for all network buses and for each harmonic distortion are shown in Fig 5.3. For this simulation, the THD_v and APLC size have same weighting factor. In other words, the APLC does not

have any restriction on the size and any size can be chosen to minimise the THD_v of the system. Due to the configuration of the network, the algorithm has chosen only bus 1 as the APLC site and it successfully controlled the THD_v values below 5% for all buses. The modelling of Case 5-II specifies the location (bus 1) and size (0.2245 p.u.) of the APLCs.

Table 5.2
Bus voltage summary of unbalanced network containing nonlinear loads (Case 5-II)

Bus No.	R.M.S Value-Phase A (p.u.)	THD_v - Phase A (%)	R.M.S Value-Phase B (p.u.)	THD_v - Phase B (%)	R.M.S Value-Phase C (p.u.)	THD_v - Phase C (%)	Allocated I_{aplc} (p.u.)
1	1.030	4.708	1.031	2.067	1.028	2.539	0.2245
2	1.028	4.348	1.028	1.938	1.024	2.877	0
3	1.027	4.102	1.025	1.996	1.020	3.122	0
4	1.026	3.976	1.024	2.045	1.017	3.256	0
5	1.024	3.637	1.020	2.202	1.015	3.642	0
6	1.024	3.637	1.019	2.202	1.015	3.642	0
7	1.023	3.637	1.018	2.202	1.013	3.642	0
8	1.021	3.637	1.016	2.202	1.011	3.642	0
9	1.026	4.028	1.026	2.020	1.022	3.201	0
20	1.017	4.140	1.022	1.966	1.020	3.079	0
21	1.008	3.730	1.016	2.119	1.016	3.522	0
22	1.008	3.730	1.016	2.120	1.016	3.523	0
23	0.995	3.160	1.007	2.481	1.009	4.350	0
24	0.995	3.160	1.005	2.481	1.009	4.351	0
25	0.989	3.159	1.007	2.482	1.008	4.352	0
26	0.989	3.159	1.007	2.482	1.008	4.353	0
50	1.049	1.429	1.049	1.338	1.049	1.282	0
51	1.050	1.340	1.050	1.340	1.050	1.340	0

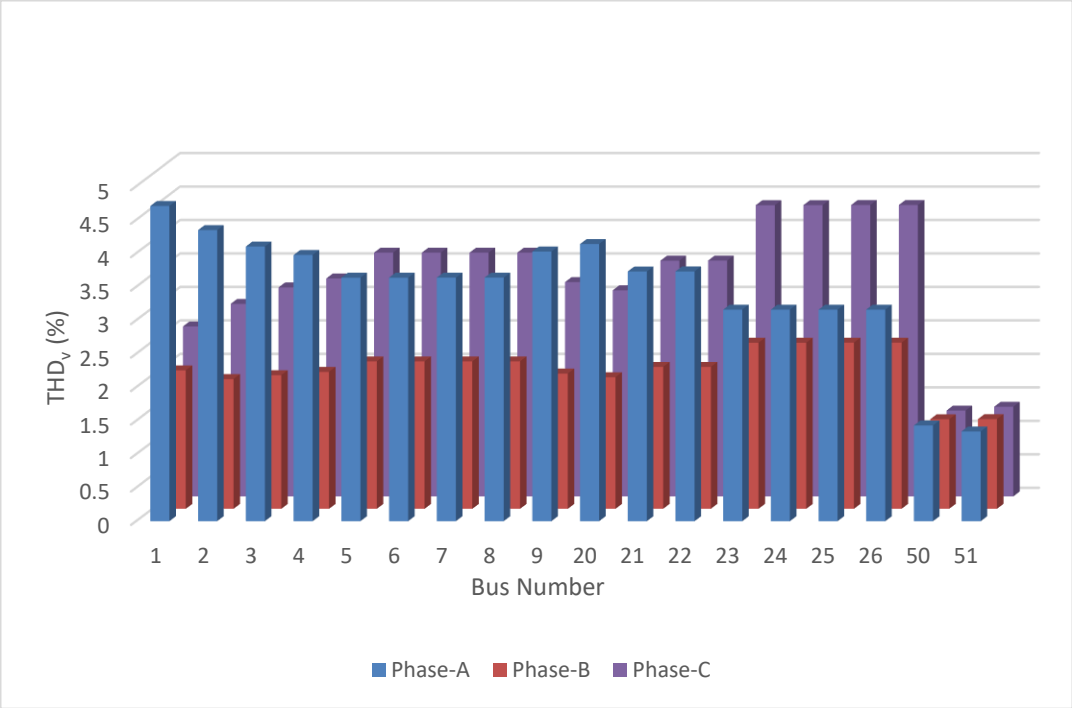
5
4.5
4
3.5
3
2.5
2
1.5
1
0.5
0
THDv (%)
1 2 3 4 5 6 7 8 9 20 21 22 23 24 25 26 50 51
Bus Number
Phase-A
Phase-B
Phase-C

(a)

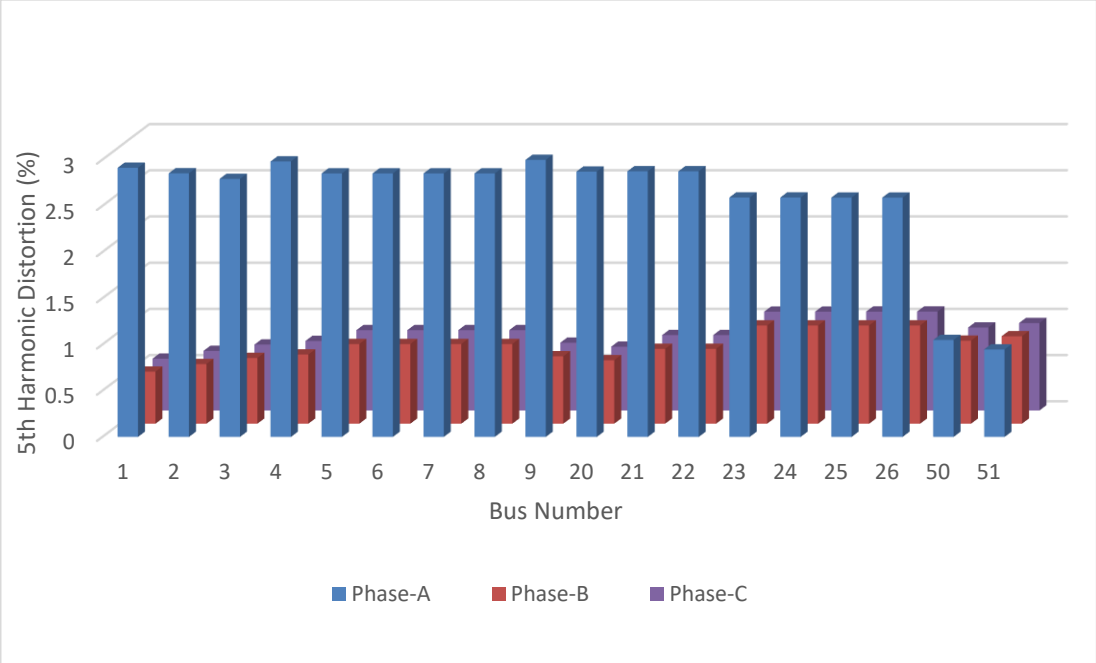
3
2.5
2
1.5
1
0.5
0
5th Harmonic Distortion (%)
1 2 3 4 5 6 7 8 9 20 21 22 23 24 25 26 50 51
Bus Number
Phase-A
Phase-B
Phase-C

(b)

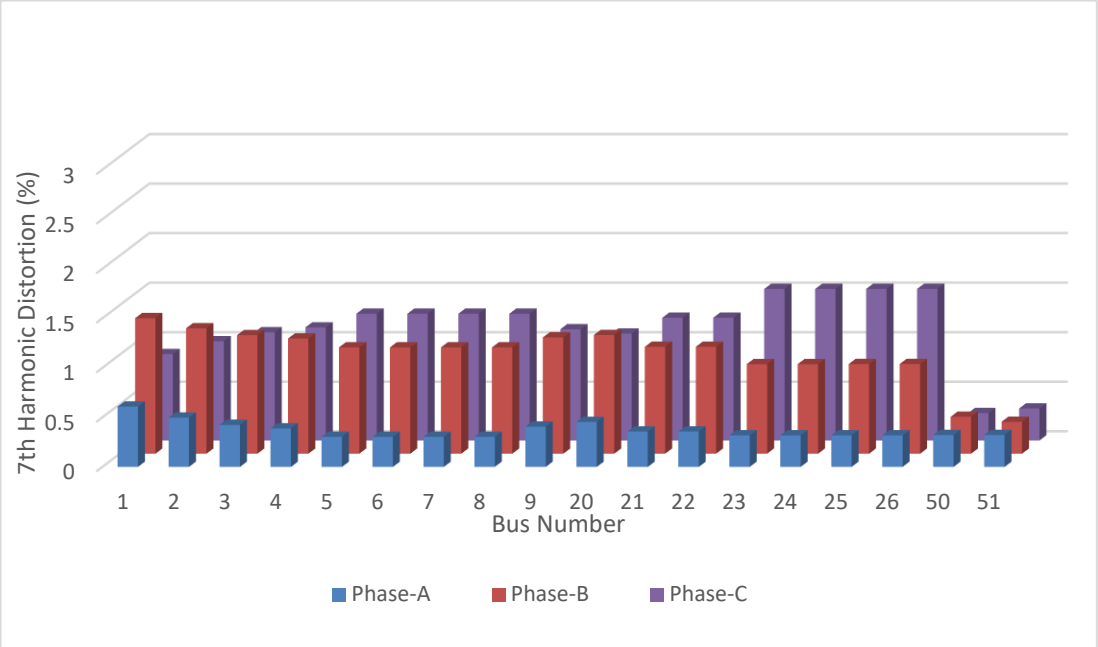

(c)

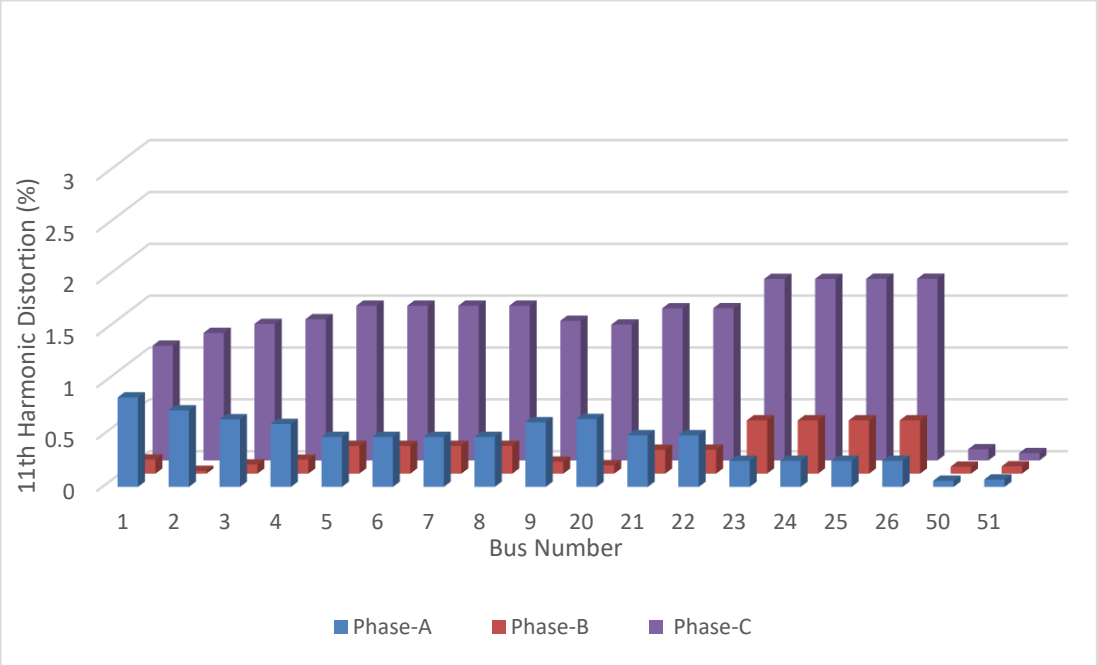

(d)

Figure 5.3: Case 5-II simulation results: (a) THD_v of system, (b) 5th harmonic distortion of system, (c) 7th harmonic distortion of system, and (d) 11th harmonic distortion of system

5.2.3 Case 5-III: Impact of Network Nonlinear Load Location on Solution of Optimal Sizing and Siting

Simulations were repeated for the same network configuration of Case 5-II but with different locations of the same nonlinear loads to investigate impact of location on the generated solution of the optimal sizing/siting by the first PSO algorithm of Fig. 4.1a in an unbalanced distribution network. For this purpose, the three nonlinear loads were relocated to buses 4, 20, and 25. The results are summarised in Table 5.3 and presented in Fig. 5.4. Case 5-III uses different optimal locations (buses 3, 4, and 6) and sizes (0.1527 p.u., 0.0116 p.u., and 0.0484 p.u.) of APLCs in contrast to Case 5-II. It means that the number of APLCs chosen by the PSO algorithm also depends on the location of nonlinear loads. Although the total size of APLCs of the system is slightly smaller than that of Case 5-II, the average THD_v of all buses is greater than that of Case 5-II, i.e. 3.462% compared to 2.965% for Case 5-II.

Table 5.3
Bus voltage summary of unbalanced network with different locations of nonlinear loads (Case 5-III)

Bus No.	R.M.S Value-Phase A (p.u.)	THD_v - Phase A (%)	R.M.S Value-Phase B (p.u.)	THD_v - Phase B (%)	R.M.S Value-Phase C (p.u.)	THD_v - Phase C (%)	Allocated I_{aplc} (p.u.)
1	1.030	3.167	1.031	3.242	1.028	2.800	0
2	1.028	3.737	1.029	3.438	1.025	2.974	0
3	1.027	4.599	1.026	3.712	1.020	3.237	0.1527
4	1.026	4.477	1.024	3.671	1.018	3.425	0.0116
5	1.025	4.477	1.022	3.671	1.017	4.126	0
6	1.025	4.477	1.021	3.671	1.017	4.363	0.0484
7	1.024	4.478	1.020	3.671	1.015	4.364	0

8	1.022	4.478	1.018	3.671	1.013	4.364	0
9	1.028	3.738	1.028	3.438	1.024	2.974	0
20	1.014	2.417	1.019	3.523	1.018	2.754	0
21	1.005	2.264	1.014	3.685	1.014	3.075	0
22	1.005	2.265	1.013	3.686	1.013	3.075	0
23	0.993	2.274	1.005	4.097	1.007	3.704	0
24	0.993	2.274	1.002	4.097	1.007	3.705	0
25	0.983	2.522	1.002	4.665	1.003	4.316	0
26	0.983	2.522	1.002	4.666	1.002	4.316	0
50	1.049	2.423	1.049	2.447	1.049	2.452	0
51	1.050	2.436	1.050	2.436	1.050	2.436	0

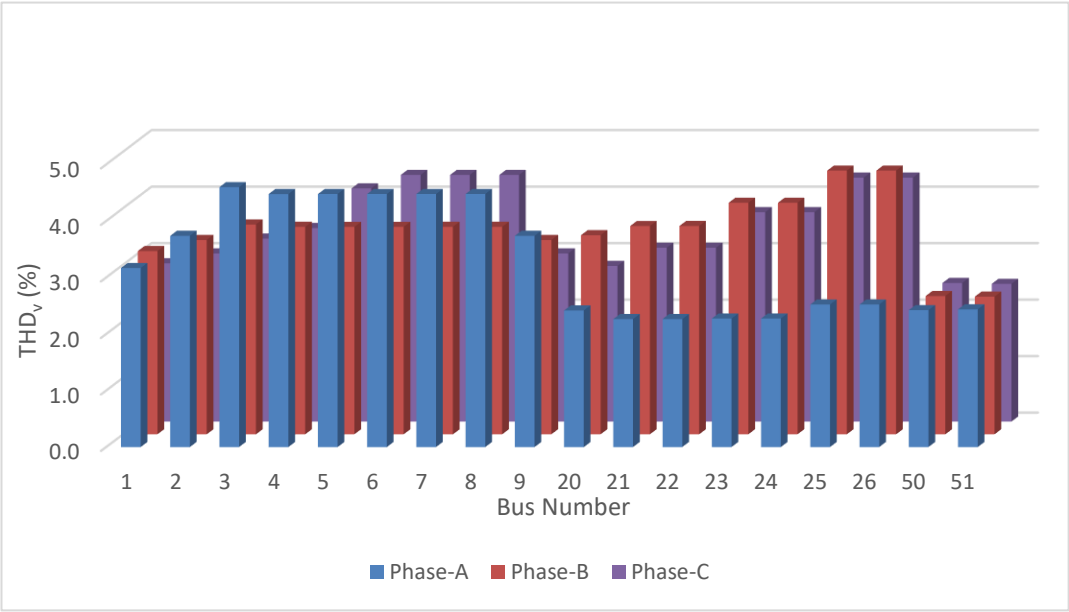

(a)

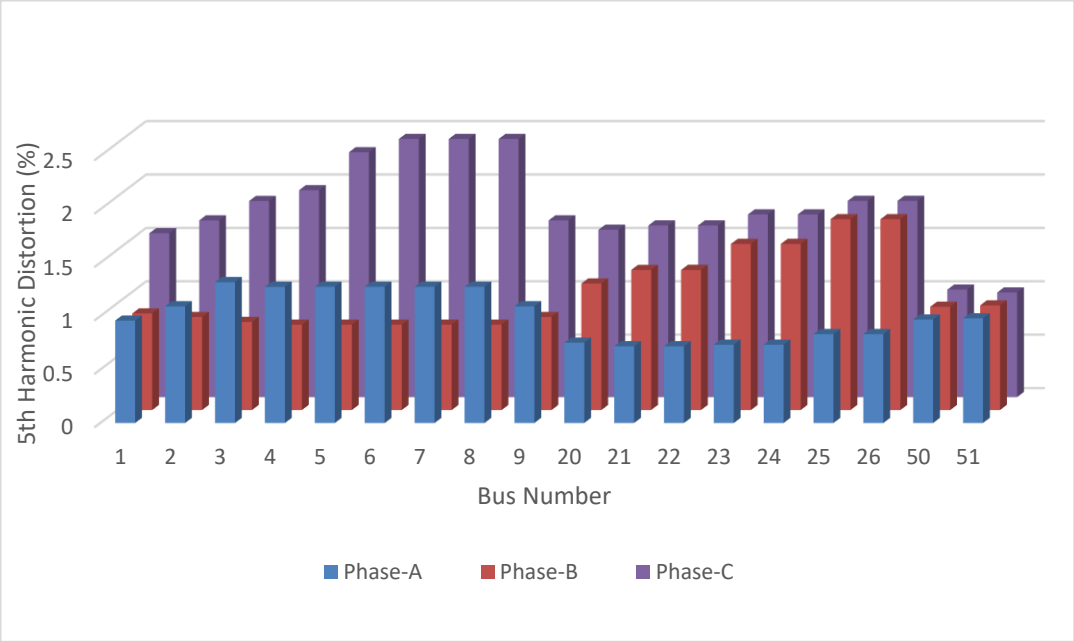
5th Harmonic Distortion (%)
2.5
2
1.5
1
0.5
0
1 2 3 4 5 6 7 8 9 20 21 22 23 24 25 26 50 51
Bus Number
Phase-A
Phase-B
Phase-C

(b)

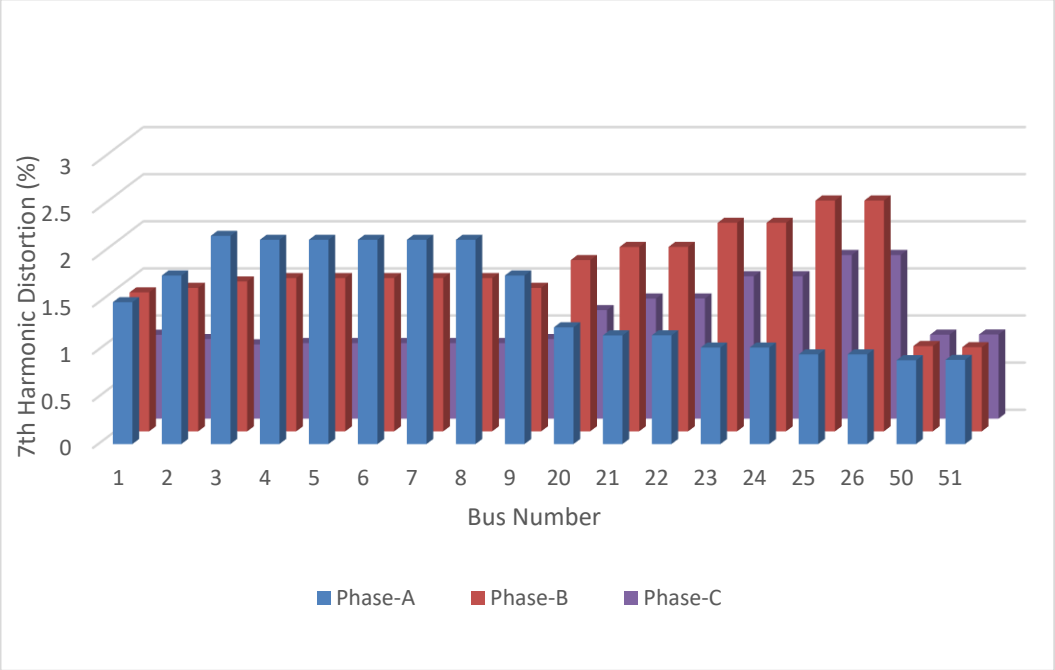
7th Harmonic Distortion (%)
3
2.5
2
1.5
1
0.5
0
1 2 3 4 5 6 7 8 9 20 21 22 23 24 25 26 50 51
Bus Number
Phase-A
Phase-B
Phase-C

(c)

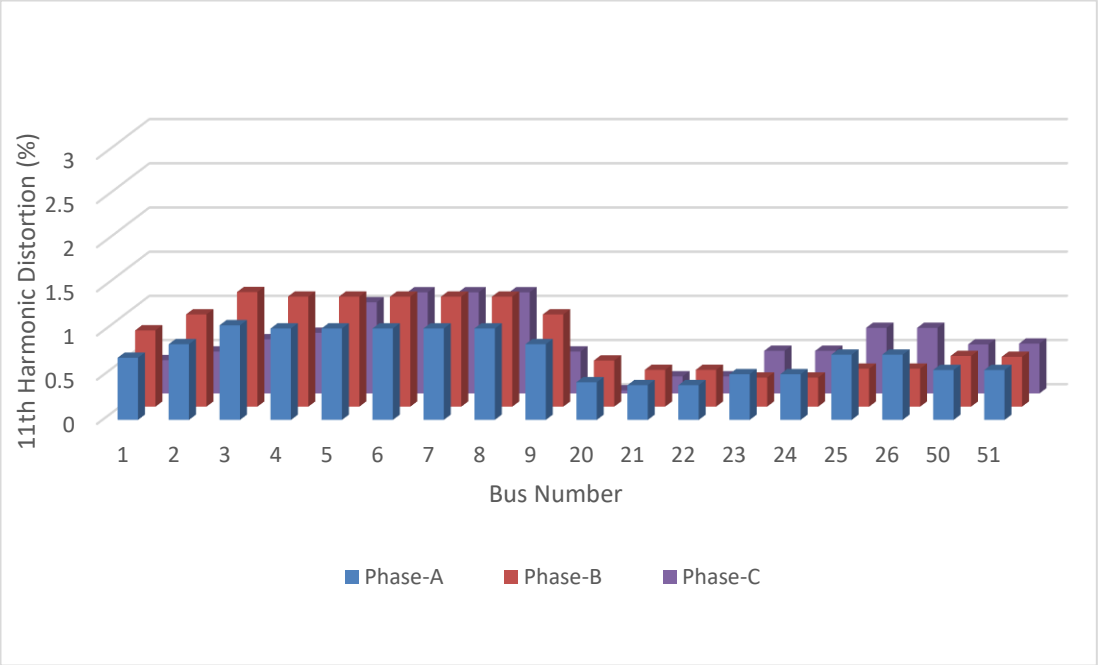

(d)

Figure 5.4: Simulation results for Case 5-III: (a) THD_v of system, (b) 5th harmonic distortion of system, (c) 7th harmonic distortion of system, and (d) 11th harmonic distortion of system

5.2.4 Case 5-IV: Impact of Greater APLC Size Weighting Factor on the Solution of Optimal Sizing and Allocating of Unbalanced Network

A larger APLC size means a higher cost for the system to keep the THD_v within the required standard range. By increasing the APLC weighting factor, the PSO algorithm decreases the size of APLC by sacrificing the system THD_v. To investigate this, simulations were conducted for the same network of Case 5-III but with greater weighting factors for APLC size than for THD_v. Table 5.4 summarises the simulation results comparing Case 5-III and Case 5-IV. The first proposed PSO-based algorithm shown in Fig. 4.1a is used for both cases. Fig. 5.5 shows the THD_v of the system for

this case. The result indicates that a greater weighting factor for APLC size caused the PSO algorithm to choose different buses for siting the APLCs. Furthermore, the APLC size in Case 5-IV is smaller than that in Case 5-III, which means savings in the system cost. However, the average THD_v is higher in this scenario. In addition, it can be observed that the THD_v values of some buses are very close to the margin of 5%, which means that a slight change in the size of nonlinear loads or configuration of the network can potentially increase the THD_v values above 5%. These values are highlighted in the table.

Table 5.4
Bus voltage summary of unbalanced network for Case 5-III and Case 5-IV

Bus No.	Case 5-III: Equal Weighting Factors				Case 5-IV: Unequal Weighting Factors			
	THD (%)			Allocated I_{aplc} (p.u.)	THD (%)			Allocated I_{aplc} (p.u.)
	Phase A	Phase B	Phase C		Phase A	Phase B	Phase C	
1	3.167	3.242	2.800	0	4.064	3.367	3.304	0.0442
2	3.737	3.438	2.974	0	4.287	3.582	3.714	0.15
3	4.599	3.712	3.237	0.1527	4.242	4.194	3.594	0
4	4.477	3.671	3.425	0.0116	4.397	4.606	3.549	0
5	4.477	3.671	4.126	0	4.800	4.681	3.656	0
6	4.477	3.671	4.363	0.0484	4.940	4.465	3.721	0
7	4.478	3.671	4.364	0	4.972	4.662	3.940	0.0017
8	4.478	3.671	4.364	0	4.963	4.235	3.940	0
9	3.738	3.438	2.974	0	4.287	3.582	3.714	0
20	2.417	3.523	2.754	0	4.972	4.137	3.387	0
21	2.264	3.685	3.075	0	4.927	4.641	3.630	0
22	2.265	3.686	3.075	0	4.914	4.581	3.631	0
23	2.274	4.097	3.704	0	4.830	4.996	4.158	0.0201
24	2.274	4.097	3.705	0	4.603	4.952	4.159	0
25	2.522	4.665	4.316	0	4.900	4.964	4.309	0

26	2.522	4.666	4.316	0	4.963	4.990	4.309	0
50	2.423	2.447	2.452	0	2.482	2.435	2.385	0
51	2.436	2.436	2.436	0	2.430	2.430	2.430	0
Ave.	3.279	3.638	3.470		4.480	4.194	3.641	

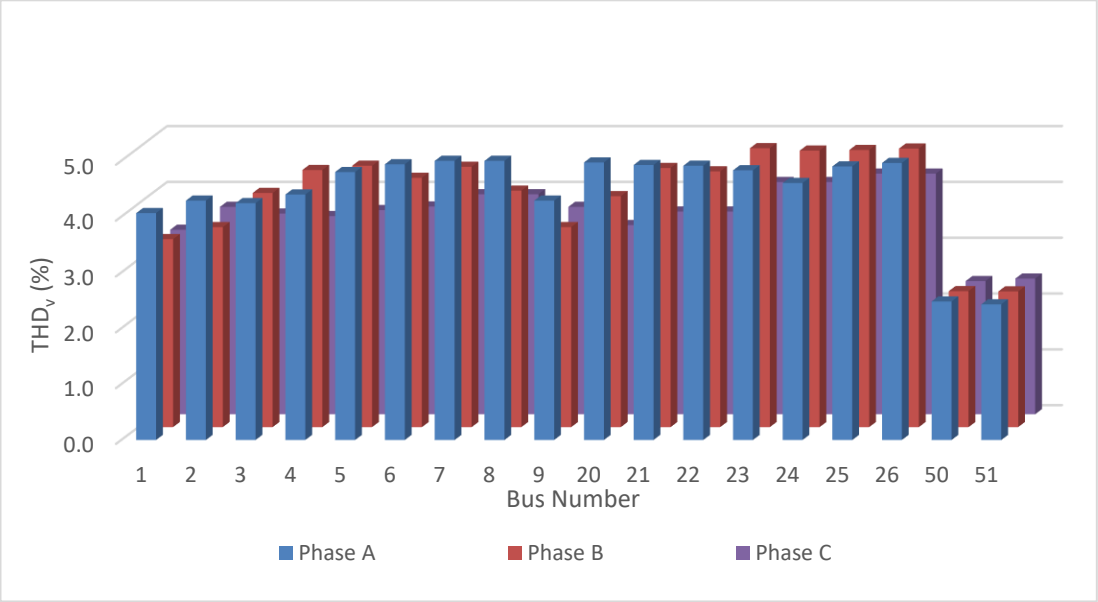

Figure 5.5: THD of all individual buses for Case 5-IV

5.2.5 Case 5-V: Optimal Operation of the Allocated APLCs for 24-Hour Period

The first step for the optimal operation of the system with multiple APLCs is performed in Cases 5-I to 5-IV, where the implemented PSO algorithm found the optimal location and size of APLCs. The APLC locations and sizes for Case 5-III are chosen to be used for this study. The network that contains three equal nonlinear loads connected to buses 4, 20, and 24 and the four optimally sized/sited APLCs of Cases 5-III and 5-IV are simulated. For the second step, at each time step (Δt), which is 1 h in this simulation, the second PSO algorithm shown Fig. 4.1b is executed to calculate the new optimal current references of APLCs. For this simulation, the load curve is used

to examine the optimal operation of the network within the 24-hour period. The concept of load interval division is based on the fact that several apparent load levels exist during a day. These intervals can therefore be used to define the optimal operation of the network containing APLCs. A load curve [117] is modified for the unbalanced three-phase scenario shown in Fig. 5.6 and is used in this simulation. A curve of rural loads containing domestic, agricultural, and industrial loads is chosen.

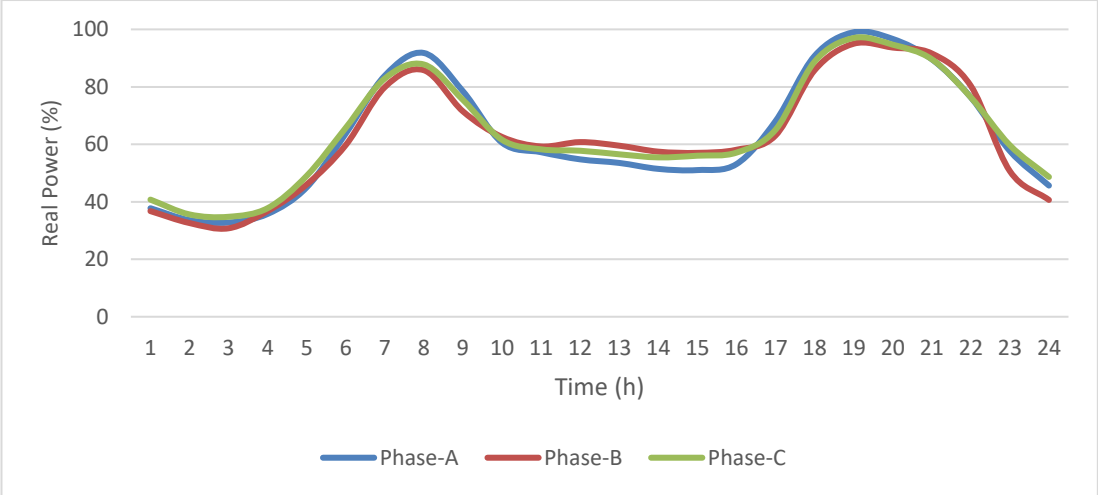

(a)

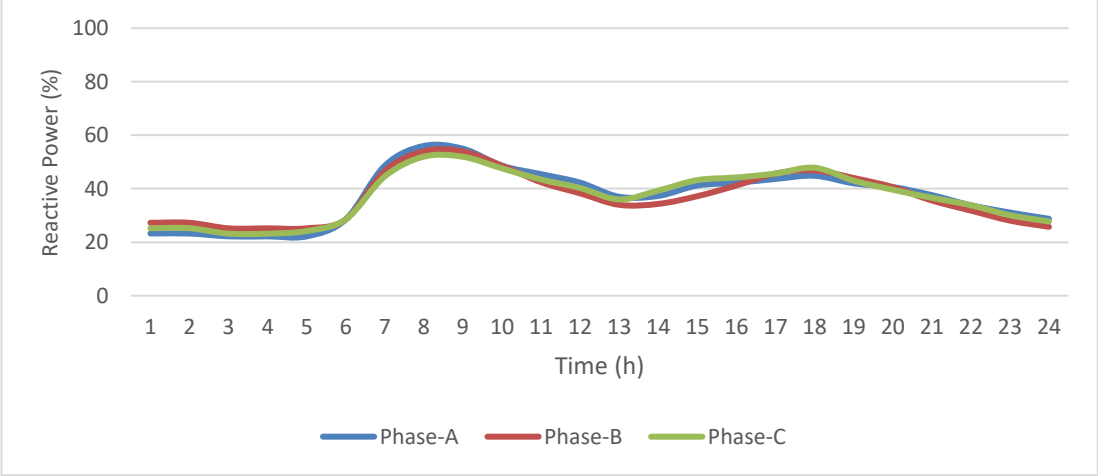

(b)

Figure 5.6: Typical daily load curves used in Case 5-V: (a) active power and (b) reactive power

The simulation results are presented in Table 5.5 and summarised in Fig. 5.7.

Table 5.5
Case 5-V network operation with three optimally sited/sized APLCs of Cases 5-III and 5-IV for a period of 24 h

Bus No.	Phase	Time (h)																							
		1	2	3	4	5	6	7	8	9	10	11	12	13	14	15	16	17	18	19	20	21	22	23	24
1	A	3.03	2.42	3.91	3.70	2.45	1.29	2.16	4.14	1.53	2.90	2.69	2.36	2.09	3.16	2.09	2.98	2.82	0.46	2.34	2.82	2.47	2.63	2.37	2.20
	B	2.94	2.43	4.00	3.73	2.53	1.28	2.36	4.37	1.49	3.14	2.83	2.22	2.26	3.21	2.03	3.20	2.97	0.57	2.18	2.96	2.58	2.97	2.29	2.36
	C	2.85	2.46	4.13	3.79	2.67	1.38	2.66	4.70	1.49	3.52	3.08	2.04	2.51	3.31	1.97	3.54	3.20	0.76	1.97	3.17	2.78	3.48	2.20	2.67
2	A	2.75	2.43	4.10	3.85	2.74	1.46	2.89	4.83	1.52	3.60	3.06	2.02	2.52	3.39	1.94	3.70	3.37	0.83	1.85	3.29	2.90	3.71	2.18	2.68
	B	2.60	2.49	4.01	3.96	2.72	1.60	3.28	4.83	1.60	3.68	3.16	1.84	2.68	3.20	2.09	3.86	3.55	1.14	1.78	3.80	2.91	4.29	2.25	2.61
	C	2.57	2.53	4.01	4.00	2.72	1.67	3.43	4.83	1.67	3.71	3.19	1.80	2.74	3.14	2.14	3.92	3.61	1.25	1.75	3.98	2.92	4.49	2.32	2.61
3	A	2.57	2.53	4.01	4.00	2.72	1.67	3.43	4.83	1.67	3.71	3.19	1.80	2.74	3.14	2.14	3.92	3.61	1.25	1.75	3.98	2.92	4.49	2.32	2.61
	B	2.57	2.53	4.01	4.00	2.72	1.67	3.43	4.83	1.67	3.71	3.20	1.80	2.74	3.14	2.14	3.92	3.61	1.25	1.75	3.98	2.92	4.49	2.32	2.61
	C	2.94	2.43	4.00	3.73	2.53	1.28	2.36	4.37	1.49	3.14	2.83	2.22	2.26	3.21	2.03	3.20	2.97	0.57	2.18	2.96	2.58	2.97	2.29	2.36
4	A	3.17	2.55	3.97	3.84	2.58	1.51	2.41	4.13	1.65	2.87	2.62	2.49	1.98	3.14	2.31	3.06	2.93	0.42	2.67	2.42	2.43	2.74	2.53	2.17
	B	3.23	2.60	4.00	3.89	2.63	1.60	2.52	4.15	1.73	2.87	2.60	2.55	1.94	3.14	2.40	3.10	2.98	0.55	2.81	2.28	2.44	2.79	2.59	2.16
	C	3.23	2.60	4.00	3.89	2.63	1.60	2.52	4.15	1.73	2.87	2.60	2.55	1.94	3.14	2.40	3.11	2.98	0.55	2.82	2.28	2.44	2.80	2.59	2.16
5	A	3.34	2.69	4.05	3.99	2.73	1.77	2.73	4.19	1.89	2.88	2.58	2.67	1.90	3.15	2.57	3.19	3.10	0.85	3.09	2.07	2.51	2.92	2.72	2.17
	B	3.34	2.69	4.05	3.99	2.73	1.77	2.73	4.19	1.89	2.88	2.58	2.67	1.90	3.15	2.57	3.19	3.10	0.85	3.09	2.07	2.51	2.92	2.72	2.17
	C	3.43	2.78	4.09	4.08	2.83	1.94	2.93	4.25	2.05	2.89	2.59	2.79	1.88	3.17	2.72	3.27	3.21	1.15	3.35	1.93	2.62	3.05	2.83	2.18
6	A	3.43	2.78	4.09	4.08	2.83	1.94	2.93	4.25	2.05	2.89	2.59	2.79	1.88	3.17	2.72	3.27	3.21	1.15	3.35	1.93	2.62	3.05	2.83	2.18
	B	3.52	2.28	3.47	3.86	2.02	2.29	1.32	3.13	1.96	2.26	2.65	2.94	1.55	3.10	2.07	1.75	2.30	0.58	2.85	2.85	2.10	1.59	2.86	2.21

3.85	4.12	4.51	4.65	4.75	4.81	4.81	4.81	4.12	4.00	4.06	4.06	4.17	4.17	4.27	4.27	2.30	2.23	2.29	2.40	2.36
3.69	3.84	4.07	4.03	4.31	4.41	4.41	4.41	3.84	3.73	3.75	3.75	3.79	3.79	3.83	3.83	2.92	3.12	3.14	3.18	3.27
1.94	1.97	2.02	2.04	1.73	1.65	1.65	1.65	1.97	2.11	2.19	2.20	2.36	2.36	2.52	2.52	1.63	3.19	3.55	4.07	4.37
2.34	2.38	2.44	2.57	2.80	2.89	2.89	2.89	2.38	2.57	2.67	2.67	2.89	2.89	3.10	3.10	2.09	1.96	2.01	2.11	2.15
2.81	2.98	3.24	3.33	3.54	3.62	3.62	3.62	2.98	2.43	2.30	2.30	2.08	2.08	1.91	1.91	2.84	3.56	3.80	4.15	4.20
3.77	3.91	4.13	4.26	4.51	4.59	4.59	4.59	3.91	4.01	4.11	4.11	4.31	4.31	4.51	4.51	2.90	3.36	3.48	3.70	3.87
2.26	2.56	2.98	3.14	3.40	3.50	3.50	3.50	2.56	2.41	2.48	2.48	2.65	2.65	2.82	2.82	0.64	1.46	1.82	2.33	2.70
2.91	3.08	3.34	3.36	3.61	3.69	3.69	3.69	3.08	2.78	2.74	2.74	2.68	2.68	2.65	2.65	2.32	2.06	2.13	2.26	2.31
1.69	1.80	2.03	2.12	2.02	1.98	1.98	1.98	1.80	1.83	1.90	1.90	2.03	2.03	2.16	2.16	1.66	1.60	1.54	1.47	1.49
2.06	2.06	2.10	2.19	2.29	2.34	2.34	2.34	2.06	2.34	2.45	2.46	2.66	2.66	2.84	2.84	2.05	2.81	2.93	3.11	3.28
3.77	3.97	4.27	4.32	4.44	4.48	4.48	4.48	3.97	3.88	3.93	3.93	4.02	4.02	4.10	4.10	3.11	3.40	3.49	3.62	3.73
1.39	1.44	1.55	1.57	1.48	1.46	1.46	1.46	1.44	1.45	1.49	1.49	1.58	1.58	1.69	1.69	1.50	1.93	2.04	2.19	2.27
3.34	3.37	3.41	3.46	3.74	3.84	3.84	3.84	3.37	3.55	3.63	3.63	3.79	3.79	3.94	3.94	2.98	3.51	3.60	3.75	3.78
2.97	3.09	3.29	3.27	3.23	3.21	3.21	3.21	3.09	2.84	2.81	2.81	2.75	2.75	2.72	2.72	2.68	3.53	3.73	4.02	4.07
3.10	3.28	3.56	3.67	3.99	4.10	4.10	4.10	3.28	3.19	3.23	3.23	3.32	3.32	3.41	3.41	2.29	2.86	3.10	3.46	3.53
2.87	3.09	3.42	3.55	3.69	3.74	3.74	3.74	3.09	2.87	2.89	2.89	2.94	2.94	3.01	3.01	2.02	2.59	2.69	2.84	2.93
1.92	1.90	1.97	2.01	2.39	2.54	2.54	2.54	1.90	1.76	1.73	1.73	1.71	1.71	1.74	1.74	3.01	3.95	4.15	4.44	4.57
3.26	3.70	4.32	4.50	4.94	4.90	4.90	4.90	3.70	3.17	3.15	3.15	3.14	3.14	3.16	3.16	1.39	1.57	1.73	2.01	2.11
3.36	3.55	3.82	3.92	4.00	4.02	4.02	4.02	3.55	3.41	3.43	3.43	3.48	3.48	3.54	3.54	2.41	3.55	3.83	4.23	4.44
2.58	2.75	3.02	3.15	3.37	3.46	3.46	3.46	2.75	2.80	2.88	2.88	3.03	3.03	3.17	3.17	1.99	2.99	3.26	3.67	3.69
4.39	4.57	4.86	4.99	4.90	4.98	4.98	4.98	4.57	4.39	4.39	4.39	4.40	4.40	4.40	4.41	3.89	4.89	5.00	4.90	4.94
3.17	3.17	3.19	3.22	3.14	3.11	3.11	3.11	3.17	3.19	3.20	3.20	3.21	3.21	3.23	3.23	3.42	3.77	3.85	3.96	4.01
3.45	3.63	3.91	4.04	4.23	4.30	4.30	4.30	3.63	3.57	3.62	3.62	3.70	3.70	3.78	3.78	2.33	2.10	2.19	2.39	2.33
4.54	4.68	4.90	4.91	4.91	4.92	4.92	4.92	4.68	4.73	4.81	4.81	4.95	4.95	4.87	4.85	3.59	3.62	3.59	3.56	3.51
C	A	B	C	A	B	C	A	B	C	A	B	C	A	B	C	A	B	C	A	B
	7			8			9			20			21			22			23	

2.22	2.19	2.19	2.19	2.29	2.25	2.26	2.26	2.30	2.30	2.34	2.34	2.23
3.51	3.60	3.60	3.60	3.14	3.30	3.38	3.38	3.52	3.52	3.65	3.65	2.89
4.77	4.91	4.91	4.91	3.55	3.32	3.38	3.38	3.51	3.51	3.63	3.63	1.65
2.33	2.39	2.39	2.39	2.01	1.90	1.91	1.91	1.97	1.97	2.06	2.06	2.08
4.32	4.37	4.37	4.37	3.80	3.30	3.22	3.22	3.10	3.10	3.02	3.02	2.88
4.15	4.25	4.25	4.25	3.48	3.58	3.68	3.68	3.88	3.88	4.07	4.07	2.88
3.27	3.46	3.46	3.46	1.82	1.26	1.23	1.23	1.24	1.24	1.33	1.33	0.55
2.66	2.79	2.79	2.79	2.13	1.89	1.84	1.84	1.77	1.77	1.73	1.73	2.28
1.68	1.80	1.80	1.80	1.54	1.79	1.88	1.88	2.04	2.04	2.19	2.19	1.69
3.49	3.56	3.56	3.56	2.93	3.00	3.08	3.08	3.22	3.22	3.36	3.36	2.09
3.52	3.46	3.46	3.46	3.49	3.40	3.41	3.41	3.43	3.43	3.45	3.45	3.11
2.51	2.59	2.59	2.59	2.04	2.00	2.03	2.03	2.11	2.11	2.20	2.20	1.53
3.81	3.83	3.83	3.83	3.60	3.59	3.63	3.63	3.71	3.71	3.80	3.80	2.99
4.03	4.02	4.02	4.02	3.73	3.56	3.59	3.59	3.64	3.64	3.69	3.69	2.69
3.67	3.74	3.74	3.74	3.10	2.87	2.88	2.88	2.92	2.92	2.97	2.97	2.26
3.02	3.06	3.06	3.06	2.69	2.83	2.94	2.94	3.13	3.13	3.32	3.32	2.01
4.65	4.68	4.68	4.68	4.15	3.96	3.98	3.98	4.03	4.03	4.09	4.09	3.11
2.18	2.22	2.22	2.22	1.73	1.86	1.99	1.99	2.23	2.23	2.47	2.47	1.28
4.75	4.85	4.86	4.86	3.83	3.49	3.47	3.47	3.45	3.45	3.44	3.45	2.41
3.84	3.90	3.90	3.90	3.26	3.03	3.05	3.05	3.10	3.10	3.14	3.14	2.03
4.90	5.00	5.00	4.90	4.90	4.93	4.95	4.95	4.99	4.99	4.92	4.92	3.93
4.11	4.15	4.15	4.15	3.85	3.83	3.85	3.85	3.89	3.89	3.93	3.93	3.46
1.78	1.62	1.62	1.62	2.19	2.26	2.32	2.32	2.44	2.44	2.54	2.54	2.24
3.49	3.48	3.48	3.48	3.59	3.81	3.88	3.88	4.01	4.01	4.13	4.13	3.55
C	**A**	**B**	**C**	**A**	**B**	**C**	**A**	**B**	**C**	**A**	**B**	**C**
	24			**25**			**26**			**50**		

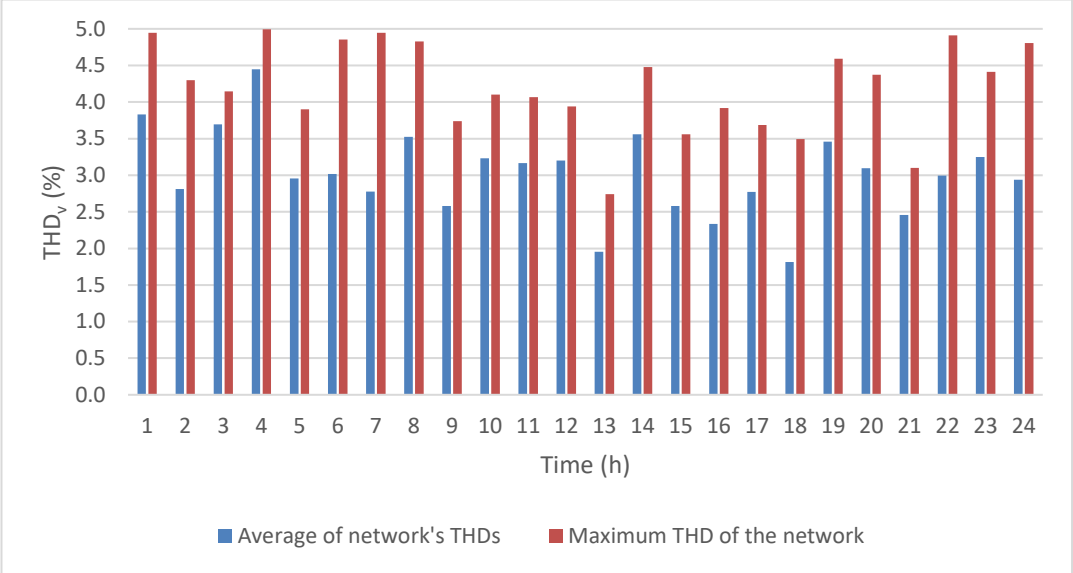

Figure 5.7: Average and maximum THD_v of network buses during 24-hour operation (Case 5-V)

According to the detailed simulation results, the optimal location/size of APLCs can effectively compensate for the nonlinear load harmonic current injections and keep the THD_v of the system within the required standard during the 24-hour operation of the unbalanced network.

Chapter 6

Conclusions and Future Work

6.1 Thesis Summary and Conclusions

A comprehensive literature review was performed on harmonic distortions and power quality issues associated with distribution networks with nonlinear loading. The optimisation of unbalanced distribution networks embedded with PVs and serving different types of nonlinear loads was carried out using APLCs. Two PSO-based algorithms for optimal sizing, allocating, and online control of APLCs were proposed and developed using the decoupled approach for harmonic load flow calculations. The algorithms were successfully employed and the results showed significant enhancements in the network operating conditions. The optimisations were carried out for both balanced and unbalanced operating conditions using both linear and harmonic-generating loads for different scenarios. Based on the simulation results, the objectives of the optimisations were successfully achieved and the associated constraints were fully satisfied. In summary, the optimisations were performed through the following two major steps:

a) The optimal sites (locations) and sizes (ratings) of multiple APLCs were calculated by the proposed first PSO-based algorithm while setting all linear and nonlinear loads at their maximum capacities. This represented the worst-case scenario for the distribution network. The objective function was the minimisation of APLC sizes and network THD_v while the upper limits for

individual voltage harmonics and individual bus THD_v levels, which were 3% and 5%, respectively, were the constraints of the algorithm. In other words, the input parameters for the first PSO algorithm were a group of candidate buses for APLC placement (generally all the network buses except for the swing bus) as well as the limits for the optimisation constraints. For a given network, the algorithm found the optimal sizes, number, and locations of the desired APLCs.

b) The APLC reference current signals were continuously calculated by the proposed second PSO-based algorithm for the online optimal control of the sited APLCs in time steps of Δt. The constraints and the allowable harmonic distortion limits were the same as in the first algorithm; however, the objective function was different. The APLC size term was excluded in the objective function while the reactive power compensation was being considered. Detailed simulations were executed for a 24-hour period simulating the operation of a real distorted system while the linear and nonlinear loads were being changed over time by the consumer; this was represented as a load curve in the network.

The optimisation results can now be summarised to highlight the research outcomes and the contributions of this research. In addition, some suggestions for future research are presented based on the obtained results.

The main conclusions resulting from this study may be summarised as follows:

1. The method of optimal sizing/allocating and control of multiple APLCs, as proposed in this thesis, is a new and effective approach for distribution system operations, which enables simultaneously mitigating the network harmonics, minimising the energy loss, and improving the power quality.
2. The PSO-based algorithm is suitable for the optimal sizing, siting, and operation of multiple APLCs under different operating conditions as it is possible to control them simultaneously by updating their reference signals while satisfying the network's constraints.

3. Owing to the fast computation time of the DHLF, the methods have also shown their potential to perform optimisation from small simple systems to large complicated systems.
4. Detailed simulations of the IEEE 18-bus network under balanced and unbalanced conditions with and without multiple single-phase PVs confirm the ability of the proposed approach to successfully maintain the power quality parameters within the acceptable levels of the IEEE 519-1992 standard while also controlling the fundamental reactive power. Simulation results also illustrate that the APLC as an enhanced APF can efficiently maintain the THDv of the entire network and individual harmonic distortions below the designated limits of 5% and 3%, respectively, which are suggested by most power quality standards.
5. The objective function's weighting factors for the size of APLC (W_{APLC}) and the network THD (W_{THD}) have significant impacts on the optimisation outcomes. These factors should be calibrated according to the user preferences. Greater values of W_{THD} cause lower THD_v values with larger total APLC size. On the other hand, greater values of W_{APLC} (APLC size) cause most THD_v values being marginally close to 5%, which increases the risk in the optimal operation and is not recommended particularly if network modifications are expected in the future.
6. Finally, the proposed second PSO-based approach for the operation and online control of multiple APLCs ensures that the designed system performs satisfactorily during a 24-hour period.

6.2 Future Work

Future work in this field may be carried out by considering the following issues:

1. It should be noted that similar to the other optimisation methods, premature convergence is still a crucial problem for the proposed methods. Due to the long computation time required by the methods, an early detection of a possible

premature convergence is necessary to avoid spending more time with no additional improvements. The optimisation algorithms developed in this research have been devised using a procedure that detects this premature convergence. However, it does not solve the problem completely and the time spent in such computation is wasted. Thus, the problem of premature convergence needs to be effectively addressed. This problem may be further resolved by intelligently constructing algorithms that do not only detect the problem but also prevent the problem in the first place so that stopping the iteration in the middle of the process is avoided.

2. The DHLF is developed and used in this research. Although the decoupled approach decreases the complexity of the problem, which significantly reduces the computing time, it can potentially decrease the accuracy of the solution. Therefore, a faster and more accurate coupled harmonic load flow algorithm is recommended for future research to enhance the optimisation results.
3. The main purpose of employing MATLAB in this research was to investigate the performance of the approach on the optimal APLC siting/sizing problem. However, MATLAB might not be a practical control software for large networks with many buses as it usually requires considerable time for calculating the operational parameters. In addition, the PSO program at each time step Δt executes the file with transferred (updated) data to calculate the optimal solution. It is recommended to use alternative practical software with a faster processor system to implement the proposed approach in real applications.

Bibliography

[1] E. Fuchs and M. A. Masoum, "Power quality in power systems and electrical machines (Second Edition)," Academic press, 2015, pp. 573-680.

[2] J. Arrillaga, B. C. Smith, N. R. Watson, and A. R. Wood, *Power system harmonic analysis*. John Wiley & Sons, 1997.

[3] F. De La Rosa, *Harmonics and power systems*. CRC press Boca Raton, 2006.

[4] I. F II, "IEEE recommended practices and requirements for harmonic control in electrical power systems," *New York, NY, USA*, 1993.

[5] T. Shuter, H. Vollkommer, and T. Kirkpatrick, "Survey of harmonic levels on the American electric power distribution system," *IEEE transactions on power delivery*, vol. 4, no. 4, pp. 2204-2213, 1989.

[6] B. Singh, K. Al-Haddad, and A. Chandra, "A review of active filters for power quality improvement," *IEEE transactions on industrial electronics*, vol. 46, no. 5, pp. 960-971, 1999.

[7] H. Sasaki and T. Machida, "A new method to eliminate AC harmonic currents by magnetic flux compensation-considerations on basic design," *IEEE Transactions on Power Apparatus and Systems*, no. 5, pp. 2009-2019, 1971.

[8] G.-H. Choe and M.-H. Park, "Analysis and control of active power filter with optimized injection," *IEEE transactions on power electronics*, vol. 4, no. 4, pp. 427-433, 1989.

[9] G.-H. Choe and M.-H. Park, "A new injection method for ac harmonic elimination by active power filter," *IEEE Transactions on Industrial Electronics*, vol. 35, no. 1, pp. 141-147, 1988.

[10] H. Akagi, "Trends in active power line conditioners," *IEEE transactions on power electronics*, vol. 9, no. 3, pp. 263-268, 1994.

[11] S. Mishra and C. Bhende, "Bacterial foraging technique-based optimized active power filter for load compensation," *IEEE transactions on power delivery*, vol. 22, no. 1, pp. 457-465, 2006.

[12] I. Ziari, A. Kazemi, and A. Jalilian, "Using active power filter based on a new control strategy to compensate power quality," in *2006 IEEE International Power and Energy Conference*, 2006, pp. 373-377: IEEE.

[13] I. Ziari and A. Jalilian, "A new control strategy for an active power filter to compensate harmonics and reactive power," in *ICHQP*, 2006.

[14] W. Chang, W. Grady, and M. Samotyj, "Meeting IEEE-519 harmonic voltage and voltage distortion constraints with an active power line conditioner," *IEEE Transactions on Power Delivery*, vol. 9, no. 3, pp. 1531-1537, 1994.

[15] W. Grady, M. Samotyj, and A. Noyola, "The application of network objective functions for actively minimizing the impact of voltage harmonics in power systems," *IEEE transactions on power delivery*, vol. 7, no. 3, pp. 1379-1386, 1992.

[16] Y.-Y. Hong, Y.-L. Hsu, and Y.-T. Chen, "Active power line conditioner planning using an enhanced optimal harmonic power flow method," *Electric Power Systems Research*, vol. 52, no. 2, pp. 181-188, 1999.

[17] W. Chang, W. Grady, and M. Samotyj, "Controlling harmonic voltage and voltage distortion in a power system with multiple active power line conditioners," *IEEE transactions on power delivery*, vol. 10, no. 3, pp. 1670-1676, 1995.

[18] W. Chang and W. Grady, "Minimizing harmonic voltage distortion with multiple current-constrained active power line conditioners," *IEEE Transactions on Power Delivery*, vol. 12, no. 2, pp. 837-843, 1997.

[19] R. Keypour, H. Seifi, and A. Yazdian-Varjani, "Genetic based algorithm for active power filter allocation and sizing," *Electric Power Systems Research*, vol. 71, no. 1, pp. 41-49, 2004.

[20] W. Grady, M. Samotyj, and A. Noyola, "Minimizing network harmonic voltage distortion with an active power line conditioner," *IEEE Transactions on Power Delivery*, vol. 6, no. 4, pp. 1690-1697, 1991.

[21] M. R. AlRashidi and M. E. El-Hawary, "A survey of particle swarm optimization applications in electric power systems," *IEEE transactions on evolutionary computation*, vol. 13, no. 4, pp. 913-918, 2008.

[22] H. Bai and B. Zhao, "A survey on application of swarm intelligence computation to electric power system," in *2006 6th World Congress on Intelligent Control and Automation*, 2006, vol. 2, pp. 7587-7591: IEEE.

[23] R. Eberhart and J. Kennedy, "A new optimizer using particle swarm theory," in *MHS'95. Proceedings of the Sixth International Symposium on Micro Machine and Human Science*, 1995, pp. 39-43: Ieee.

[24] J.-B. Park, K.-S. Lee, J.-R. Shin, and K. Y. Lee, "A particle swarm optimization for economic dispatch with nonsmooth cost functions," *IEEE Transactions on Power systems,* vol. 20, no. 1, pp. 34-42, 2005.

[25] A. Zobaa, "A new approach for voltage harmonic distortion minimization," *Electric Power Systems Research,* vol. 70, no. 3, pp. 253-260, 2004.

[26] A. F. Zobaa and A. Aziz, "LC compensators based on transmission loss minimization for nonlinear loads," *IEEE transactions on power delivery,* vol. 19, no. 4, pp. 1740-1745, 2004.

[27] C. K. Duffey and R. P. Stratford, "Update of harmonic standard IEEE-519: IEEE recommended practices and requirements for harmonic control in electric power systems," *IEEE Transactions on Industry Applications,* vol. 25, no. 6, pp. 1025-1034, 1989.

[28] J. S. Subjak and J. S. Mcquilkin, "Harmonics-causes, effects, measurements, and analysis: an update," *IEEE transactions on industry applications,* vol. 26, no. 6, pp. 1034-1042, 1990.

[29] R.-H. Liang and C.-K. Cheng, "Dispatch of main transformer ULTC and capacitors in a distribution system," *IEEE Transactions on Power Delivery,* vol. 16, no. 4, pp. 625-630, 2001.

[30] R.-H. Liang and Y.-S. Wang, "Fuzzy-based reactive power and voltage control in a distribution system," *IEEE Transactions on Power Delivery,* vol. 18, no. 2, pp. 610-618, 2003.

[31] A. Ulinuha, M. Masoum, and S. Islam, "The accuracy and efficiency issues of decouple approach for harmonic power flow calculation," in *Regional Postgraduate Conference on Engineering and Science (RPCES)*, 2006, vol. 1, pp. 213-218.

[32] A. Ulinuha, M. Masoum, and S. Islam, "Harmonic power flow calculations for a large power system with multiple nonlinear loads using decoupled approach," in *2007 Australasian Universities Power Engineering Conference*, 2007, pp. 1-6: IEEE.

[33] P. Didsayabutra, N. Mithulananthan, and B. Eua-Aroporn, "Static voltage stability study on Thailand power system network," *12th International Conference on the Electric Power Supply Industry, 12th CEPSI, Pattaya, Thailand*, pp. No. 34-31, 1998.

[34] N. Mithulananthan and S. C. Srivastava, "Investigation of a voltage collapse incident in Sri Lankan power system network," (in English), *Proceedings of Empd '98 - 1998 International Conference on Energy Management and Power Delivery, Vols 1 and 2 and Supplement*, pp. 47-53, 1998.

[35] A. Kusko and M. T. Thompson, *Power quality in electrical systems*. McGraw-Hill New York, 2007.

[36] M. Salem, L. Talat, and H. Soliman, "Voltage control by tap-changing transformers for a radial distribution network," *IEE Proceedings-Generation, Transmission and Distribution*, vol. 144, no. 6, pp. 517-520, 1997.

[37] J. C. Vasquez, R. A. Mastromauro, J. M. Guerrero, and M. Liserre, "Voltage support provided by a droop-controlled multifunctional inverter," *IEEE Transactions on Industrial Electronics*, vol. 56, no. 11, pp. 4510-4519, 2009.

[38] M. Morati, D. Girod, F. Terrien, V. Peron, P. Poure, and S. Saadate, "Industrial 100-MVA EAF voltage flicker mitigation using VSC-based STATCOM with improved performance," *IEEE Transactions on Power Delivery*, vol. 31, no. 6, pp. 2494-2501, 2015.

[39] T. Tadivaka, M. Srikanth, and T. V. Muni, "THD reduction and voltage flicker mitigation in power system base on STATCOM," in *International Conference on Information Communication and Embedded Systems (ICICES2014)*, 2014, pp. 1-6: IEEE.

[40] G. A. Taylor, "Power quality hardware solutions for distribution systems: Custom power," 1995.

[41] N. G. Hingorani, "Introducing custom power," *IEEE spectrum*, vol. 32, no. 6, pp. 41-48, 1995.

[42] N. G. Hingorani, "FACTS-flexible AC transmission system," in *International Conference on AC and DC Power Transmission*, 1991, pp. 1-7: IET.

[43] E. Fuchs and M. S. Masoum, *Power quality in electrical machines and power systems*. Elsevier, 2008.

[44] C.-J. Chou, C.-W. Liu, J.-Y. Lee, and K.-D. Lee, "Optimal planning of large passive-harmonic-filters set at high voltage level," *IEEE Transactions on Power Systems*, vol. 15, no. 1, pp. 433-441, 2000.

[45] H. Fujita and H. Akagi, "A practical approach to harmonic compensation in power systems-series connection of passive and active filters," *IEEE Transactions on industry applications,* vol. 27, no. 6, pp. 1020-1025, 1991.

[46] A. Ghosh and G. Ledwich, "Compensation of distribution system voltage using DVR," *IEEE Transactions on power delivery,* vol. 17, no. 4, pp. 1030-1036, 2002.

[47] H. K. Al-Hadidi, A. Gole, and D. A. Jacobson, "A novel configuration for a cascade inverter-based dynamic voltage restorer with reduced energy storage requirements," *IEEE Transactions on Power Delivery,* vol. 23, no. 2, pp. 881-888, 2008.

[48] C. Zhan *et al.*, "Dynamic voltage restorer based on voltage-space-vector PWM control," *IEEE transactions on Industry applications,* vol. 37, no. 6, pp. 1855-1863, 2001.

[49] C. Zhan, A. Arulampalam, and N. Jenkins, "Four-wire dynamic voltage restorer based on a three-dimensional voltage space vector PWM algorithm," *IEEE Transactions on Power Electronics,* vol. 18, no. 4, pp. 1093-1102, 2003.

[50] S. Bhattacharyya, S. Cobben, P. Ribeiro, and W. Kling, "Harmonic emission limits and responsibilities at a point of connection," *IET generation, transmission & distribution,* vol. 6, no. 3, pp. 256-264, 2012.

[51] A. M. Massoud, S. J. Finney, and B. W. Williams, "Review of harmonic current extraction techniques for an active power filter," in *2004 11th International Conference on Harmonics and Quality of Power (IEEE Cat. No. 04EX951)*, 2004, pp. 154-159: IEEE.

[52] M. Hannan and A. Mohamed, "PSCAD/EMTDC simulation of unified series-shunt compensator for power quality improvement," *IEEE Transactions on power delivery,* vol. 20, no. 2, pp. 1650-1656, 2005.

[53] Y. Tang, P. C. Loh, P. Wang, F. H. Choo, F. Gao, and F. Blaabjerg, "Generalized design of high performance shunt active power filter with output LCL filter," *IEEE Transactions on Industrial Electronics,* vol. 59, no. 3, pp. 1443-1452, 2011.

[54] A. Ghosh, A. K. Jindal, and A. Joshi, "A unified power quality conditioner for voltage regulation of critical load bus," in *IEEE Power Engineering Society General Meeting, 2004.*, 2004, pp. 471-476: IEEE.

[55] A. K. Jindal, A. Ghosh, and A. Joshi, "Interline unified power quality conditioner," *IEEE transactions on power delivery,* vol. 22, no. 1, pp. 364-372, 2006.

[56] M. I. Marei, E. F. El-Saadany, and M. M. Salama, "A new approach to control DVR based on symmetrical components estimation," *IEEE Transactions on Power Delivery*, vol. 22, no. 4, pp. 2017-2024, 2007.

[57] R. Arnold, "Solutions to the power quality problem," *Power Engineering Journal*, vol. 15, no. 2, pp. 65-73, 2001.

[58] C. Madtharad and S. Premrudeepreechacharn, "Active power filter for three-phase four-wire electric systems using neural networks," *Electric Power Systems Research*, vol. 60, no. 3, pp. 179-192, 2002.

[59] H. A. Ramos-Carranza and A. Medina, "Single-harmonic active power line conditioner for harmonic distortion control in power networks," *IET Power Electronics*, vol. 7, no. 9, pp. 2218-2226, 2014.

[60] I. Ziari and A. Jalilian, "Optimal allocation and sizing of active power line conditioners using a new particle swarm optimization-based approach," *Electric Power Components and Systems*, vol. 40, no. 3, pp. 273-291, 2012.

[61] K. Kennedy, G. Lightbody, R. Yacamini, M. Murray, and J. Kennedy, "Development of a network-wide harmonic control scheme using an active filter," *IEEE transactions on power delivery*, vol. 22, no. 3, pp. 1847-1856, 2007.

[62] K. Kennedy, G. Lightbody, R. Yacamini, M. Murray, and J. Kennedy, "Online control of an APLC for network-wide harmonic reduction," *IEEE transactions on power delivery*, vol. 21, no. 1, pp. 432-439, 2005.

[63] I. Ziari and A. Jalilian, "A new approach for allocation and sizing of multiple active power-line conditioners," *IEEE Transactions on Power Delivery*, vol. 25, no. 2, pp. 1026-1035, 2009.

[64] H. Ying-Yi and C. Ying-Kwun, "Determination of locations and sizes for active power line conditioners to reduce harmonics in power systems," *IEEE Transactions on Power Delivery*, vol. 11, no. 3, pp. 1610-1617, 1996.

[65] T.-H. Chen, M.-S. Chen, K.-J. Hwang, P. Kotas, and E. A. Chebli, "Distribution system power flow analysis-a rigid approach," *IEEE Transactions on Power Delivery*, vol. 6, no. 3, pp. 1146-1152, 1991.

[66] V. Ajjarapu and C. Christy, "The continuation power flow: a tool for steady state voltage stability analysis," in *[Proceedings] Conference Papers 1991 Power Industry Computer Application Conference*, 1991, pp. 304-311: Ieee.

[67] J. J. Grainger, W. D. Stevenson, and W. D. Stevenson, *Power system analysis*. 2003.

[68] P. Murty, "Power systems analysis," vol. Second: Butterworth-Heinemann, 2017, pp. 205-276.

[69] L. Powell, *Power system load flow analysis*. McGraw-Hill, 2005.

[70] V. M. da Costa, N. Martins, and J. L. R. Pereira, "Developments in the Newton Raphson power flow formulation based on current injections," *IEEE Transactions on power systems*, vol. 14, no. 4, pp. 1320-1326, 1999.

[71] H. Le Nguyen, "Newton-Raphson method in complex form [power system load flow analysis]," *IEEE transactions on power systems*, vol. 12, no. 3, pp. 1355-1359, 1997.

[72] H.-C. Chin, "Optimal shunt capacitor allocation by fuzzy dynamic programming," *Electric Power Systems Research*, vol. 35, no. 2, pp. 133-139, 1995.

[73] J. Arrillaga, N. R. Watson, and G. N. Bathurst, "A multifrequency power flow of general applicability," *IEEE transactions on power delivery*, vol. 19, no. 1, pp. 342-349, 2004.

[74] G. Bathurst, B. Smith, N. Watson, and J. Arillaga, "A modular approach to the solution of the three-phase harmonic power-flow," in *8th International Conference on Harmonics and Quality of Power. Proceedings (Cat. No. 98EX227)*, 1998, vol. 2, pp. 653-659: IEEE.

[75] A. Semlyen and M. Shlash, "Principles of modular harmonic power flow methodology," *IEE Proceedings-Generation, Transmission and Distribution*, vol. 147, no. 1, pp. 1-6, 2000.

[76] W. Xu, Z. Huang, Y. Cui, and H. Wang, "Harmonic resonance mode analysis," *IEEE Transactions on Power Delivery*, vol. 20, no. 2, pp. 1182-1190, 2005.

[77] M. A. Masoum, M. Ladjevardi, A. Jafarian, and E. F. Fuchs, "Optimal placement, replacement and sizing of capacitor banks in distorted distribution networks by genetic algorithms," *IEEE transactions on power delivery*, vol. 19, no. 4, pp. 1794-1801, 2004.

[78] M. A. Masoum, A. Jafarian, M. Ladjevardi, E. F. Fuchs, and W. Grady, "Fuzzy approach for optimal placement and sizing of capacitor banks in the presence of harmonics," *IEEE Transactions on Power Delivery*, vol. 19, no. 2, pp. 822-829, 2004.

[79] M. Masoum, M. Ladjevardi, E. Fuchs, and W. Grady, "Application of local variations and maximum sensitivities selection for optimal placement of shunt capacitor banks under nonsinusoidal operating conditions," *International*

Journal of Electrical Power & Energy Systems, vol. 26, no. 10, pp. 761-769, 2004.

[80] K. Islam and A. Samra, "Effect of condensers on harmonic propagation in AC power system," in *Proceedings IEEE Southeastcon'95. Visualize the Future*, 1995, pp. 425-428: IEEE.

[81] Y. Baghzouz, "Effects of nonlinear loads on optimal capacitor placement in radial feeders," *IEEE Transactions on Power Delivery*, vol. 6, no. 1, pp. 245-251, 1991.

[82] T. Ghose and S. Goswami, "Effects of unbalances and harmonics on optimal capacitor placement in distribution system," *Electric Power Systems Research*, vol. 68, no. 2, pp. 167-173, 2004.

[83] M. Shlash and A. Semlyen, "Efficiency issues of modular harmonic power flow," *IEE Proceedings-Generation, Transmission and Distribution*, vol. 148, no. 2, pp. 123-127, 2001.

[84] I. M. Elamin, "Fast decoupled harmonic loadflow method," in *Conference Record of the 1990 IEEE Industry Applications Society Annual Meeting*, 1990, pp. 1749-1756: IEEE.

[85] J.-H. Teng and C.-Y. Chang, "Fast harmonic analysis method for unbalanced distribution systems," in *2003 IEEE Power Engineering Society General Meeting (IEEE Cat. No. 03CH37491)*, 2003, vol. 2, pp. 1244-1249: IEEE.

[86] J.-H. Teng and C.-Y. Chang, "A fast harmonic load flow method for industrial distribution systems," in *PowerCon 2000. 2000 International Conference on Power System Technology. Proceedings (Cat. No. 00EX409)*, 2000, vol. 3, pp. 1149-1154: IEEE.

[87] Z. Mariños, J. Pereira, and S. J. Carneiro, "Fast harmonic power flow calculation using parallel processing," *IEE Proceedings-Generation, Transmission and Distribution*, vol. 141, no. 1, pp. 27-32, 1994.

[88] G. Carpinelli, T. Esposito, P. Varilone, and P. Verde, "First-order probabilistic harmonic power flow," *IEE Proceedings-Generation, Transmission and Distribution*, vol. 148, no. 6, pp. 541-548, 2001.

[89] Y.-Y. Hong, J.-S. Lin, and C.-H. Liu, "Fuzzy harmonic power flow analyses," in *PowerCon 2000. 2000 International Conference on Power System Technology. Proceedings (Cat. No. 00EX409)*, 2000, vol. 1, pp. 121-125: IEEE.

[90] T. Chung and H. Leung, "A genetic algorithm approach in optimal capacitor selection with harmonic distortion considerations," *International Journal of Electrical Power & Energy Systems,* vol. 21, no. 8, pp. 561-569, 1999.

[91] M. Valcarel and J. G. Mayordomo, "Harmonic power flow for unbalanced systems," *IEEE Transactions on Power Delivery,* vol. 8, no. 4, pp. 2052-2059, 1993.

[92] D. Xia and G. T. Heydt, "Harmonic power flow studies part I-formulation and solution," *IEEE Transactions on Power Apparatus and systems,* no. 6, pp. 1257-1265, 1982.

[93] D. Xia and G. Heydt, "Harmonic power flow studies-part II implementation and practical application," *IEEE transactions on power apparatus and systems,* no. 6, pp. 1266-1270, 1982.

[94] S. Williams, G. Brownfield, and J. Duffus, "Harmonic propagation on an electric distribution system: field measurements compared with computer simulation," *IEEE transactions on power delivery,* vol. 8, no. 2, pp. 547-552, 1993.

[95] S. Rios and R. Castaneda, "Newton-Raphson Probabilistic Harmonic Power Flow Through Montecarlo Simulation," in *MIDWEST SYMPOSIUM ON CIRCUITS AND SYSTEMS*, 1995, vol. 38, pp. 1297-1300: PROCEEDINGS PUBLISHED BY VARIOUS PUBLISHERS.

[96] J.-H. Teng and C.-Y. Chang, "A novel and fast three-phase load flow for unbalanced radial distribution systems," *IEEE Transactions on Power Systems,* vol. 17, no. 4, pp. 1238-1244, 2002.

[97] C. Chen and Y. Yan, "Optimal capacitor placement for power systems with nonlinear loads," *International Journal of Electrical Power & Energy Systems,* vol. 14, no. 6, pp. 387-392, 1992.

[98] Z. Wu and K. Lo, "Optimal choice of fixed and switched capacitors in radial distributors with distorted substation voltage," *IEE Proceedings-Generation, Transmission and Distribution,* vol. 142, no. 1, pp. 24-28, 1995.

[99] S. Ertem and Y. Baghzouz, "Optimal shunt capacitor sizing for distribution systems with multiple nonlinear loads," in *Conference on Industrial and Commercial Power Systems,* 1990, pp. 51-56: IEEE.

[100] T. Esposito, G. Carpinelli, P. Varilone, and P. Verde, "Probabilistic harmonic power flow for percentile evaluation," in *Canadian Conference on Electrical and Computer Engineering 2001. Conference Proceedings (Cat. No. 01TH8555)*, 2001, vol. 2, pp. 831-838: IEEE.

[101] X.-m. Yu, X.-y. Xiong, and Y.-w. Wu, "A PSO-based approach to optimal capacitor placement with harmonic distortion consideration," *Electric Power Systems Research*, vol. 71, no. 1, pp. 27-33, 2004.

[102] M. M. L. de Saa and J. U. Garcia, "Three-phase harmonic load flow in frequency and time domains," *IEE Proceedings-Electric Power Applications*, vol. 150, no. 3, pp. 295-300, 2003.

[103] Y. Baghzouz *et al.*, "Time-varying harmonics. I. Characterizing measured data," *IEEE Transactions on Power Delivery*, vol. 13, no. 3, pp. 938-944, 1998.

[104] Y. Baghzouz *et al.*, "Time-varying harmonics. II. Harmonic summation and propagation," *IEEE Transactions on Power Delivery*, vol. 17, no. 1, pp. 279-285, 2002.

[105] Y. Baghzouz and S. Ertem, "Shunt capacitor sizing for radial distribution feeders with distorted substation voltages," *IEEE Transactions on Power Delivery*, vol. 5, no. 2, pp. 650-657, 1990.

[106] B. Singh, K. Al-Haddad, and A. Chandra, "A universal active power filter for single-phase reactive power and harmonic compensation," in *Power Quality'98*, 1998, pp. 81-87: IEEE.

[107] W. R. N. Santos *et al.*, "The transformerless single-phase universal active power filter for harmonic and reactive power compensation," *IEEE Transactions on Power Electronics*, vol. 29, no. 7, pp. 3563-3572, 2013.

[108] K. B. Nikilesh and P. N. Rao, "Harmonic compensation using D-STATCOM in combination with Renewable Energy Sources to enhance power quality," in *2015 International Conference on Electrical, Electronics, Signals, Communication and Optimization (EESCO)*, 2015, pp. 1-5: IEEE.

[109] T. B. Kumar and M. V. G. Rao, "Mitigation of Harmonics and power quality enhancement for SEIG based wind farm using ANFIS based STATCOM," in *2014 International Conference on Smart Electric Grid (ISEG)*, 2014, pp. 1-7: IEEE.

[110] L. Dinesh, H. Sesham, and V. Manoj, "Simulation of D-Statcom with hysteresis current controller for harmonic reduction," in *2012 International Conference on Emerging Trends in Electrical Engineering and Energy Management (ICETEEEM)*, 2012, pp. 104-108: IEEE.

[111] P. Lauttamus and H. Tuusa, "Three-level VSI based low switching frequency 10 MVA STATCOM in reactive power and harmonics compensation," in *2007 7th Internatonal Conference on Power Electronics*, 2007, pp. 536-541: IEEE.

[112] S. Ganguly, "Multi-objective planning for reactive power compensation of radial distribution networks with unified power quality conditioner allocation using particle swarm optimization," *IEEE Transactions on Power Systems,* vol. 29, no. 4, pp. 1801-1810, 2014.

[113] V. Khadkikar and A. Chandra, "UPQC-S: A novel concept of simultaneous voltage sag/swell and load reactive power compensations utilizing series inverter of UPQC," *IEEE transactions on power electronics,* vol. 26, no. 9, pp. 2414-2425, 2011.

[114] B. B. Ambati and V. Khadkikar, "Optimal sizing of UPQC considering VA loading and maximum utilization of power-electronic converters," *IEEE transactions on power delivery,* vol. 29, no. 3, pp. 1490-1498, 2014.

[115] V. Khadkikar, "Enhancing electric power quality using UPQC: A comprehensive overview," *IEEE transactions on Power Electronics,* vol. 27, no. 5, pp. 2284-2297, 2011.

[116] W. H. Kersting, "Radial distribution test feeders," *IEEE Transactions on Power Systems,* vol. 6, no. 3, pp. 975-985, 1991.

[117] A. Shenkman, "Energy loss computation by using statistical techniques," *IEEE Transactions on Power Delivery,* vol. 5, no. 1, pp. 254-258, 1990.

Every reasonable effort has been made to acknowledge the owners of copyright material. I would be pleased to hear from any copyright owner who has been omitted or incorrectly acknowledged.

Saeed Kazemi

Date: 15/03/2022